

UNIVERSITÀ
DEGLI STUDI
DI PADOVA

UNIVERSITÀ DEGLI STUDI DI PADOVA

Dipartimento di Ingegneria Industriale - DII

CURRICULUM: CHEMICAL AND ENVIRONMENTAL ENGINEERING
SERIES 32nd

MICROPATTERN TECHNOLOGY APPLIED TO THE IN VITRO STUDY OF THE EARLY HUMAN EMBRYONIC DEVELOPMENT

Direttore della Scuola: Ch.mo Prof. Paolo Colombo

Coordinatore d'indirizzo: Ch.mo Prof. Andrea Claudio Santomaso

Supervisore: Ch.mo Prof. Nicola Elvassore

Ph.D. student: Yang Yang

INDEX

SOMMARIO	V
SUMMARY	XIII
CHAPTER 1: INTRODUCTION.....	1
1.1 MICRO-ENGINEERING: MICROPATTERN TECHNOLOGY.....	3
1.1.1 Basis of micropattern technology.....	3
1.1.1.1 Cellular patterning.....	3
1.1.1.2 Micropatterning steps.....	6
1.1.1.3 Micropatterning scales.....	8
1.1.2 Soft lithography.....	12
1.1.2.1 Microcontact printing.....	12
1.1.2.2 Microfluidic patterning.....	14
1.1.2.3 Stencil patterning.....	17
1.1.3 Patterning with photolithography.....	18
1.1.4 Conclusions.....	19
1.2 HUMAN EARLY EMBRYONIC DEVELOPMENT.....	23
1.2.1 Germinal stage.....	24
1.2.2 Gastrulation.....	26
1.2.3 Neurulation or neural tube formation.....	28
1.2.4 Signaling pathways in human embryonic development.....	30
1.2.4.1 TGF- β signaling pathway.....	30
1.2.4.2 WNT signaling pathway.....	31
1.2.4.3 Hedgehog signaling pathway.....	33
1.2.4.4 NOTCH signaling pathway.....	35

1.3 HUMAN PLURIPOTENT STEM CELLS.....	37
1.3.1 Human embryonic stem cells.....	38
1.3.2 Human induced pluripotent stem cells.....	40
1.4 Advanced technologies to generate <i>in vitro</i> research models.....	45
1.4.1 Neural subtype specification form human pluripotent stem cells.....	45
1.4.2 3D <i>in vitro</i> models of central nervous system.....	48
1.4.3 Organ-on-a-chip engineering.....	51
CHAPTER 2: MOTIVATION AND AIM.....	55
CHAPTER 3: METHODS AND MATERIALS.....	59
3.1 METHODS.....	61
3.1.1 H9 human embryonic stem cells (H9 hESCs) culture.....	61
3.1.1.1 Medium preparation.....	61
3.1.1.2 Cell thawing.....	61
3.1.1.3 Passaging.....	62
3.1.1.4 Single-cell splitting.....	63
3.1.1.5 Cryopreservation.....	64
3.1.2 Lentiviral production and stable cell line generation.....	64
3.1.2.1 Lentivirus infection.....	64
3.1.2.2 Single-cell picking and expansion.....	66
3.1.3 Micropatterned surface preparation.....	67
3.1.3.1 Glass slide functionalization.....	67
3.1.3.2 Sterilization and coating.....	68
3.1.4 Mouse embryonic fibroblast conditioned medium preparation.....	68
3.1.5 Micropatterned cell culture.....	70
3.1.5.1 Micropatterned neural induction.....	70

3.1.5.2 Standard and micropatterned meso-endoderm induction.....	71
3.1.5.3 Micropatterned neuroectoderm cultured with meso-endoderm	72
3.1.6 Micropatterns inside of microfluidic chips.....	72
3.1.7 Immunofluorescence.....	75
3.2 MATERIALS.....	77
3.2.1 Media and supplements.....	77
3.2.2 Reagents.....	77
3.2.3 Antibodies.....	78
3.2.4 Small molecules.....	79
CHAPTER 4: RESULTS.....	81
4.1 ESTABLISHMENT OF THE MICROPATTERN TECHNOLOGY.....	83
4.2 MICROPATTERNED NEURAL INDUCTION.....	89
4.2.1 Standard neural induction protocol with dual-Smad inhibition.....	89
4.2.2 Micropatterned neural induction.....	93
4.3 MICROPATTERNED CO-CULTURE SYSTEM.....	99
4.3.1 H9 hESCs-GFP cell line.....	99
4.3.2 Characterization of meso-endoderm fates.....	101
4.3.3 Micropatterned neuroectoderm co-culture with meso-endoderm...	103
4.3.4 Micropatterned meso-endoderm culture.....	107
4.3.5 Micropatterns inside of microfluidic chips.....	110
CHAPTER 5: DISSCUSSION.....	115
CHAPTER 6: CONCLUSIONS AND FUTURE PERSPECTIVES.....	121
CHAPTER 7: REFERENCES.....	125
ACKNOWLEDGEMENT.....	141
致谢.....	145

SOMMARIO

Oggi, la *micropattern technology* che consente il controllo dell'architettura cellulare e tissutale *in vitro*, è stata dimostrata essere uno strumento utile ed efficiente nel modellare i microambienti su scale e complessità diverse. Negli ultimi 20 anni, l'utilizzo di tale tecnologia ha permesso agli scienziati di: - analizzare nel dettaglio, addirittura "dissezionare" il meccanismo di comunicazione tra le cellule ed i tessuti circostanti fino ad arrivare alla scoperta di importanti funzioni responsabili degli stessi meccanismi; - coltivare le cellule in un ambiente geometrico confinato ben definito avendo così la possibilità di controllare non solo la forma, le dimensioni, la posizione delle cellule, ma addirittura l'architettura a più strati, caratteristica dei tessuti biologici. Dallo studio della biologia cellulare e della biologia dello sviluppo, infatti, sappiamo che sia i segnali geometrici che meccanici, presenti nel microambiente, influenzano molto il comportamento cellulare. Tuttavia, non vi è alcuna possibilità di testare entrambi questi segnali in colture tissutali standard. Al giorno d'oggi, sono disponibili molti *micropattern methods* per affrontare questo problema. In generale, questi nuovi metodi forniscono una potente piattaforma per rispondere a quesiti fondamentali sul meccanismo della biologia cellulare e sull'ingegneria dei tessuti, tra cui la sopravvivenza cellulare, la proliferazione, la differenziazione, la migrazione cellulare, la citochinesi e la polarità cellulare.

Le cellule staminali pluripotenti umane (hPSCs), comprese le cellule staminali embrionali (hESC) e le cellule staminali pluripotenti indotte (hiPSCs), sono ampiamente utilizzate nella medicina rigenerativa, così come nel modello sperimentale di organogenesi normale e patologico a causa del loro potenziale

pluripotente capace di differenziare nei lignaggi di tutti e tre gli strati germinali: strati germinali di endoderma, ectoderma e mesoderma. Come sappiamo, i destini di differenziazione delle hPSCs sono altamente sensibili ai fattori ambientali locali che possono modulare la segnalazione autocrina o paracrina, nonché i processi di meccano-trasduzione mediati da segnali fisici. Il micropatterning cellulare comprende una serie di strategie tecniche che sono state sviluppate per organizzare spazialmente la geometria e la posizione di una popolazione cellulare allo scopo di controllare il microambiente cellulare locale, come le interazioni cellula-cellula e cellula-matrice. Nel contesto delle hPSCs, il micropattern cellulare è stato impiegato per ottenere e approfondire studi significativi su come i segnali geometrici e chimici modulano la decisione sui destini e sull'organizzazione delle cellule, nei primi schemi di differenziazione embrionale. Allo stesso tempo, micropattern di colture di hPSCs 2D e 3D sono stati usati per controllare la dimensione della colonia cellulare in modelli multicellulari, che a loro volta influenzeranno poi le decisioni di differenziazione nei tre strati germinali. Negli ultimi anni, sono stati sviluppati numerosi metodi di *micropatterning cellulare*, ma solo pochissimi, come la *microcontact printing*, *micro-well culture*, *photo-patterning*, e la *micro-stencil*, sono stati applicati con successo ai micropattern di hPSCs. La sfida con i micropattern di hPSCs risiede nella loro fragilità e nel requisito più rigoroso del microambiente che include la matrice extracellulare specifica (ECM) e le condizioni di crescita per l'adesione e la sopravvivenza delle cellule.

Fino ad oggi, l'uso del *micropattern* ha dimostrato che l'auto-organizzazione delle hESC può essere influenzata da segnali sia geometrici che chimici e generare così diverse popolazioni di cellule con una distribuzione ad anello indicativa dei diversi destini cellulari, simili, inoltre, a quelle osservate durante la gastrulazione. Questi

schemi auto-organizzanti emergono come conseguenza dell'interazione tra localizzazione del recettore e produzione dell'inibitore del BMP NOGGIN. Questo sistema rappresenta un modello in vitro ideale per rivelare la complessa interazione tra segnalazione, destino e forma cellulare, nonché per esplorare gli eventi di perdita della simmetria e le proprietà di auto-organizzazione delle cellule staminali pluripotenti. In risposta a fattori specifici, ad esempio l'inibitore *dual-Smad* e l'inibitore del WNT pathway, i *micropattern*, derivati dalle colture di hESCs, possono essere differenziati rispettivamente in progenitori neurali e popolazioni caratteristiche della striscia primitiva. È interessante notare come le tecniche di *micropatterning* possano anche essere applicate alla medicina rigenerativa, ad esempio, le cellule organizzate in *micropattern* possono essere trapiantate nell'embrione di pollo e portare alla formazione di un asse secondario che successivamente inizierà un destino neurale, all'interno dell'ospite stesso. In conclusione, la tecnologia dei *micropattern* applicata allo studio in vitro può aiutarci a comprendere e svelare il segreto dello sviluppo embrionale umano in vari modi. Nel frattempo, sempre più metodiche di ingegneria tissutale, che includono sia quelle bidimensionali che tridimensionali, saranno stabilite e combinate con la tecnologia dei *micropattern* per sviluppare un microambiente ben definito, che aiuterà le persone a generare modelli *in vitro* più complessi.

In questo lavoro di tesi, abbiamo sviluppato una nuova tecnica per la generazione di *micropattern* attraverso l'applicazione di una procedura di funzionalizzazione superficiale rapida. Inoltre, grazie all'uso di diversi *photomask*, possiamo realizzare i *micropattern* in varie forme e dimensioni, da 50 μ m a 1000 μ m. La generazione del substrato di coltura cellulare prevede due passaggi di poli-L-lisina superficiale ed un successivo rivestimento di ECM. Dopo una prima fase di settaggio del protocollo, per l'ottenimento di una coltura cellulare stabile, attraverso l'uso delle tecniche di

micropatterning, possiamo affermare che siamo in grado di raccogliere colonie cellulari stabili e ben formate dopo più di 8 giorni di coltura. Il nostro scopo è dunque quello di indagare come sarà influenzata l'induzione neurale, in caso di confinamento geometrico, per questo motivo abbiamo eseguito un esperimento di induzione neurale avvalendoci di tecniche di *micropatterning*; ciò usando il protocollo di induzione neurale caratterizzato da inibizione del *dual-Smad pathway*, sviluppato in precedenza. Nella coltura cellulare standard, è stato dimostrato che le doppie inibizioni della via segnalazione Smad sono altamente efficienti nella conversione neurale sia di hESC che di hiPSCs. L'azione sinergica di due inibitori, SB431542 e NOGGIN, è sufficiente per indurre una conversione neurale rapida (~ 6 giorni) e completa (> 80%) in condizioni di coltura aderente. Sempre nello stesso lavoro, i risultati hanno suggerito che la densità cellulare, ovvero la densità iniziale, al momento della semina, influenza in modo significativo l'esito dei destini cellulari, durante il processo di induzione neurale: l'alta densità di semina promuove un destino cellulare orientato verso la generazione del sistema nervoso centrale mentre la bassa densità di semina promuove il differenziamento di cellule della cresta neurale. Quindi, ipotizziamo che la nostra piattaforma di induzione neurale, generata con tecnologia di *micropatterning*, potrebbe essere utile per generare diversi destini cellulari localizzati individualmente lungo l'asse della colonia, e questa diversa localizzazione potrebbe essere un modello in vitro per imitare il modello di ectoderma. Come ci aspettavamo, abbiamo dimostrato che nella colonia sottoposta ad induzione neurale "micro-strutturata", le cellule si autoorganizzavano in 3 popolazioni principali, dall'interno verso l'esterno. Al centro della colonia, le cellule mostravano una densità relativamente bassa ed esprimevano sia AP-2 α sia P75 (marcatori della cresta neurale). Al contrario, le cellule esterne esprimevano NESTIN, SOX1 e PAX6 (marcatore di progenitore neurale) e si

distribuiscono come una struttura ad anello tra il centro e il bordo. Questa popolazione presenta un destino cellulare che riflette quello del sistema nervoso centrale. Confrontando la densità cellulare dal centro al confine, della colonia, abbiamo dimostrato come le basse densità cellulari promuovano la generazione di cellule della cresta neurale nel centro, mentre l'alta densità promuove la formazione di cellule del sistema nervoso centrale all'esterno. Inoltre, le cellule localizzate al confine della colonia avevano una morfologia più compatta e NESTIN risultava essere l'unico marcatore altamente espresso; questa popolazione cellulare presenta il destino tipico delle cellule ectodermiche superficiali. Possiamo quindi affermare che il nostro modello di induzione neurale, basato su tecniche di *micropatterning*, può essere utilizzato come piattaforma in vitro per imitare il modello ectodermico umano.

Successivamente, abbiamo esteso il nostro modello sperimentale per stabilire un sistema di co-coltura in vitro con lo scopo di studiare come i 3 strati germinali comunicano tra loro durante l'embriogenesi. Durante questo studio, una nuova linea cellulare hESCs-GFP è stata generata mediante infezione con Lentivirus, ed è stata utilizzata nel sistema di co-coltura per contrassegnare le cellule di *pre / sub-seeding*. Per generare cellule mesodermiche ed endodermiche co-coltivate, *in vitro*, abbiamo sviluppato un protocollo di differenziazione meso-endoderma, in condizioni di coltura cellulare standard, e questa popolazione meso-endodermica può essere successivamente seminata sulla popolazione cellulare neuroectodermica, al fine di simulare l'architettura presente *in vivo*. È interessante notare come la stragrande maggioranza delle cellule meso-endodermiche, successivamente seminate, può solo aderire a livello della porzione del neuroectoderma, area in cui le cellule si sono organizzate in una struttura ad anello vicino alle cellule PAX6+. Questa proprietà di adesione può essere determinata dalle differenze intrinseche che caratterizzano i

diversi destini del foglietto ectodermico. Inoltre, abbiamo dimostrato che quando le cellule meso-endodermiche vengono coltivate in un contesto di co-cultura con neuroectoderma, una nuova popolazione cellulare può essere generata a partire dalle cellule *sub-seeded*, e tutte hanno co-espresso PAX6 ma non esistono nella coltura cellulare meso-endodermica. Inoltre, con una co-cultura di 3 giorni, abbiamo sorprendentemente verificato che alcune cellule situate al di sopra delle cellule neuroectodermiche PAX6 + erano caratterizzate da una morfologia cellulare completamente diversa, rispetto alle altre popolazioni cellulari. Possiamo, per tanto ipotizzare, che queste cellule si siano auto-organizzate in una morfologia lineare e siano diventate, in questo sistema di co-cultura, una struttura di collegamento. Questo sistema di co-cultura sviluppato si è rivelato una solida piattaforma nello studio dell'interazione e della comunicazione tra i diversi strati germinali.

Infine, per studiare la capacità di auto-organizzazione del meso-endoderma abbiamo successivamente eseguito una coltura cellulare meso-endodermica, in un contesto di *micropatterning*. In breve, abbiamo innanzitutto indotto l'induzione meso-endodermica applicando lo stesso protocollo studiato precedentemente e secondariamente seminato questa popolazione mista sui micropattern. Al fine di simulare, al meglio, la stessa condizione di coltura, sono state utilizzate uguale densità di semina ed è stato effettuato lo stesso numero di cambi medium al giorno, uguale a 3. Le cellule meso-endodermiche, differenziate con tecniche di *micropatterning*, si sono differenziate in diverse popolazioni cellulari con morfologie diverse. Generalmente, le cellule localizzate nel centro della colonia mostravano una struttura compatta e multistrato, mentre le cellule situate all'altezza del bordo si differenziavano in strutture lineari. In conclusione, è evidente che il destino delle cellule meso-endodermiche è regolato da proprietà intrinseche di auto-organizzazione sotto

confinamento geometrico, ma non è ancora chiaro come tale organizzazione sia influenzata, quando co-coltivata con neuroectoderma. Da questo punto di vista, stiamo affrontando l'opportunità e sfide, allo stesso tempo, e sono necessarie ulteriori attività di ricerca, per il prossimo futuro.

SUMMARY

Micropattern technology, which enables control of cell and tissue architecture *in vitro* has been demonstrated as a useful and efficient tool for modeling the microenvironments at different scales and complexities. In the last 20 years, scientists have benefited a lot in revealing and dissecting the mechanism of communication between cells and the surrounding tissues and leading to the function from the breakthroughs in micropattern technology. Moreover, micropattern technology allows users to culture cells under well-defined geometric confinement by controlling cell shape, size, position, or multi-layered architecture. From the study of cell biology and developmental biology, we know that both geometric and mechanical cues present in the microenvironment affect cell behavior a lot. However, there is no possibility that we can test both these cues under standard tissue culture. Nowadays, many micropattern methods are available to address this problem at various scales. Generally speaking, these new methods provide a powerful platform for asking fundamental and mechanism questions in cell biology and tissue engineering, including cell survival, proliferation, differentiation, cell migration, cytokinesis, and cell polarity.

Human pluripotent stem cells (hPSCs), including embryonic stem cells (hESCs) and induced pluripotent stem cells (hiPSCs), are widely used in regenerative medicine as well as experimental model of normal and diseased organogenesis because of their nearly pluripotent differentiation potential into all cell lineages of all the three germ layers: endoderm, ectoderm and mesoderm germ layers. As we know, the differentiation fates of hPSCs are highly sensitive to local environmental factors that can modulate autocrine or paracrine signaling as well as mechanotransduction

processes mediated by physical cues. Cell micropatterning encompasses a set of technical strategies that have been developed to spatially organize the geometry and location of a cell population with the purpose to control the local cellular microenvironment, such as cell-cell and cell-matrix interactions. In the context of hPSCs, cell micropattern has been employed to gain significant insights into how geometric and chemical cues modulate cell fates decision and cell organization into early embryonic differentiation patterns. At the same time, 2D and 3D micropatterned hPSCs have been used to control the colony size of multicellular patterns, which in turn will influence differentiation decisions into three germ layers. In recent years, numerous cell micropattern methods have been established and developed, but only very few, such as microcontact printing, micro-well culture, photo-patterning, and micro-stencil, have been successfully applied to micropatterned hPSCs. The challenge with micropatterned hPSCs lies in their fragility and a most stringent requirement of the microenvironment which include the specific extracellular matrix (ECM) and growth conditions for cell adhesion and survival.

To date, the use of micropattern has shown that the self-organization of hESCs can be influenced by both geometric and chemical cues and generate several ring-like cell populations of different cell-fates, similar to those observed at gastrulation. These self-organizing patterns emerge as a consequence of the interaction between receptor localization and the production of the BMP-inhibitor NOGGIN. This system represents an *in vitro* model ideally suited to reveal the complex interaction between signaling, fate, and shape, as well as explore symmetric-breaking events and the self-organization properties of pluripotent stem cells. In response to specific factors, for example, dual-Smad inhibitor and WNT inhibitor, the micropatterned hESCs can be

differentiated into neural progenitors and primitive streak-like populations respectively. Interestingly, micropattern technology can also be applied to regenerative medicine, for example, the micropatterned organizer cells can be transplanted into the chicken embryo and subsequently induces a secondary axis which later initiates a neural fate in the host. As a conclusion, micropattern technology applied to the *in vitro* study can help us understand and reveal the secret of human embryonic development in various ways. In the meantime, more and more tissue engineering methods, include both 2-dimensional and 3-dimensional, will be established and combined with micropattern technology to develop a well-defined microenvironment, which will help people to generate more complex *in vitro* model.

Here in this thesis, we have established our micropattern technique by applying a fast and convenient surface functionalization procedure. By using different photomasks, we can make the micropatterns in various shapes, and sizes ranged from 50 μ m to 1000 μ m. Then a two-steps of surface Poly-L-lysine and ECM coating is necessary to generate the cell culture substrate. For the micropatterned cell culture, we tested and modified the protocol, and now we can harvest stable and well-formed cell colonies in culture for more than 8 days. With the purpose to investigate how the neural induction will be affected when under geometric confinement, we performed a micropatterned neural induction experiment by using a dual-Smad inhibitor neural induction protocol we have developed previously. In standard cell culture, it has been reported and demonstrated that the dual inhibitions of Smad signaling is highly efficient in the neural conversion of both hESCs and hiPSCs. The synergistic action of two inhibitors, SB431542 and NOGGIN, is sufficient to induce rapid (~6days) and complete (>80%) neural conversion under adherent culture conditions. Also in the same work, the future

date suggested that the cell density, which means the initial seeding density, influences the outcome of cell fates of neural induction significantly: High seeding density promoted cell fate presents central nervous system while low seeding density promoted neural crest cell fate. So, we hypothesis that, our micropatterned neural induction platform could be useful to generate different cell fates located individually along the colony axis, and this different allocation could be an *in vitro* model to mimic the patterning of ectoderm. As we expected, we found that in the micropatterned neural induction colony, cells self-organized themselves into 3 main populations from inner to outer. In the center of the colony, cells showed a relatively low density and expressed both AP-2 α and P75 (neural crest markers). On the contrary, cells outside expressed NESTIN, SOX1, and PAX6 (neural progenitor markers) and distributed as a ring structure between the center and border. This population presents a central nervous system cell fate. By comparing the cell density distributed form the center to the border, we found that the low density promotes neural crest cell fate in the center while high density promotes central nervous system cell fate outside, and the cells at the border had a more compact morphology and highly expressed only NESTIN, this cell population presents the surface ectoderm cell fate. General speaking, our micropatterned neural induction model can be used as an *in vitro* platform to mimic the human ectodermal patterning.

Later on, we extended our experimental model to establish an *in vitro* co-culture system with the purpose to investigate how the 3 germ layers communicate with each other during embryogenesis. During this period, a new hESCs-GFP cell line was established by Lentivirus infection, and it was used in the co-culture system to mark the cells of pre/sub seeded. To mimic the co-cultured mesodermal and endodermal

cells, we developed a meso-endoderm differentiation protocol under standard cell culture condition, and this meso-endoderm population can be seeded on top of the neuroectoderm cell population to simulate the *in vivo* architecture. Interestingly, we found that the vast majority subsequently seeded meso-endoderm cells can only adhere to the border of neuroectoderm fate, and they arranged into a ring-like structure close to PAX6+ cells. This adhesion property may be determined by the intrinsic differences between specific cell fates of ectoderm. Moreover, we also found that when the meso-endoderm cells were co-cultured with neuroectoderm, a new cell population can be generated from sub-seeded cells, and they all co-expressed PAX6 but are not exist in meso-endoderm cell culture. Additionally, with 3 days' co-culture, we surprisingly found some cells located above the PAX6+ neuroectoderm cells, and they showed a totally different cell morphology form other cell populations. It seems these cells were self-organized into a linear morphology and became the connecting cross-structure in this co-culture system. At all events, this co-culture system we developed has been demonstrated a robust platform in the study of interaction and communication between different germ layers.

To investigate the self-organization ability of subsequently seeded meso-endoderm, we next performed a micropatterned meso-endoderm cell culture. Briefly, we initiated meso-endoderm induction by applying the same protocol with 24 hours and then seeded this mixed population on the same micropatterns. To simulate the same condition, we repeated all the same seeding density, medium, and medium change for 3 days. Unexpectedly, the micropatterned meso-endoderm cells differentiated into distinct different cell populations with diverse morphologies. Generally, cells in the colony center showed a compact and multi-layered structure while cells at the border

differentiated into many linear structures. As a conclusion, it is evident that the meso-endoderm cell fate has intrinsic self-organization property under geometric confinement, but how the organization is affected when co-cultured with neuroectoderm are still not clear. From this perspective, we are facing the opportunity and challenging at the same time, and more research activities are necessary for the coming future.

CHAPTER 1

INTRODUCTION

1.1 MICROPATTERN TECHNOLOGY

1.1.1 Basis of micropattern technology

1.1.1.1 Cellular patterning

Micropattern technology is one kind of microfabrication technique which combined with material science and surface chemistry, has provided new approaches to explore and dissect, *in vitro*, the interaction between cells and tissue architecture (Ingber 2003, They 2010). Cellular behaviors such as cell adhesion, migration, proliferation, differentiation, and apoptosis are controlled by multiple surface cues remodeled during cell culture. The cell responses are regulated by intracellular signaling pathways that are originally triggered by the interactions between the transmembrane proteins and the engineered surface (Hynes 2002). For cellular patterning, the surface chemistry (Keselowsky, Collard et al. 2003) and spatial distribution (Rajagopalan, Marganski et al. 2004), as well as their conformation (Luk, Kato et al. 2000) have been demonstrated crucial to cell adhesion and other cellular behaviors. The ability to spatial and temporally control the surface geometry, the substrate stiffness, the location of cells, and the multiphase tissue architecture will provide new application into the study of cell-cell and cell-environment interactions (Whitesides, Ostuni et al. 2001, Engler, Griffin et al. 2004, Wong, Leach et al. 2004, McNulty, Klann et al. 2014).

In any cellular patterning, the ability to suppress the adhesion or interaction between the surface and the cells is vital to generate cellular patterning model. For example, the native molecules including agarose, mannitol, and albumin are used to reduce the adsorption of proteins at the surface (Luk, Kato et al. 2000, Nelson, Raghavan et al. 2003). Moreover, advances in material science and surface chemistry have made it

possible to synthesize the cell repellent surface that significantly reduces and eliminates the non-specific adhesion of protein, culture medium, and cells. Due to the limitation and stability, the most widely used synthetic materials have been developed in the recent 15 years (Ratner and Bryant 2004). PEG or poly (ethylene glycol) is one synthetic material developed in this period, and many different PEG surface-immobilization strategies have been successfully applied in cell-repellent surface functionalization (Pasche, De Paul et al. 2003, Wagner, Pasche et al. 2004, Pasche, Vörös et al. 2005). Another widely used PEG-chemistry-based approach relies on oligo-EG or PEG-modified alkanethiol assembled monolayers (SAMs) (Nuzzo and Allara 1983). This approach has the potential to link with other polymer architectures such as gels and polymeric SAMs (Bearinger, Castner et al. 1998, Barber, Golledge et al. 2003, Revzin, Tompkins et al. 2003). Polycationic surface, such as poly (L-lysine)-g-poly (ethylene glycol) has been proved as a useful system for patterning negatively charged surface (Kenausis, Vörös et al. 2000). The synthesized lipid bilayers constitute another class of cell or protein repellent surface (Andersson, Glasmästar et al. 2003). However, the practical limitation restricts this application only in aqueous solution. A smart polymer, which can switch between interactive and non-interactive properties in response to temperature, has been used to induce the surface transition between hydrophobic and hydrophilic (Langer and Tirrell 2004). This class of smart polymers is believed as one promising technique to achieve not only spatial control but also “on-demand” change of local surface properties.

The choice of protein or cell resistant chemistry is often decided by the type of substrate material used in the system. For example, PLL-g-PEG is highly versatile and can be used on different surfaces, while others require a particular substrate. However,

each method has its own strengths and weakness. We also note that, in different cell culture system, different protocols use serum-free or serum-depleted media. Some groups start cell seeding initiate with no serum and later add adequate amounts of serum. This will influence cell adhesion property and result in poor cell pattern quality. Moreover, cellular patterning varies with cell types. Some cells produce a large amount of ECM during cell culture and will ruin the surface repellent property while others are less delicate. In neural patterning, neurons are relatively easy to pattern since they need a specific adhesion protein, which can be geometrically patterned and emphasized from the background.

Base on the surface modification techniques introduced above, a myriad of cell micropattern technologies have been established. Considering the application perspectives, only some sorts of them, such as microcontact printing (Peerani, Rao et al. 2007, Bauwens, Peerani et al. 2008, Lee, Peerani et al. 2009), micro-well culture (Khademhosseini, Ferreira et al. 2006, Mohr, de Pablo et al. 2006), photopatterning (Warmflash, Sorre et al. 2014) and micro-stencils (Yao, Wang et al. 2014, Sahni, Yuan et al. 2016) have been successfully applied to hPSCs maintenance and differentiation. The challenge here lies in: 1) The vulnerability of hPSCs; 2) Cell type-specific ECM for cell adhesion; 3) Growth condition for cell adhesion and survival. For 2D micropatterned hPSCs culture, microcontact printing is the most widely used technique to pattern both tissue culture and glass substrate. The crucial evaluation criterion is whether the surface modification can build appropriate ECM patterns under desired geometric confinement while minimizing unwanted cell adhesion to the repellent surface.

1.1.1.2 Micropatterning steps

For all the micropattern technologies, they all involve 3 main basic steps : 1) Generation of patterned cell adhesion or repellent surface; 2) Cell seeding to adhere to the surface. In some applications, especially the hPSCs-derived culture model, additional ECM coating step is necessary to increase the adhesion ability of the cells; 3) Washing to remove cells outside the adhesion region and thus generate the patterns. It is crucial to modify the washing procedure, including both the time point and duration. For surface modification, microcontact printing technology is widely used to print cell adhesion islands on both tissue culture and the glass substrate, the ECM (e.g. Laminin or Matrigel) is known as the standard ink applied. In some other applications, to reduce and eliminate the cell adhesion potential outside patterns, one additional inactivation step is always introduced. Moreover, if a multiphase tissue co-culture with different cell types is to be patterned, 3 extra steps are required: 4) Re-activation of cell repellent surface; 5) Second cell population seeding; 6) Washing again to remove excess cells and thus to generate the patterned co-culture. The main steps are illustrated in Figure 1.1.

The practical application determines strategy selection, and the strength and weakness balance results in different cell adhesion properties. For example, in the so-called photopatterning or photolithography method, the patterning steps need to be modified in the different cell culture systems. Variety parameters are adjusted in different applications even when they use the same commercial micropatterned chip (CYTOOTM Chip) (Hurtado, Caballero et al. 2011, Tseng, Duchemin-Pelletier et al. 2012, Aragona, Panciera et al. 2013, Warmflash, Sorre et al. 2014).

In one application, Aryeh Warmflash and colleagues published a practical micropatterned stem cell culture protocol and concluded a troubleshooting table (Table 1.1) to explain the critical theory for cellular patterning which can solve most of the problem people will meet in their experiment. In this protocol, they succeeded in seeding hESCs on Poly-L-lysine/Matrigel or Laminin 521 (LN-521) matrix coated surface. Cells are maintained in growth medium and seeded as a single cell. To increase the cell proliferation, a small molecule Rock-inhibitor Y-27632 was used within 24 hours after seeding and then removed before the initiation of differentiation.

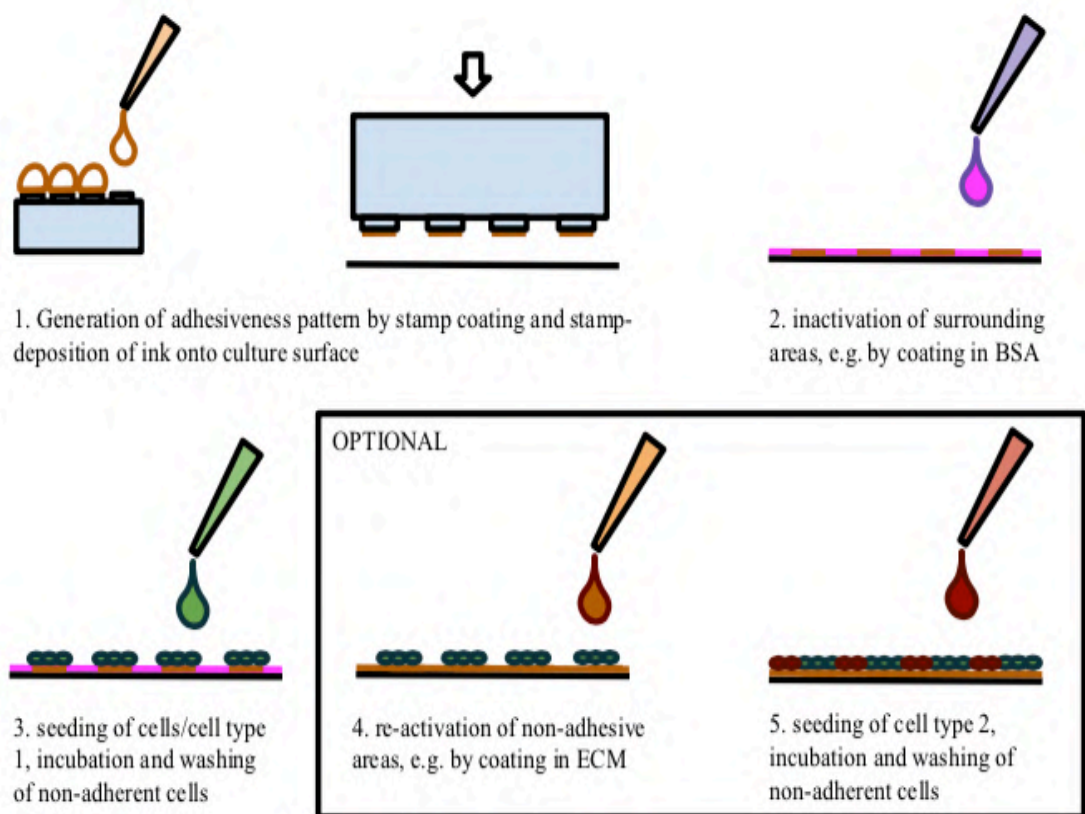


Figure 1.1: Overview of the main patterning steps (D'Arcangelo and McGuigan 2015).

Problem	Possible reason	Solution
Cell attach outside of the micropatterned colonies	Concentration of LN-521 is too high.	Find the working dilution of LN-521 for each batch; test in the range of 1:5 to 1:20
	Substrate dried up during coating or washing steps	Ensure that the chips are kept immersed in liquid
	Substrate was not washed properly	Properly wash the substrate according to the protocol
	Cells were left in Rock inhibitor too long	Ensure that the cells are exposed to Y-27632 for the appropriate time
	Too many cells were seeded	Adjust the number of cells used in Step 8 such that surface coverage of the colonies is 95-100% 2 h after seeding
Uneven seeding	Poor mixing	Gently mix the cells when seeding the chip, taking care not to swirl, as this will concentrate cells in the center of the dish
	Cells were not reduced to a single-cell suspension	Single cells are critical for accurate counting and seeding; if colonies are difficult to break up into single colonies, incubate them longer with Accutase
	Too many or too few cells were seeded	Adjust the number of cells used in Step 8 such that surface coverage of the colonies is 95-100% 2 h after seeding
Holes form in colonies upon removal of RI	Poor seeding	Adjust the number of cells used in Step 8 such that surface coverage of the colonies is 95-100% 2 h after seeding
Cells or colonies detach from the chip	Problems with coating	Try a higher concentration of LN-521 or a longer coating time
	Cell density is too high	Try lowering the cell concentration

Table 1.1: Troubleshooting table of micropatterned hESCs on the commercial CYTOO™ chip

(Deglincerti, Etoc et al. 2016).

1.1.1.3 Micropatterning scales

The micropattern techniques have opened access to achieve a controlled spatial cell patterning with diverse shapes and sizes, and also the patterned forms could range from single-cell patterns to tissue level patterns. Considering the complexity of the

micropatterning system, the spatial controlling has developed from 2D to 3D structures by engineering the microenvironment. Hence, here, I will discuss briefly the recent advantages in engineering the 3D stem cell culture.

As illustrated in Figure 1.2, we reviewed the general scales of micropatterns from single-cell to micro-sheets to confluent sheets.

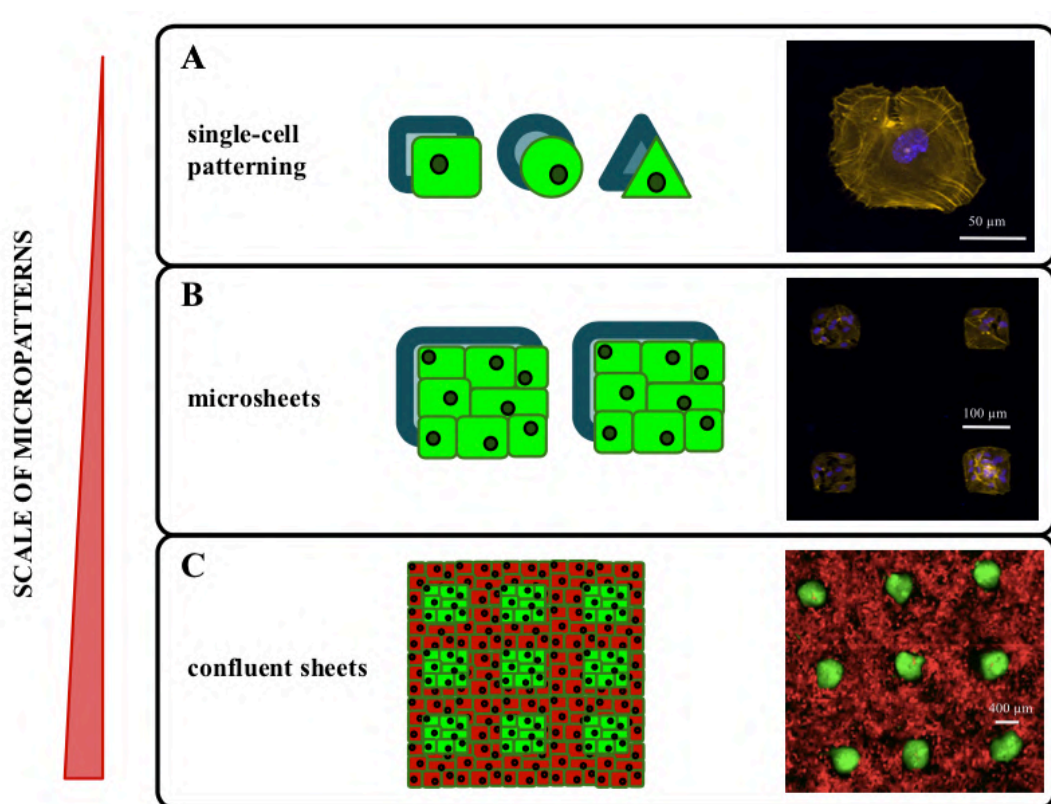


Figure 1.2: Micropatterning at different scales. (A) Schematic and micrograph of Single-cell patterns in different shapes for single-cell array. (B) Schematic and micrograph of micro-sheets. (C) Schematic and micrograph of confluent patterned co-culture cell culture. Underlying ECM pattern in dark blue, adhesion cells in green. In the co-culture system, the pre-seeded and sub-seeded cells in green and red respectively (D'Arcangelo and McGuigan 2015).

Micropatterns at single-cell level allow researchers to investigate the effects of geometric confinement on single-cell phenotype and behavior by limiting cell spread and migration only on restricted adhesion region (Azioune, Storch et al. 2009). In this micropatterning level, the crucial requirement is that the cell adhesion area must be less than the optimal spreading area. As a result, cells under this confinement will adjust themselves according to the patterns, and the cytoskeletal organization and the contractility information will be transmitted into the nucleus, and thus regulate the downstream gene expression. This approach is flexible to reveal the relationship between physic factors and cell behaviors, such as mechanotransduction (Wang, Ostuni et al. 2002), migration (Jiang, Bruzewicz et al. 2005), polarization (James, Goluch et al. 2008) and differentiation potential (Bédurier, Vieu et al. 2012).

At the multi-cellular scale, micropatterning has been used to pattern only one population of cells into individual islands, and thus generate a monolayer or multilayer cell culture system. Here, the geometry of the patterns is always controlled, but the shape of the individual cells within the sheet is not. When the cells are cultured in confluent cell sheets, the individual cell in different locations will have different shapes because of the local contractility, and this contractility and cell communication will influence the cell behaviors. Micropatterned hPSCs model is a research hotspot in recent 10 years. Cells inside the same micropattern with similar diameter can generate different cell populations in response to different differentiation factors, and these applications can enrich the experimental models for the study of embryogenesis by mimicking *in vivo* development processes such as germ-layer formation (Warmflash, Sorre et al. 2014), primitive streak formation (Martyn, Kanno et al. 2018), beating heart chamber (Ma, Wang et al. 2015) and singular neural rosette or neural tube

formation (Knight, Sha et al. 2015, Knight, Lundin et al. 2018, Xue, Sun et al. 2018). The representative works are reviewed in Figure 1.3.

Input	Differentiation/Induction protocol	Output	In vitro model
 hESCs	BMP4	(1)  Trophectoderm (CDX2) Endoderm (SOX17) Mesoderm (BRA) Ectoderm (SOX2)	Germ layers
	Wnt3A + ActinA	(2)  Endoderm (SOX17) Mesoderm (BRA)	Primitive streak formation in gastrulation
	Wnt activation/inhibition	(3)  Cardiomyocytes (cTnT) Myofibroblast (SM22)	Beating heart chambers
	Neural induction	(4)  Neural progenitors (PAX6) Neural rosette (N-Cadherin)	Neural tube

Figure 1.3: Examples of differentiation of hESCs on micropatterns. Upon stimulation with different signals, different tissues can be generated in a reproducible manner in order to study (1) Germ layers; (2) Primitive streak formation in gastrulation model; (3) Beating heart chamber; (4) Neural rosette formation (Metzger, Simunovic et al. 2018).

Compared with single- and multi-cellular micropatterning, the confluent sheet contains micro-sheet patterns of multiple cell populations or types, this micropatterning scale is also known as cell co-culture. Users can control the architecture of the interface between different cell layers or cell colony boundaries. This co-culture method contains detailed steps as introduced above. The ability to switch specified regions from non-adhesive to adhesive on demand is critical when generating multi-cell populations patterns. This approach is widely used to generate the *in vitro* models that could be used to answer questions about the *in vivo* mechanisms. Recently, this approach has been used to probe signaling mechanisms at

the tumor-stromal interface (Shen, Luk et al. 2014), and examine the establishment of tissue boundaries. Importantly, the stability of patterns generated using this method depends on the characteristic of the cell populations being patterned and their interactions, and pattern remodeling and degradation over time, due to cell re-organization within then sheet, is possible (Londono, Loureiro et al. 2014)

1.1.2 Soft lithography

“Soft lithography” is widely used to create chemical structures on surfaces to control the cell-substrate interactions (Xia and Whitesides 1998). The name of “soft” indicates that some elastomeric materials are used to create the patterned surface. Here, in this thesis, we will review the two related techniques of soft lithography technology: 1) Microcontact printing (μ CP); 2) Microfluidic patterning (μ FLP).

1.1.2.1 Microcontact printing

Microcontact printing technique was designed for creating patterns in microelectronic applications, but was soon adapted to cell culture. This method developed a lot and resulted in a lot of applications within a short time because of its simplicity, cost-effectiveness, and flexibility, with regards to both the choice of substrate and the material to be transferred during imprinting. The major processes of the microcontact printing technique include the design of master, the stamp production, the protein coating of the stamp, contact printing and cell adhesion. Silicon master and polydimethylsiloxane (PDMS) stamp are widely used in applications. In this section, the individual steps are discussed in more detail.

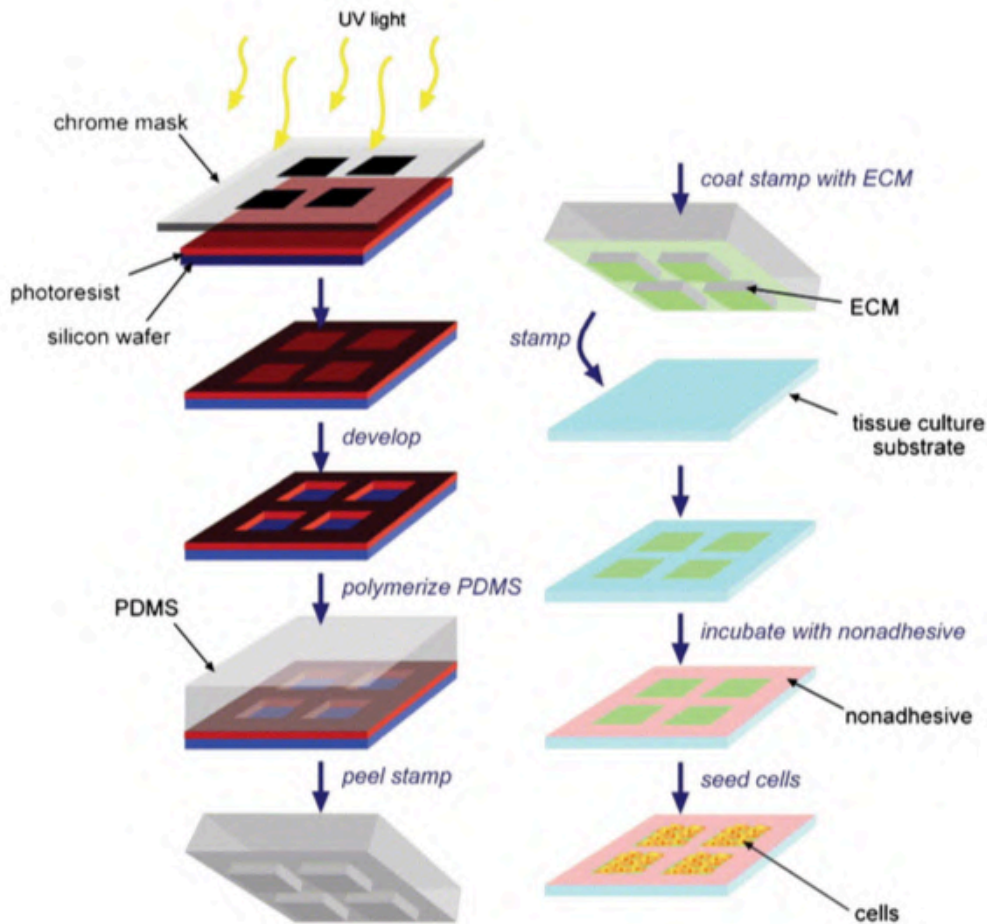


Figure 1.4: Schematic representation of the microcontact printing (Goubko and Cao 2009).

In the microcontact printing technique, the master used is traditionally designed and created by photolithography, mechanical scribing, or acoustic micromachining. The stamps are formed by casting the elastomer over this master, and the correct topological design of the stamp master is important to make all the printing reproduced (Bietsch and Michel 2000).

The stamp material used affects the printing quality a lot. In most of the applications, the PDMS is one of the widely-used materials in the past 20 years. Additionally, this material can also be applied after an oxygen/air plasma treatment, which can facilitate the absorption of the ink to the surface of the stamp. The surface functionalization of

the stamp and the material used can offer more possibilities for future applications. The ink or printing material is the molecular layer that will transfer from the stamp surface to the substrate surface during the printing procedure. Kaufmann and Ravoo reviewed the mostly used substrates and inks, especially the polymers in the microcontact printing technique (Kaufmann and Ravoo 2010). In nearly all the applications to pattern hPSCs, ECM or ECM related proteins are the only choices, and the stamping step is crucial to the aim of the cellular patterning. In the simplest case, the type of printed ECM molecules need to be matched to the cellular system. As an example, neurons were successfully patterned by using laminin or polypeptides containing cell binding sequences (Lauer, Klein et al. 2001).

Although in most of the published work, the printing is used to generate the cell adhesion region or the subsequent backfill to passivate the non-stamp areas, there are exceptions. For instance, the octadecyltrichlorosilane (OTS) are printed as cell repellent region onto silicon wafer to create no-adhesion areas, while a backfill with N1[3-(trimethoxysilyl) propyl] diethylenetriamine (DETA) is used to form the cell adhesion areas (John, Kam et al. 1997, Kam, Shain et al. 1999). The negative patterning technique is rare even now, but it still keeps the potential to open access in the opposite direction.

1.1.2.2 Microfluidic patterning

As demonstrated by numerous researches, scientists can benefit a lot by scaling down the fluidic processes to microscale. Microfluidic technology and microfluidic device are well developed during recent years. Here, I will introduce the theory and application of microfluidic and microfluidic patterning briefly. The practical

technology mentioned here refers mainly to the PDMS based microfluidics, which was developed as an extension of conventional soft lithography.

In PDMS microfluidic technology, the first essential feature of soft lithography is the possibility to obtain a sealed microfluidic device. Typically, the microchannels imprinted in the PDMS layer are closed with a glass slide (Figure 1.5). Alternatively, another PDMS slide can be used. The bonding between PDMS/Glass or PDMS/PDMS determines if we can get permanent or temporary fabrication. In device fabrication, a plasma treatment is necessary to increase the bonding force between two surfaces. Once the microchannels are properly sealed, fluids can be pumped at pressure as $\sim 350\text{kPa}$ without leaking.

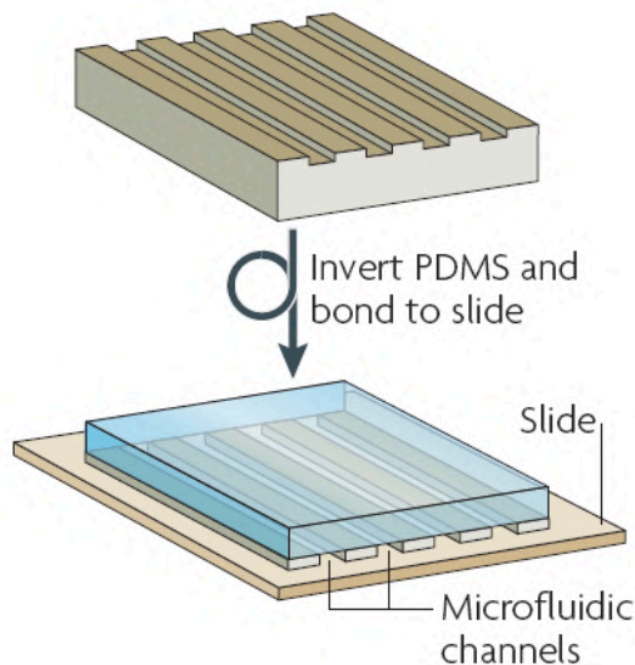


Figure 1.5: Fabrication of a microfluidic chip. A PDMS layer incorporating microchannels is sealed to a glass slide (Weibel, Diluzio et al. 2007).

In microfluidic patterning, the patterns generated on the wafer by applying photolithography result in specific microchannel networks (μ FN) that can be filled with the protein solution. As with microcontact printing, the elastomeric stamps such as the PDMS layer, which contain the channels modeled from the wafer can be removed from the template and then clamped to the substrate. Later, the coating or patterning solution can fill the channels as a series flow (Figure 1.6). PDMS layer then is removed before cell seeding. Additionally, cells can also be deposited together with the coating/patterning solution, rather than being added after a protein pattern is generated. This makes microfluidic micropatterning more flexible when a multi-component surface is needed.

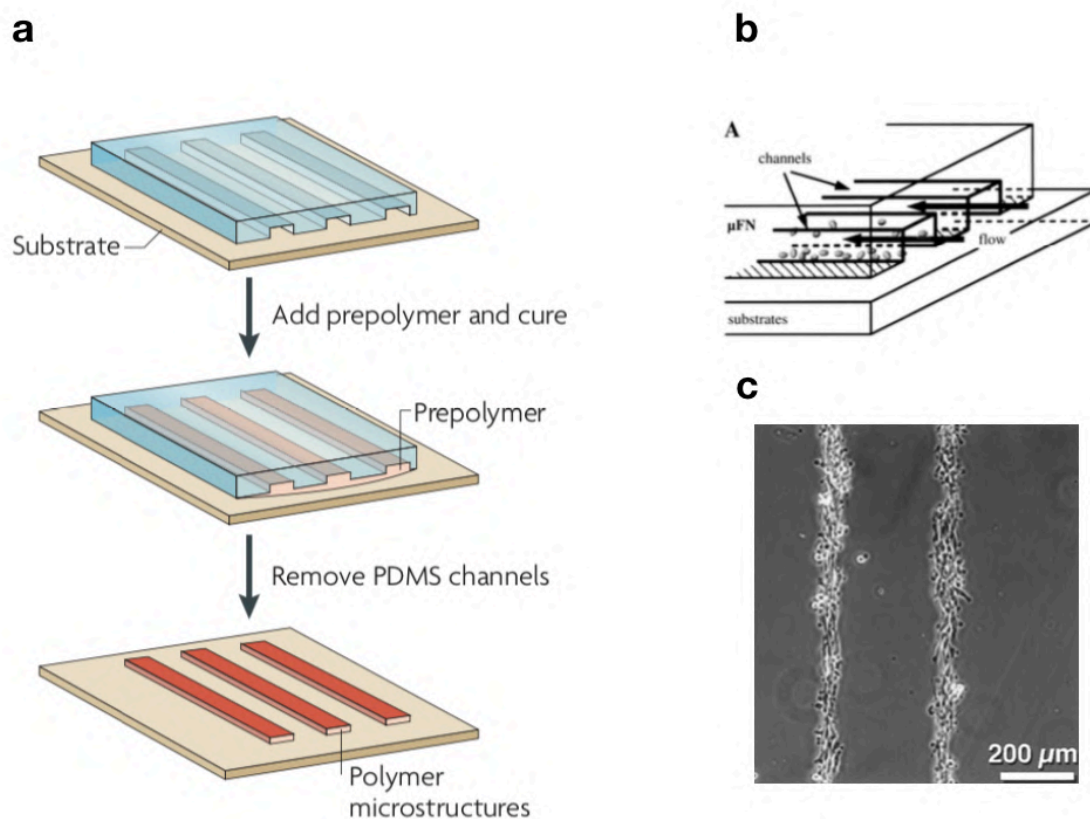


Figure 1.6: Schematic of microfluidic patterning. (a) Patterning strategies. (b) Flow solution inside the microfluidic network. (c) Strip-shaped cell patterns. Scare bar = 200 μ m.

1.1.2.3 Stencil patterning

Stencil technique was developed a lot for micropatterning by creating holes with diverse shapes and sizes through a thin sheet. PDMS is a suitable material for stencil patterning as it can adhere stable onto most flat dry surfaces. The general stencil fabrication is similar to PDMS stamps, but the PDMS prepolymer should not fully cover the model (wafer). After PDMS polymerized, peeling it off the model (wafer) produces the stencil. In cellular patterning, the through-holes are exposed to cell solution while the rest of the substrate is covered by the PDMS. Thus the patterns of the cells or cell colonies will be shaped when the PDMS is removed (Folch, Jo et al. 2000, Ostuni, Kane et al. 2000).

The most recent application of stencil patterning was published by Sahni and colleagues (Sahni, Yuan et al. 2016). In this protocol, they use a laser to cut and make through-hole on a thin (120-150 μm) sheet. Another 2mm thick PDMS sheet was laser-cut to produce the gasket. Later, these two components are glued together with uncured PDMS to assemble the stencil (Figure 1.7). In this method, the PDMS stencil can be plated onto tissue culture petri-dish, glass slides, or even another PDMS layer with different stiffness.

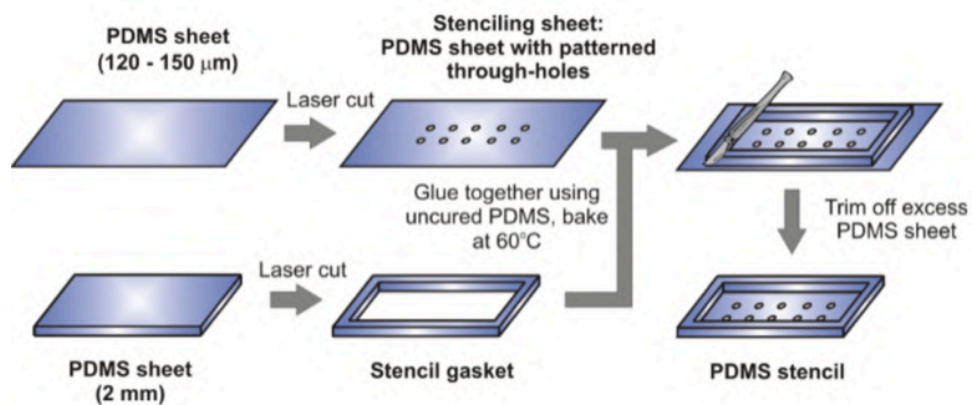


Figure 1.7: Schematic of PDMS stencil fabrication (Sahni, Yuan et al. 2016).

1.1.3 Patterning with photolithography

In the photolithography technique, the desired geometric features on the photomask are “printed” onto a substrate via UV activated reactions. Then the surface functionalization can be carried out in a “coating” or “etching” method (Figure 1.7). Here, the silicon wafer which is originally designed for the fabrication of semiconductor devices is widely used in PDMS based photolithography patterning. Photomasks to shape the substrate are generally designed with any computer-aided design (CAD) software and created by manufacturing companies.

As the first step, the UV sensitive photoresist (PR) layer is deposited or spin-coated onto the wafer. Later on, the substrate is incubated on the hot plate to make a hard layer of PR. The PR-coated wafer is then covered and in close contact with the photomask, as a consequence, the irradiated regions become soluble and are then removed by washing procedure (Figure 1.8, step 1 and 2). Upon development, the surface is compared to patterns with “windows” providing access to the substrate and a background protected with PR. At this point, any future processing steps will mainly be dictated by the type of chemical pattern one needs (Figure 1.7, route a or b).

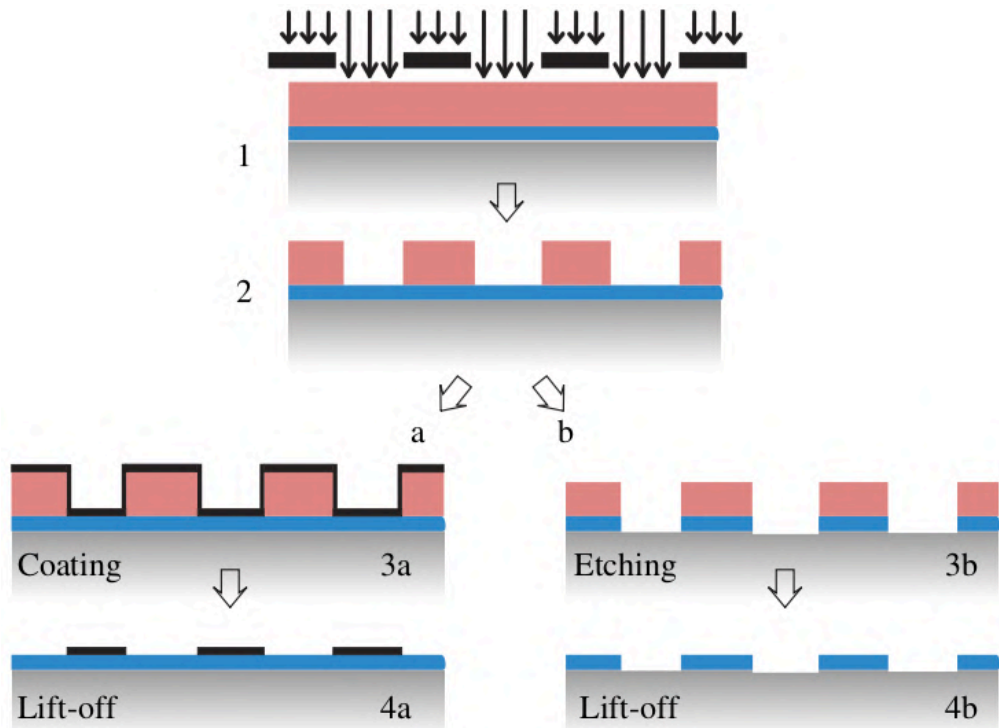


Figure 1.8: The photolithography process: (1) The spin-coating step with photoresist (PR) on the substrate. Top black lines present photomask in close contact with the surface. (2) Patterned surface after UV exposure. There are two alternative following routes: Route a, (3a) Deposit a thin layer of either metal or bioactive molecule and then (4a) lift-off in an organic solvent. Route b, (3b) Utilize the patterned PR as the mask for local dry etching of the metal layer and then (4b) lift-off the residual PR

(Falconnet, Csucs et al. 2006).

1.1.4 Conclusions

Micropattern technologies have improved rapidly with the breakthrough of several methodologies such as microcontact printing, microfluidic printing, and stencil patterning. They all benefit from the development of both “soft-lithography” and “photolithography” (Figure 1.9).

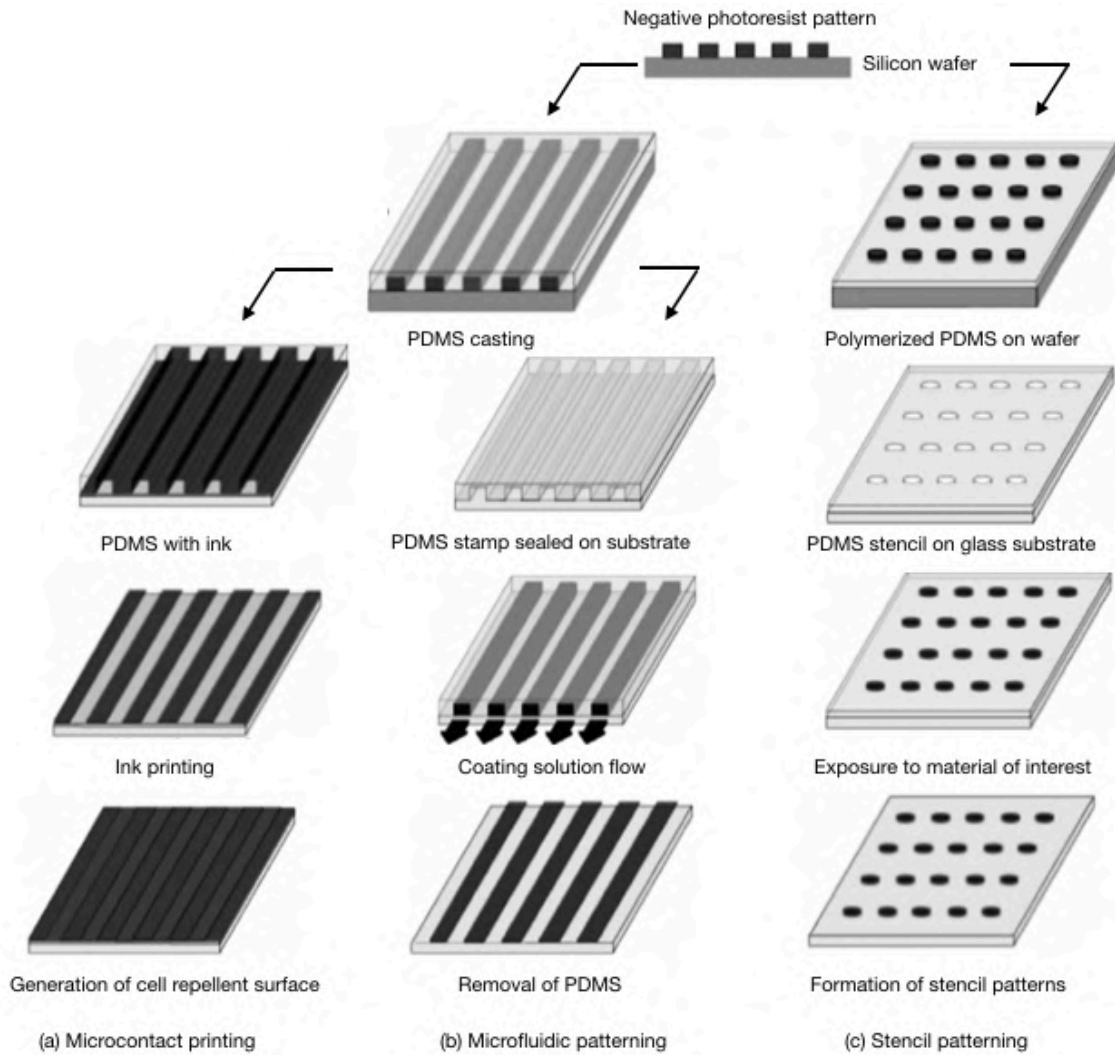


Figure 1.9: Schematic procedure for patterning using soft lithography. (a) Microcontact printing. (b) Microfluidic patterning. (c) Stencil patterning (Wen-Wen, Zhen-Ling et al. 2009).

A critical aspect of micropatterning is the choice of techniques for a proposed application. Both the advantages and disadvantages of different strategies make great sense. As the widely used micropattern technologies, the key advantages and disadvantages are concluded in Table 1.2 (D'Arcangelo and McGuigan 2015). Generally speaking, the single important point to consider is the scale and complexity of the interactions of patterning. Other factors such as laboratory conditions, costs of

experiments, the potential of modification, and throughput are effective but not crucial.

Technology	Patterning scale	Advantages	Limitations
Microcontact printing on SAMs	Single-cell Micro-sheets	Complex geometries possible Patterns stable for days Micron scale patterns feasible	Requires clean room access Requires surface coating Multi-steps procedure Fixed surface property Low throughput
Direct ECM microcontact printing	Single-cell Micro-sheets Confluent sheets	Complex geometries possible Switchable surface property Enables patterning at all scales	Requires clean room access Multi-steps procedure Low pattern stability Low throughput
Microfluidic patterning	Micro-sheets Confluent sheets	Complex geometries possible Cell patterning along channels	Requires clean room access Coasts Multi-steps procedure
Stencil patterning	Single-cell Confluent sheets	Patterns stable Cells can be released Co-culture possible Complex geometries possible	Handling issue Low throughput Fabrication is challenge

Table 1.2: Key advantages and limitations of different micropattern technologies (D'Arcangelo and McGuigan 2015).

On the one hand, physical methods (not introduced here) for cell trapping such as inkjet printing, optoelectronic, laser-based, and magnetic-based patterning provide the potential to apply in new technology for high-throughput analysis. However, with these methods, the side effects on cells such as cell damage can appear because of the thermal effects caused by external energy sources. On the other hand, the use of surface chemistry patterning procedure provides an efficient way to pattern the surface with different properties which allow high adhesion, specificity or the opposite effect such as repelling adhesion. Microcontact printing techniques have an extension even in the application in the microfluidic area. The patterned cellular *in vitro* models are now increasing and impacting on future studies of intracellular sensing. All these technological benefits have significant impacts on the development of biomedical

microdevices and high-throughput platforms to analyze human- or patient-derived samples automatically.

1.2 HUMAN EARLY EMBRYONIC DEVELOPMENT

Human embryonic development or human embryogenesis refers to the development procedures and formation of the organs and organ systems (Figure 1.10). It is characterized as several steps including cell division, cellular differentiation of the embryo that occurs during the early stages of development. In mammals, the embryogenesis starts from the fertilization. When fertilized, the ovum is referred to as a zygote, which is single at the very beginning. Embryonic development in the human covers the first 8 weeks of development and then begin the formation of a fetus from the ninth week. Generally speaking, human embryology is the study of this development during the first 8 weeks after fertilization (Vaillancourt and Lafond 2009).

In this chapter, we will focus on the stage of early human embryonic development, which contains the germinal stage, the gastrulation, and the neurulation. Additionally, the signaling pathways that play important and crucial roles during embryogenesis are well summarized here.

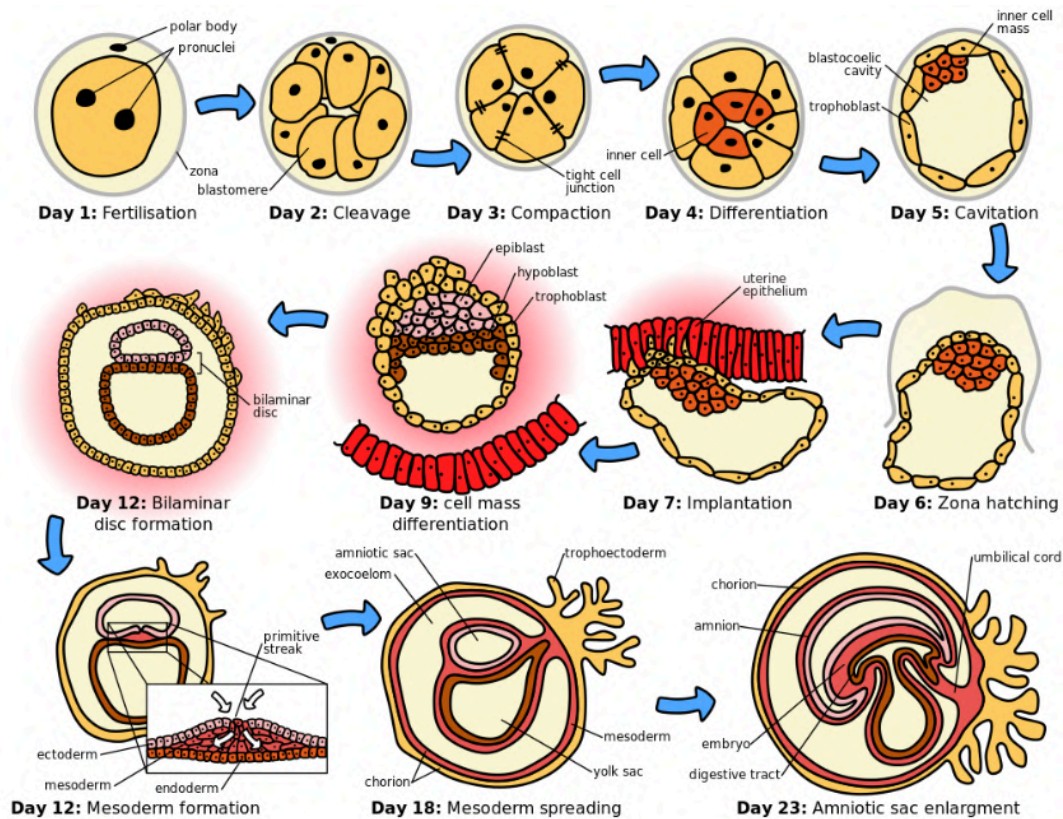


Figure 1.10: The initial stages of human embryonic development in the first 12 days.

1.2.1 Germinal stage

The germinal stage refers to the time from fertilization from the very beginning to the implantation is completed in the uterus. All the germinal stage lasts around 10 days and the cells proliferate and differentiate a lot. During this stage, the zygote begins to divide in a process called cleavage. A blastocyst is formed and implanted in the uterus. Embryogenesis then continues and goes into the next stage of gastrulation.

Fertilization happens when the sperm has successfully entered into the ovum and the two sets of the genetic materials carried by the gametes fuse together, resulting in the zygote (Asch, Simerly et al. 1995). Successful fertilization is ensured by three processes, which also act as a control of the species-specificity. The first is the

movement of the sperm towards the ovum. Secondly, there is an adhesive compatibility between the sperm and the egg. With the sperm attached to the ovum. The third process called the acrosomal reaction.

When the zygote divides through mitosis into 2 cells, the cell cleavage process starts (Figure 1.10 day1-3). The mitosis continues and then the first 2 cells divide into 4 cells, then into 8 cells and so on. Each division takes 12-24 hours. When the cell number reaches around 16, the solid sphere of cells within the zona pellucida is referred to as a morula. At this stage, the cells bind firmly and cellular differentiation occurs (Figure 1.10 day4).

Cleavage itself is the first stage in blastulation, the process of forming the blastocyst. Cells differentiation results in the outer trophoblast and inner cell mass layers. With further compaction, the trophoblasts become indistinguishable and this compaction serves to make the structure watertight, containing the fluidic that the cells will later secrete. The important cell source: inner cell mass, later differentiated into embryoblasts and polarize at one end. They close together and form gap junction, which facilitate cell communication. In this stage, the increase in the size of the blastocyst causes the zona hatching as a result (Figure 1.10 day5-6). Later the implantation happens, and the inner cell mass also develops at the same time (Figure 1.10 day 7-9). Interestingly, the inner cell mass is the most important cell source to produce the embryonic stem cells, which are pluripotent and can be differentiated into all the germ layers and thus give rise to all the somatic cells. The human pluripotent stem cells including human embryonic stem cells will be well-reviewed in the following chapter. The last procedure of the germinal stage is the formation of the embryonic disc. During

this period, the embryoblast forms the embryonic disc, which is a bilaminar disc with two individual layers: the upper layer is called the epiblast and the lower layer is called the hypoblast. They are also known as the primitive ectoderm and primitive endoderm. The epiblast is adjacent to the trophoblast and made of columnar cells while the hypoblast is close to the blastocyst cavity and made of cuboidal cells. The epiblast migrates and then form the amniotic cavity. At the same time, the hypoblast is pushed down and forms the yolk sac (Figure 1.10 day12-28).

1.2.2 Gastrulation

The gastrulation happens at week 3 after fertilization and characterized by the formation of the primitive streak. The process of gastrulation reorganizes the epiblast and hypoblast into a three-layer embryo and also gives the embryo a specific head-to-tail and front-to-back orientation (Figure 1.11).

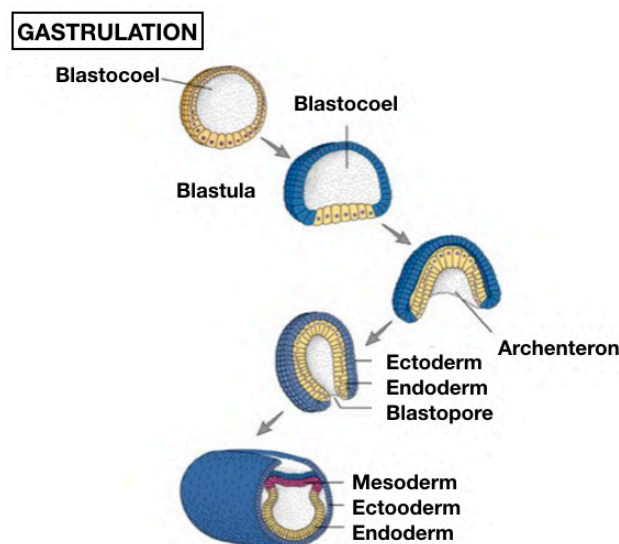


Figure 1.11: Human gastrulation.

A primitive node forms in front of the primitive streak which is known as the organizer

cells of the neurulation. A primitive pit later forms as a depression in the center of the primitive node. The node has arisen from epiblasts of the amniotic cavity floor, and later induce the formation of the neural plate, which serves as the basis of the nervous system. After the formation of the neural plate, cells from the epiblast region move down into the streak under the primitive pit and later form the mesoderm layer in the way called ingression. The transition happens in this stage is known as epithelial-mesenchymal transition (EMT) and the cells transmit from epithelial cells to the mesenchymal stem cells. In the meantime, the hypoblast is pushed out of the way and goes on to form the amnion.

The three germ layers formed in the gastrulation are ectoderm, mesoderm, and endoderm. They form an overlapped flat structure and share the communications between tissues and the environment. It is from these three germ layers that all the structure and organs of the body will be derived (Montero and Heisenberg 2004). The embryonic endoderm is formed by the invagination of epiblast cells that migrate to the hypoblast, while the mesoderm is formed by the cells migrate from the primitive ectoderm layer and develop between ectoderm and endoderm. The upper layer of ectoderm will give rise to the outermost layer of skin, central and peripheral nervous system, eyes, inner ear, and many connective tissues. The mesoderm will give rise to the heart and the beginning of the circulatory system as well as then bones, muscles, and kidneys. The inner layer of the endoderm will serve as the starting point for the development of the lungs, intestine, thyroid, pancreas, and bladder (Figure 1.12). Additionally, because of the great importance, the neural crest is sometimes considered as the fourth germ layer even it is derived from the ectoderm (Hall 2000).

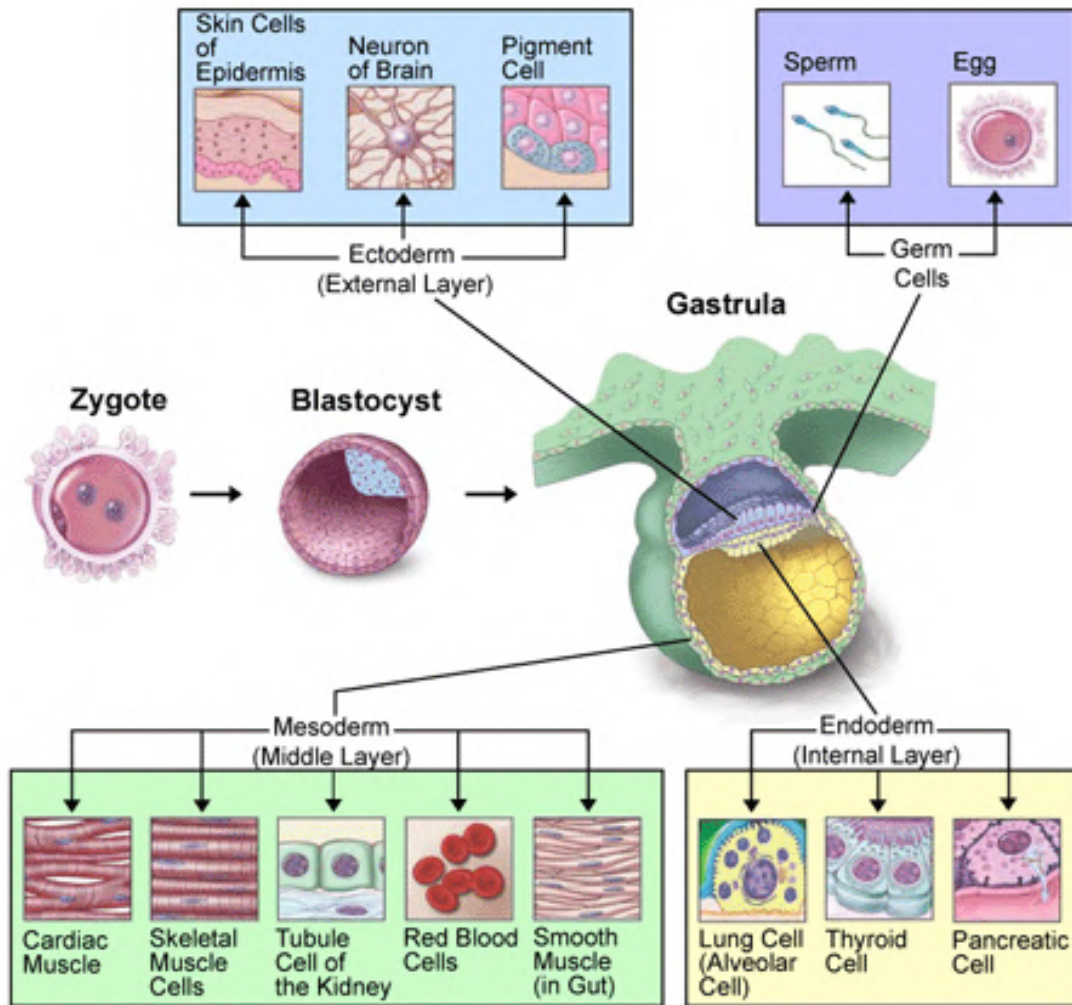


Figure 1.12: Organs derived from each germ layer.

1.2.3 Neurulation or neural tube formation

Following gastrulation, the ectoderm gives rise to epithelial and neural tissue, and the gastrula is now referred to as the neurula. The neural plate that has formed as a thickened plate from the ectoderm, which later start to fold and form the border and then form the structure called neural folds. Neurulation refers to this folding process whereby the neural plate (NP) will transfer into the neural tube. During the neural plate formation, the changes in cell shape and cell adhesion cause the edge fold and rise, meeting in the midline to form a tube. The cells at the tips of the neural folds come to lie between the neural tube and the overlying epidermis. These cells become the neural

crest (NC) cells, and both the epidermis and neural plate are capable of giving rise to the neural crest cells. The notochord is an essential structure during neurulation, and induce and regulate the proper location and formation of the neural tube (Fleming, Keynes et al. 2001, Stemple 2005). The detailed neurulation or neural tube formation stages are shown in Figure 1.13.

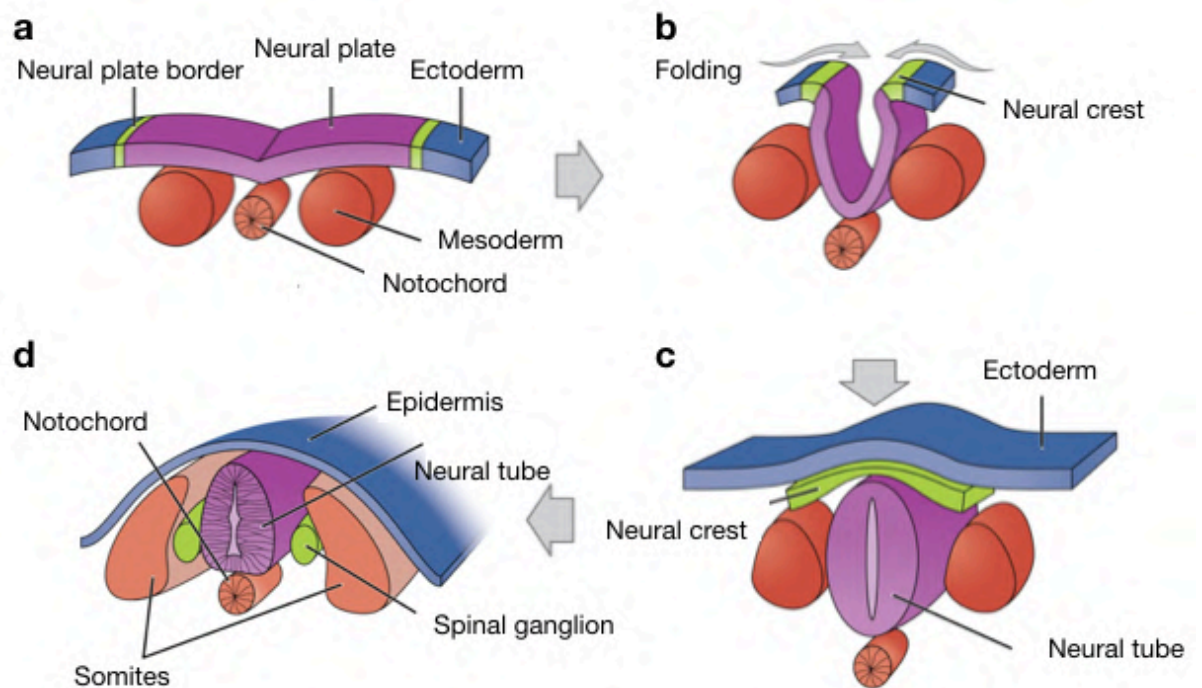


Figure 1.13: Neurulation (neural tube formation) processes. (a) Neuroectoderm tissues differentiate from the ectoderm and thicken into the neural plate. The neural plate border separates the ectoderm from the neural plate. (b) The neural plate bends dorsally, with the two ends eventually joining at the neural plate border, which are now referred to as the neural crest. (c) The closure of the neural tube disconnects the neural crest from the epidermis. Neural crest cells differentiate to form most of the peripheral nervous system (PNS). (d) The notochord degenerates and only persists as the nucleus pulposus of the intervertebral discs. Other mesoderm cells differentiate into the somites, the precursors of the axial skeleton and skeletal muscle.

1.2.4 Signaling pathways in human embryonic development

The formation of a complex multicellular structure contains different tissues and organs is one of the most fantastic parts of developmental biology. The embryogenesis is referred to as a dynamic process by the careful regulation of cellular behaviors including cell proliferation, migration, and form tissues which locate correctly. These processes depend on the cell lineage and also controlled by the deep mechanism known as the activation and inactivation of some critical signaling pathways. Here in this part, we will give a brief introduction of TGF- β , WNT, Hedgehog, and NOTCH signaling pathways (Sanz-Ezquerro, Münsterberg et al. 2017).

1.2.4.1 TGF- β signaling pathway

The transforming growth factor β (TGF- β) superfamily contains more than 30 different members which including TGF- β s, bone morphogenetic proteins (BMPs), growth and differentiation factors (GDFs), Activins, and Nodal. They regulate a variety of cellular activities, especially play an important role in stem cell differentiation. The ligand dimers bind and activate type I and II transmembrane receptors. The activation of the receptor will phosphorylate the downstream Smad mediator, which subsequently regulate the target gene expression (Figure 1.14).

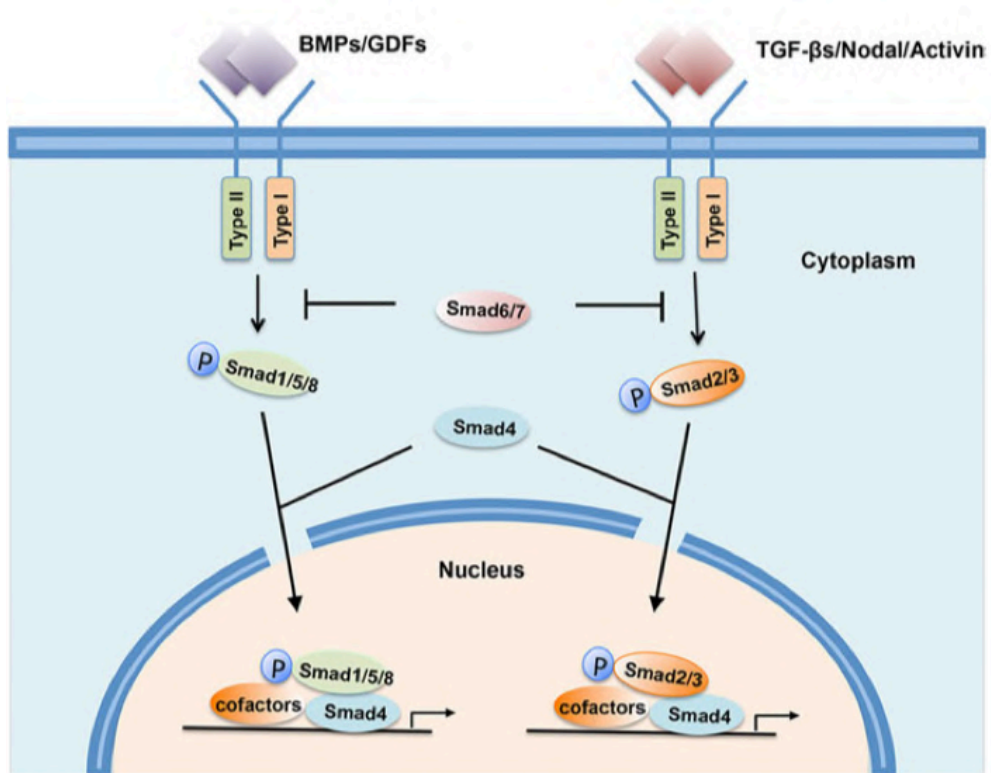


Figure 1.14: TGF- β superfamily signaling components. Extracellular signaling ligands bind to the receptor, and then R-Smad will be activated, which later forms the complex with Smad4.

Phosphorylated Smad complex then bind to the target gene and regulate the transcription (Liu, Peng et al. 2017).

The variables that influence the formation of the three germ layers are characterized by both extracellular and intracellular molecules and from the impact of different growth factors on the TGF- β signaling pathway. The antagonistic proteins, such as noggin, chordin, and follistatin, are demonstrated as important inhibitors in the neuroectoderm induction. Moreover, SB431542 was reported as an effective induction factor, and the combination of SB431542 with LDN193189 (BMP inhibitor) was widely used as a famous neural induction protocol called “dual-Smad inhibitor”.

1.2.4.2 WNT signaling pathway

The WNT signaling pathways are a group of signal transduction pathways that begin with proteins that pass signals into a cell through cell surface receptors. There are three WNT signaling pathways that have been characterized, and they are: 1) the canonical WNT pathway, 2) the non-canonical planar cell polarity pathway, and 3) the non-canonical WNT/Calcium pathway. Generally, the WNT signaling pathways are activated by the binding of WNT ligand-protein with a Frizzled receptor. The Dishevelled protein plays an important role here to pass the information through the membrane (Figure 1.15).

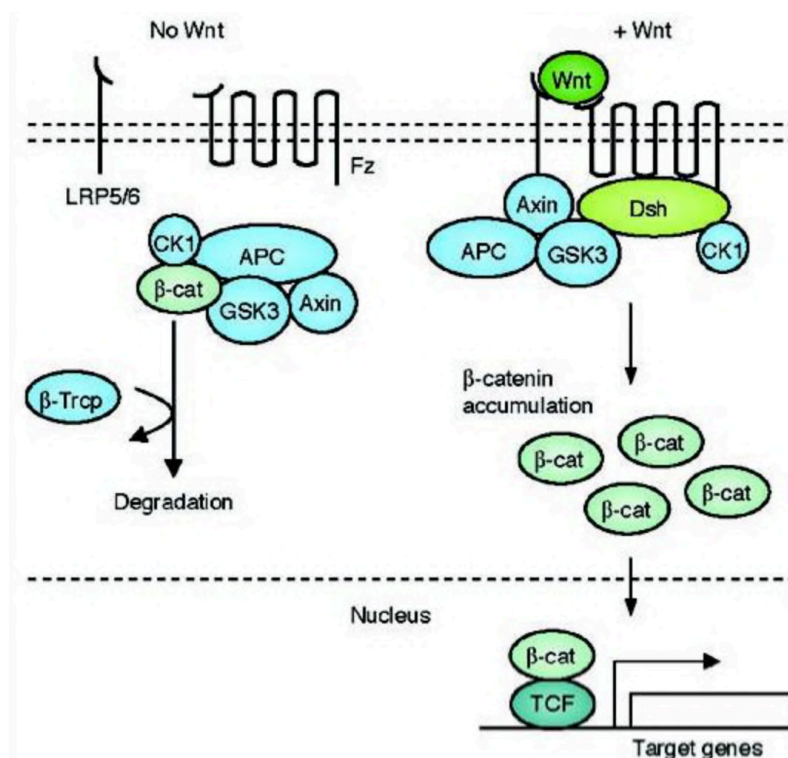


Figure 1.15: Canonical WNT signaling pathway. (Left) The inactivated condition with no WNT ligand. The complex (APC, Axin, GSK3, CK1, and β-catenin) locates in the cytosol. β-catenin phosphorylation by β-Trcp results in the degradation. (Right) The activated condition with WNT ligand. When WNT binds Fz and LRP5/6, the translocation of the Axin happens. The phosphorylation

of the destruction complex (Fz and LRP5/6) later binds to Axin to LRP5/6. The Dsh recruited in the complex becomes activated and inhibits the GSK3 activity, and this allows the β -catenin to accumulate and localize to the nucleus and subsequently regulate the cellular response (Komiya and Habas 2008).

The WNT signaling pathway plays an essential role in human embryonic development. The WNT ligands can bind to multiple receptors and regulate several downstream signaling cascades. The same signal can elicit diverse cellular responses in different cell populations and tissues. For instance, the canonical WNT signaling pathway regulates eye development and plays a crucial impact on tissue patterning (Fujimura 2016). The disorder of WNT cascade can lead to eye malformations and related diseases. Additionally, in the application of *in vitro* neural induction, WNT signaling pathways has demonstrated as an important factor for the neural crest formation (Dorsky, Moon et al. 1998).

1.2.4.3 Hedgehog signaling pathway

The hedgehog signaling is an important pathway in embryonic development that transmits information into the embryonic cells and then cause the proper cell differentiation (Arias and Stewart 2002). Different parts of the embryo have different concentrations of hedgehog proteins. Hedgehog signaling pathway, named from an intercellular molecule called hedgehog (Hh), which was found firstly in the genus *Drosophila*. In mammals, there are three hedgehog homologs they are Desert (DHH), Indian (IHH), and Sonic (SHH), of which the SHH is the best studied. The mechanism of the hedgehog signaling pathway is shown below in Figure 1.16.

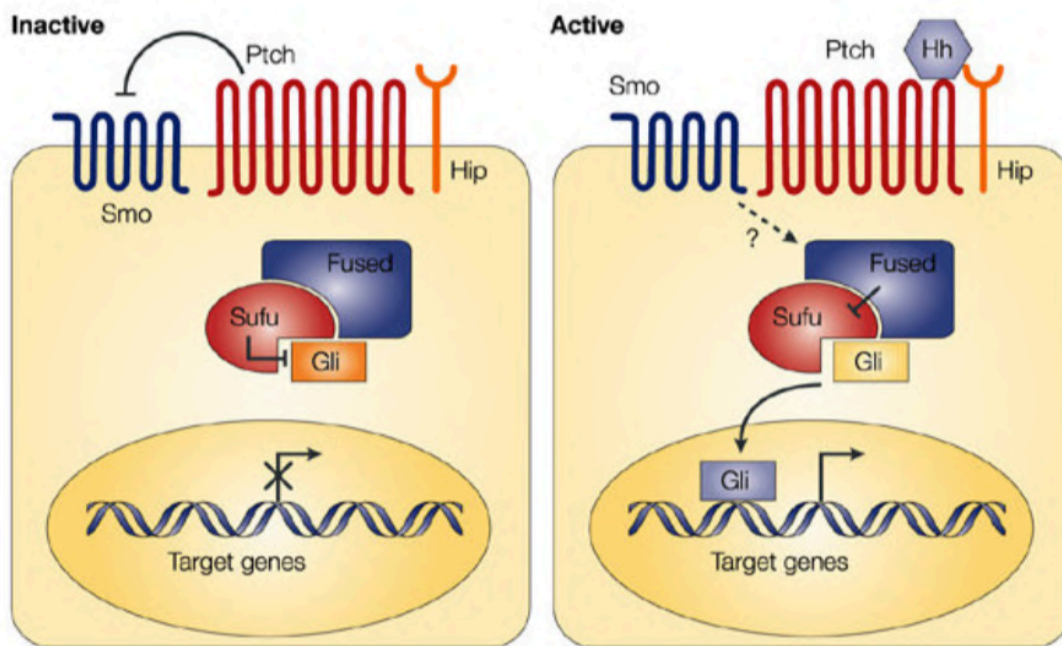


Figure 1.16: Hedgehog signaling pathway. (Left) Signaling pathway off when in the absence of ligand. The transmembrane protein receptor Patched (Ptch/Ptc) inhibits the activity of Smoothed (Smo). The Gli, referred to as the downstream signaling, is prevented from entering the nucleus because of the interaction between Fused and Sufu. The target gene is inactivated in this condition. (Right) Signaling pathway on through the binding between the receptor and ligand. The binding results in a de-repression of Smo and then activate the Gli in the cytoplasm. Nuclear Gli activates the target gene expression (di Magliano and Hebrok 2003).

Among all the hedgehog family, the sonic hedgehog signaling pathway during the development of the vertebrate limb is widely investigated and explained. The classic study on SHH was carried out in 1968 on a developing chicken embryo, and the found one diffusible factor (hedgehog protein) in the chicken limb determined the digit identity. The following study in the mammal model showed the same pattern during development. Additionally, Hedgehog signaling remains important in the adult body. Sonic hedgehog is demonstrated to promote adult stem cell proliferation from various

tissues, including primitive hematopoietic cells, mammary, and neural stem cells.

1.2.4.4 NOTCH signaling pathway

NOTCH signaling pathway is a highly conserved cell signaling presents in most animals (Artavanis-Tsakonas, Rand et al. 1999). The mechanism is shown in Figure 1.17. Mammals have four different Notch receptors (NOTCH1/2/3/4), and all the receptors are called single-pass transmembrane protein. In this signaling pathways, the NOTCH protein spans the cell membrane, which means the whole protein has part inside and part outside of the cells. After inactivation, the ligand proteins binding to the extracellular domain initiate the proteolytic cleavage and later on release the intracellular domain. The free domain enters into the nucleus and binds with MAML and CSL to regulate the downstream gene expression.

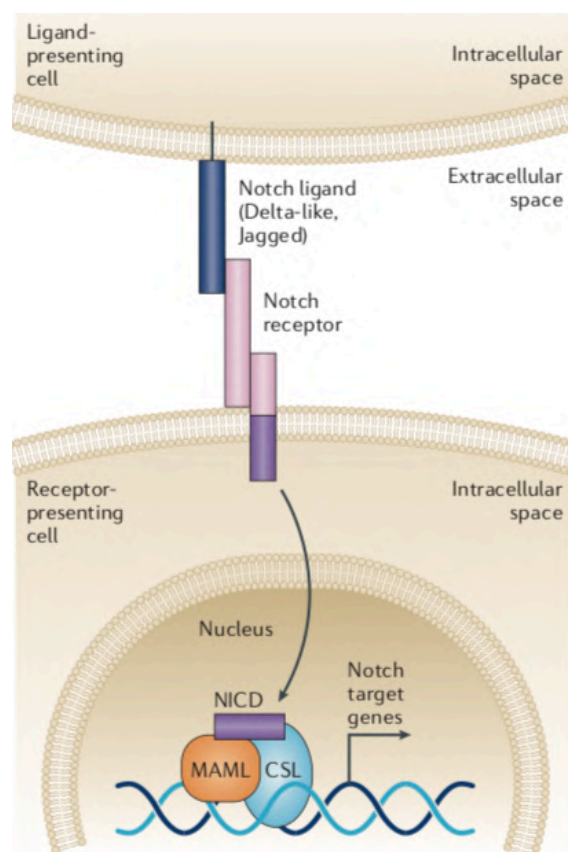


Figure 1.17: NOTCH signaling pathway. The ligand on the membrane of one cell induces a series of proteolytic cleavage events in a receptor on a coating cell. These events release the NOTCH intracellular domain (NICD), which later will translocate into the nucleus and activate the target gene expression.

The NOTCH signaling pathway is essential for cell-cell communication, which involves gene regulation that controls cell differentiation both in embryonic and adult life. In cancer biology, the NOTCH signaling pathway is also found dysregulated in some conditions, and the faulty NOTCH signaling is implicated in many diseases, such as T-cell acute lymphoblastic leukemia (T-ALL). Moreover, the Rex1 protein, which is critical in maintaining the proliferative state in mesenchymal stem cells (MSC), has the inhibitory effects on the expression of NOTCH, thus preventing the initiation of differentiation.

1.3 HUMAN PLURIPOTENT STEM CELLS

Human pluripotent stem cells (hPSCs), which include human embryonic stem cells (hESCs) and human induced pluripotent stem cells (hiPSCs), can be cultured while maintaining the potential to become nearly all cell types of somatic cells in human body (Thomson, Itskovitz-Eldor et al. 1998, Takahashi, Tanabe et al. 2007, Yu, Vodyanik et al. 2007). hESCs are the cell source derived from the early human embryo (ICM from the blastocyst) while hiPSCs are obtained by reprogramming of somatic cells (Figure 1.14). Now, the derivation and culture of these two pluripotent stem cells are widely used in the study of cell biology, development biology, regenerative medicine, *in vitro* disease modeling.

Human embryonic stem cells are derived from the inner cell mass of the cultured preimplantation human blastocyst. When the cells are maintained on the substrate of mouse embryonic fibroblast (MEF), the human embryonic stem cells can self-renew in culture and differentiate and become the three germ layers. Now more culture methods are developed even with not feeder layer and with a more chemical defined medium. These methods have enriched the application of hESCs and made the *in vitro* culture system more robust.

Different from hESCs, human induced pluripotent stem cells are the reprogrammed cells from the somatic cells. The main processes can be concluded as 1) Ectopic expression of transcription factors; 2) Ectopic expression of transcription factors together with small molecules; and 3) Ectopic expression of microRNA. These reprogramming factors can be divided into somatic cells via viral infection, transposon

transgenesis, plasmid transfection direct delivery of cell-permeable proteins or synthetic mRNA.

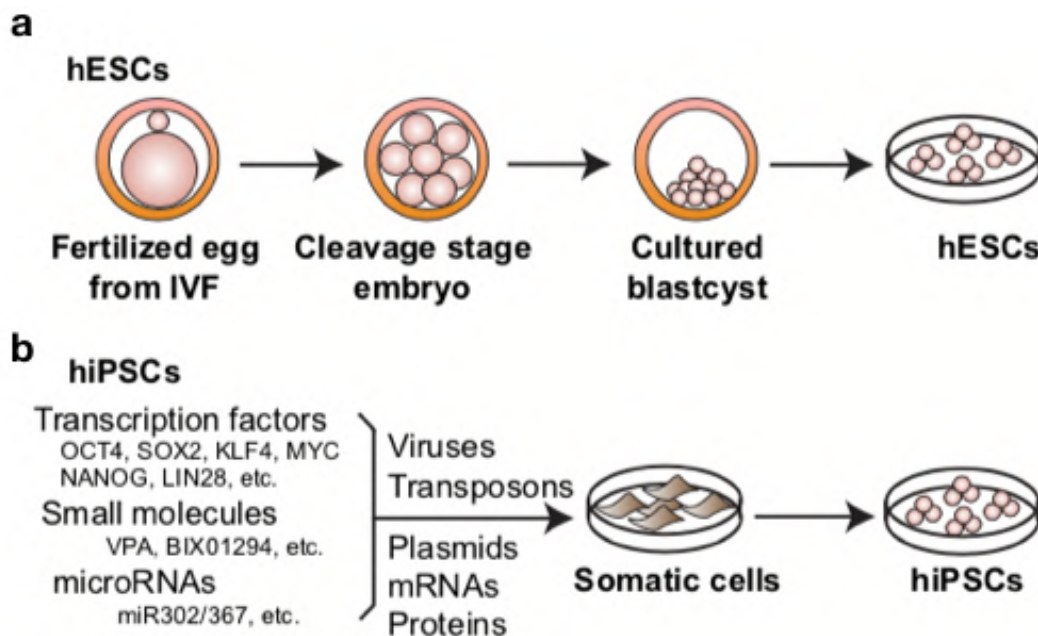


Figure 1.18: The derivation of hESCs and hiPSCs (Zhu and Huangfu 2013).

1.3.1 Human embryonic stem cells

Human embryonic stem cells are pluripotent stem cell lines derived from the ICM of the human blastocyst stage (Rathjen 2014). Even the pluripotency of the cells from ICM is transient, but they still have the potentiality to be maintained *in vitro* in an undifferentiated state. The first report about the *in vitro* culture of cell source from the embryo came out in the 1980s, and the finding of culture conditions which could be used to maintain the pluripotent characteristics of cells isolated from teratoma was reported in the same year (Barbaric and Harrison 2012). In 1981, two independent groups reported the mouse embryonic stem cells (mESCs) derived from a mouse embryo, but this condition was not easy to obtain with primate-derived cells. In the same year, another group announced that the cell survival rate could be increased

significantly when the derived embryonic stem cells are maintained in the medium conditioned by teratoma stem-cell line. In the year of 1998, a further breakthrough came out, James Thomson and colleagues described the first isolation of human embryonic stem cells from the human blastocyst, and they confirmed that this cell line could keep the pluripotent state in culture after more than 4-5 month (Thomson, Itskovitz-Eldor et al. 1998). Unfortunately, the discovery aroused an ethical argument about if the human embryos constitute human beings. To circumvent this problem, the research method called somatic-cell nuclear transfer was developed, and the human embryo after this process can be used to derive the hESCs.

However, in the last 10 years, lots of the researches were carried out and focused on the pluripotent property of these cells to differentiate into the three germ layers and later nearly all the somatic cells.

The main research topic in the study of stem cell biology focuses on the differentiation ability, which ensures the broad application potential of stem cells in therapeutic and clinical applications. As we know, human embryonic stem cells have the potential to differentiate into nearly all cell types of the human body. In vitro, they are able to generate an experimental model, the embryoid body (EB), which express markers present the generation of three germ layers. Generally, the hESCs have the ability to differentiate into neuron, skin, keratinocyte, pancreas and liver cells. Moreover, the studies in animal models show that the transplantation of ES-derived cell sources can be successfully used to treat a variety of chronic diseases. The potential applications reviewed here all underline the promising role of hESCs in tissue regeneration and modern medicine.

1.3.2 Human induced pluripotent stem cells

Induced pluripotent stem cells (iPSCs) are cell sources derived from the adult somatic cells with the typical molecular and functional properties of embryonic stem cells. The two main characteristics that associate iPSCs and ESCs are the self-renewal and possibility to give rise to form the three germ layers. The applications of hiPSCs offer a broad potential to the regenerative medicine, the possibility to work with autologous cell source in the replacement therapies, and with the patient-specific iPSCs for the in vitro disease modeling and drug discovery (Singh, Kalsan et al. 2015). The inventor of iPSCs, Shinya Yamanaka won the 2012 Nobel Prize because of this revolutionary discovery. In his research, he found that twenty-four genes are determined important for the pluripotency of stem cells. Surprisingly, when these genes were introduced into mouse fibroblast cells by retroviral vectors, only four of them were necessary to generate the iPSCs. As conclusion, OCT4, SOX2, KLF4, and C-MYC are collectively named as “OSKM FACTORS”, and now they are known as the transcription factor genes used for the adult cells reprogramming. In the same year, the factors, Oct3/4, Sox2, Nanog, and Lin28 also applied to induce human stem cells (Yu, Vodyanik et al. 2007). These results have inspired a lot of studies in the field of cell-type specification, such as neural stem cells, pancreatic B cells, melanocytes, stomach and liver cells. The timeline review of all the main reprogramming and induced pluripotency researches are showed here, in Figure 1.15.

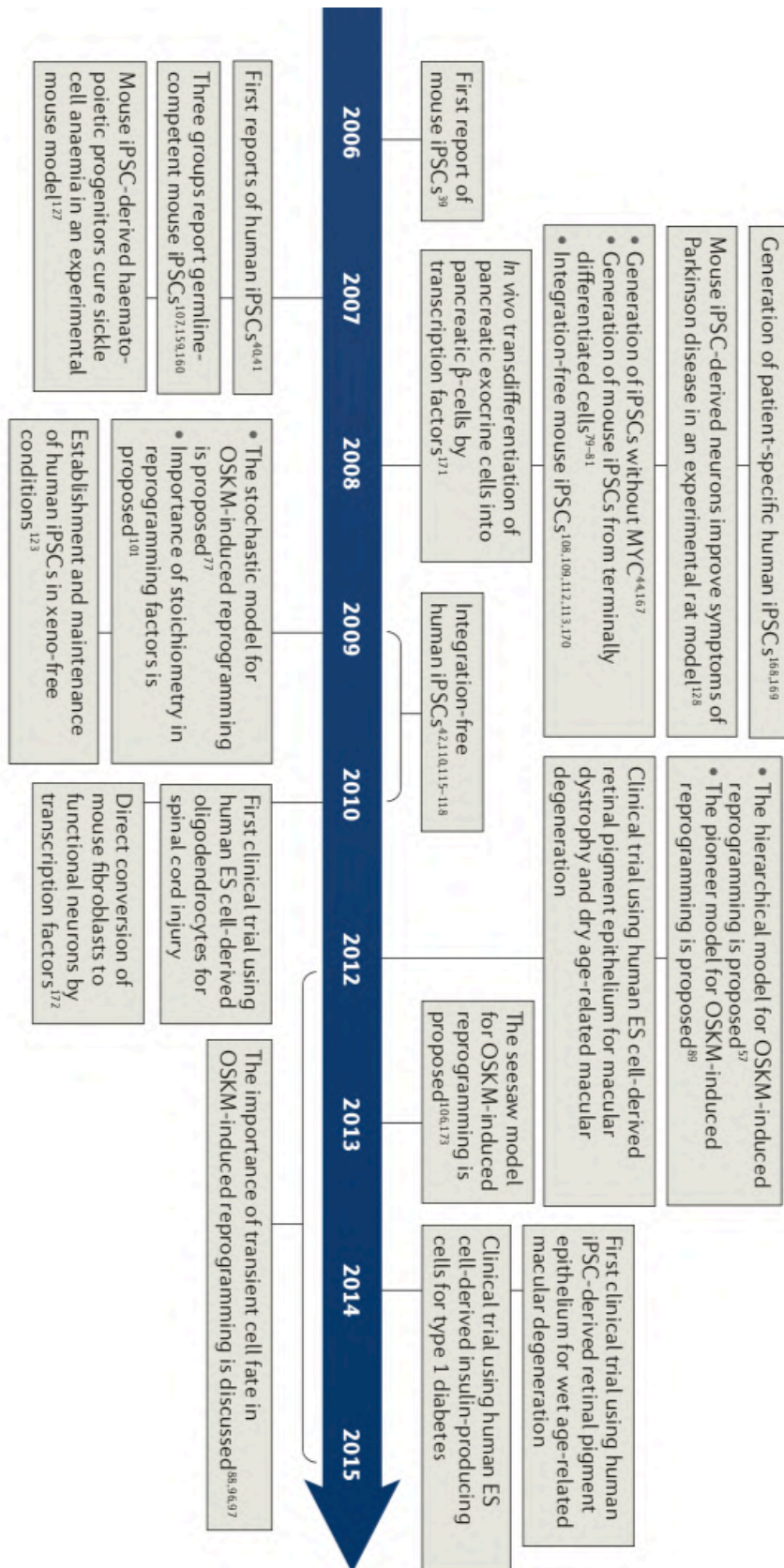


Figure 1.19: The timeline of human induced pluripotent stem cell researches from 2006 to 2015

(Takahashi and Yamanaka 2016).

Considering the early iPSCs based researches, the culture model frequently uncovered the cell-cell phenotypes in monogenic diseases, but the translation to tissue-level (include the microenvironment) and organ-level diseases has required the development of more complex, such as 3D or multicellular cell culture system. To reveal the key influence in human embryonic development, the experimental models, such as hiPSCs-derived organoids and human-rodent chimeras, are established during this period (Rowe and Daley 2019).

Following the isolation of hESCs, differentiation protocols typically modulated the morphogen exposure condition in 2D tissue culture or within the embryoid bodies. These culture conditions can only mimic the early patterning events and thus induce the cell differentiation into a target cell lineage (Kaufman, Hanson et al. 2001, Reubinoff, Itsykson et al. 2001, Zhang, Wernig et al. 2001). In a different level, the hiPSCs-derived organoids were developed, and this model was applied in generating a more complex *in vitro* model. Organoids are 3D multicellular aggregates derived from stem cells that differentiate and self-organize to recapitulate the structure and cell-cell interactions of the *in vivo* tissue. Furthermore, researchers have achieved particular regions of organs such as the brain and gastrointestinal tract. A brief introduction of the phenotypes modeled in 2D and 3D systems based on iPSCs is reviewed in table 1.3. The most widely used organoids are neural organoids, gastrointestinal organoids, liver organoids, lung organoids, and cardiac organoids. These 3D *in vitro* organoids are perfect models for disease modeling and drug discovery.

Tissue	2D phenotype	3D phenotype
Blood	Oligopotent differentiation	Multipotent differentiation and engraftment
Neural	Neural differentiation, gene expression and neurite formation	Cortical organization, regional specification, cell-cell interactions and neuronal migration
Cardiac	Action potential and contractility	Self-organization and integration of biophysical cues
Gastrointestinal	Differentiation	Bile secretion, motility and cell-cell interactions

Table 1.3: Phenotypes modelled in 2D and 3D system based on iPSCs (Rowe and Daley 2019).

1.4 ADVANCED TECHNOLOGIES TO GENERATE THE IN VITRO RESEARCH MODELS

Here in this part we list and talk about some advanced technologies used to generate the *in vitro* models that could be used to mimic the *in vivo* developmental events. Most of the cell source talked here are human embryonic stem cells (hESCs) and human induced pluripotent stem cells (hiPSCs), also here, the comparison between 2D and 3D has given form the aspect of *in vitro* neural models.

1.4.1 Neural subtype specification from human pluripotent stem cells

Human pluripotent stem cells (hPSCs) provide the possibility to mimic early neural development, which benefits the study of model pathological processes and help to develop new therapeutics. The human brain is built by a huge number of neurons and glial cells from ordered but intricate networks (Lake, Ai et al. 2016). The complexity of the brain network and how the brain cellular diversity arises to make the research task more difficult. In these 20 years, a new cell source, human pluripotent stem cells, came out and offered a model/platform to examine the specification of neural subtypes in humans. Neurons and glia undergo degenerative changes with age, but most of the neurological diseases showed cellular damage even at the early stage. In Parkinson's disease (PD) and Huntington's disease, the specific neurons have degenerated as the prime target. In spinal muscular atrophy (SMA) and amyotrophic lateral sclerosis (ALS), motor neurons are affected. Moreover, some researchers reported that the motor neuron is sensitive to pathological damage (Kanning, Kaplan et al. 2010). Based on the requirement of the experimental model in practical application, the desire for pure neural subtypes is aware presented. Lots of progresses have been made to

generate the functionally and regionally specialized subtypes of brain tissue by applying both human embryonic stem cells (hESCs) and human induced pluripotent stem cells (hiPSCs). Studies based on these neural subtype specification processes can help to reveal both the principles and strategies and in turn, manipulation of these principles in a well-defined way can also help to enrich pure cell subtypes for future research.

The development of the human nervous system starts from gastrulation after the formation of the neuroectoderm. The initiation of neural cell fate is also called neural induction. During this period, the “organized” cells move underneath ectoderm and release molecules that inhibit the BMP signaling pathway and/or activate the FGF pathway. The entire induction principle is concluded in Figure 1.20. Human PSCs are cultured in the induction medium and switched from the self-renewal state to the neural state, thus resulting in the neuroepithelia (NE) or neural stem cells (NSCs). In human embryogenesis, the neuroepithelia, which refer to the neural plate *in vivo*, fold and form the neural tube and later form the brain and spinal cord. This patterning is regulated by the distribution of morphogens in a temporarily and spatially way. It is the patterning procedure results in the neural progenitor specification. The progenitors can also give rise to different types of neurons and then glial cells according to the intrinsic time course. During the development, the glia cells will differentiate into astrocytes at subventricular zone (SVZ) while the strategy for hPSCs differentiation takes similar but 3 individual steps. 1) Cell specification to NE, 2) Expansion of NE until the onset of gliogenesis, and 3) Differentiation of glial progenitors into astrocytes. As talked above, the process of neural differentiation from hPSCs mirrors the *in vivo* development, and it thus offers a good model for the research of human neural

development.

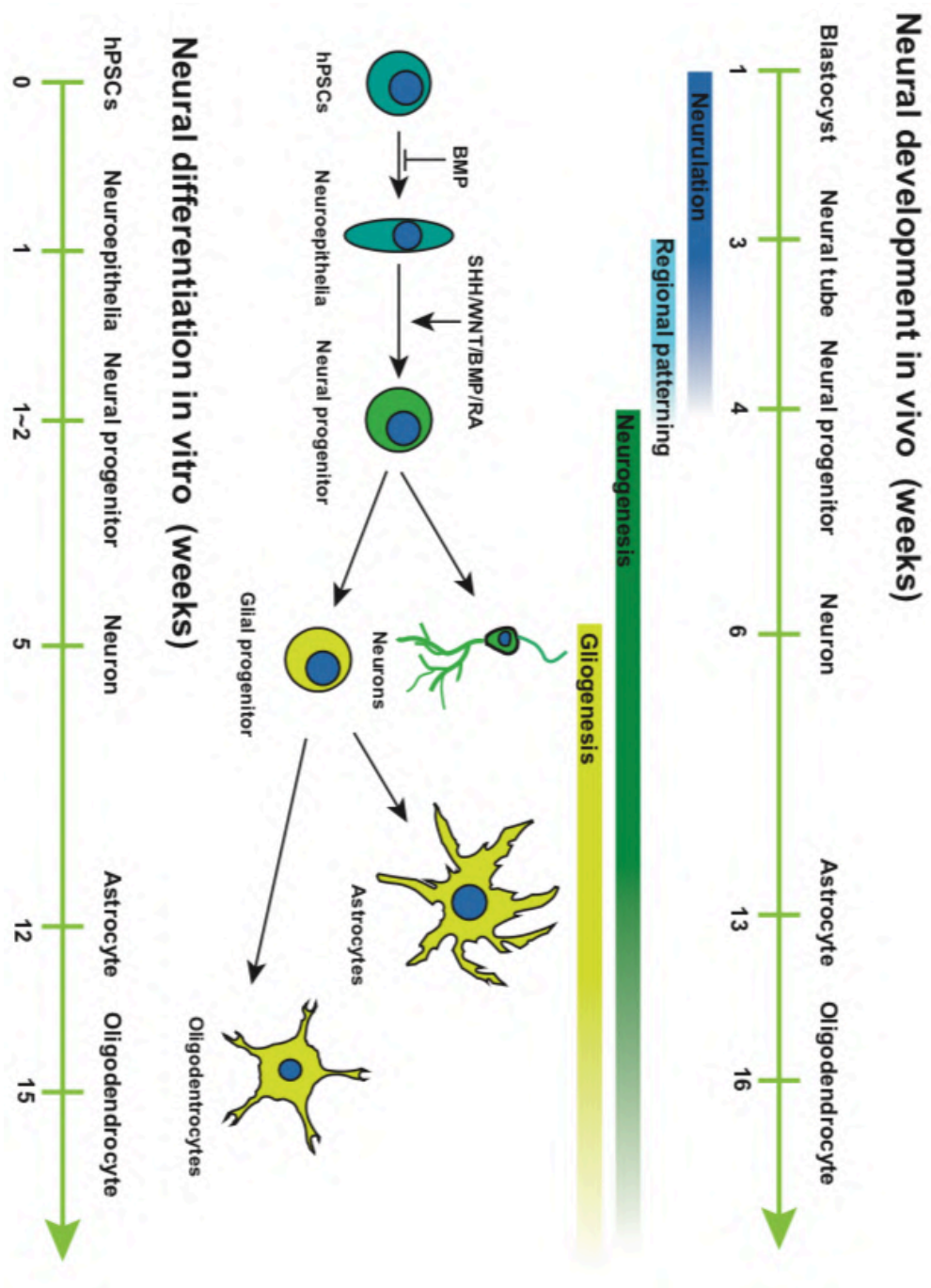


Figure 1.20: Parallel between in vitro differentiation and in vivo neural development (Tao and Zhang

2016).

1.4.2 3D *in vitro* models of central nervous system (CNS)

The study of neurons in 2D culture became possible in 1907 when Rose Harrison realized the *in vitro* nerve cell culture (Harrison, Greenman et al. 1907). There are lots of available approaches to modeling the CNS, and they can be broadly categorized as *in vivo*, *in vitro*, *ex vivo*, and *in silico*. *In vivo* methods use rodents as animal models to answer basic questions. *Ex vivo* method, in which the brain tissue dissected from the animal samples are usually utilized. 2D *in vitro* model is the most widely used experimental system, in which cells are normally cultured on a functionalized 2D surface. The traditional *in vitro* models have provided useful to study the information about the neural cell types and cell-cell interaction but not the interaction between cells and the microenvironment. This may limit the application of 2D models to mimic the real brain tissue in the body. Hence, we need to extend the *in vitro* model from 2D to 3D architecture with the aim to recapitulate the human brain tissue system outside of the body. During the past 15 years, the 3D *in vitro* neural model has developed a lot, it referred to as cell aggregates (Kato-Negishi, Morimoto et al. 2013), organoids (Lancaster, Renner et al. 2013) and neurospheres (Hogberg, Bressler et al. 2013, Urich, Patsch et al. 2013), in which the stem cells or different types of cells are cultured in high cell density with spontaneous self-organized 3D structure. The cell-cell contact and cell-environment communication ensure the reliability of the models. However, these models still suffer from high variability due to the stem cell clone-ability and commonly form necrotic cores due to the insufficient oxygen and nutrient diffusion, subsequently leading to size limitation. Refer to Table 1.4 for the comparison of current modeling approaches.

Type of model	Advantages	Disadvantages
<i>In vivo</i>	High complexity, particularly pathological modeling Suitable for long-term studies Anatomical relevance	Limited sample size Low reproducibility High volume and low control over variables Limited relevance to humans Difficult to quantify results
<i>Ex vivo</i> (Tissue slices)	Complexity architecture Capability for functional tests used on 2D slices Contains all cell type	Loss of tissue function Short-term culture only Low access to human tissue
<i>2D in vitro</i>	Inexpensive Highly reproducible Capable of high throughput studies Quantifiable Ability to carefully control environment conditions Numerous, well-characterized assays	Limited complexity Short-term culture only Limited cell sources available Limited insights into biological mechanisms and functions, particularly on the whole-tissue scale
<i>In silico</i>	Inexpensive High-throughput Highly quantitative Highly reproducible	Currently, impossible to model all parameters Input parameter limited to animal studies
<i>3D in vitro</i> (cell aggregate)	High throughput Quantifiable Simultaneous examination of biological mechanisms and functional outputs 3D	Typically, cannot have both high complexity and high variable control Formation of necrotic core
<i>3D in vitro</i> (tissue-engineered approaches)	Reproducible Controlled complexity Capability for long-term studies Quantifiable Capability to probe biological mechanisms Possibility for human and physical relevance	Lack of protocols and technology for functional evaluation Limited human cell sources Bioreactors required for longer cultures (≥ 6 months) Currently, limited to tissue scale (cannot model whole organ)

Table 1.4: Advantages and disadvantages of current approaches to modeling CNS (Hopkins, DeSimone et al. 2015).

The brain organoids are a new and transformative investigational tool for neuroscience research, especially CNS. As introduced before, the brain organoid is a spontaneously self-organized 3D architecture that typically derived from hPSCs. They are cell aggregates that more recapitulate the *in vivo* tissues and can also reproduce organ

function. The timeline of major events in the developmental milestone of brain organoids is reviewed in Figure 1.21 (Vaez Ghaemi, Co et al. 2019). The brain organoids are promising models for drug screening because of the stability of both genes and phenotype. Also, the reconstructed structure can be used to modulate and detect the distribution of drug leads, and reveal the mechanical response of the *in vivo* tissue to the chemical stimulation. Beyond the drug discovery, the use of brain organoids can be also extended to the study of early human development, especially uncover the deep mechanisms of neurodegenerative disease.

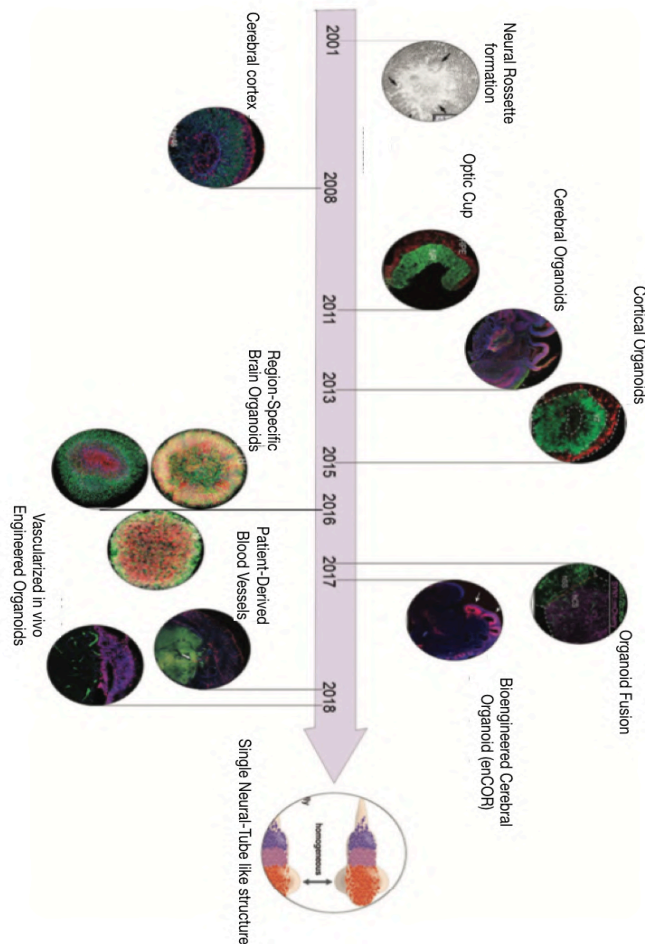


Figure 1.21: Timeline of major events in the technical development of brain organoids (Vaez Ghaemi, Co et al. 2019).

1.4.3 Organ-on-a-chip engineering

The organoids refer to the self-organized hPSCs *in vitro* and are capable of reproducing specific features of native tissues or organs. This *in vitro* model can give a perfect example to reveal the cell-cell and cell-environment communications that bridge the gap between animal studies and traditional 2D culture platform (Sasai 2013). At present, brain organoids are widely used in research, and the emerging organ-on-a-chip are biomimetic 3D systems stemmed from microfluidic technology. The mini-brain organs generated from the microfluidics can recreate the minimal functional units of the living brain to recapitulate the structural and physiological properties (van der Meer and van den Berg 2012, Bhatia and Ingber 2014).

The CNS comprises neurons, astrocytes, and glia. To mimic the communications between cells and extracellular matrix (ECM), the control of physical and chemical cues and the proper ratio of different cell types are important. In the microfluidic platform, various surface topological technologies are used to generate the desired ECM constructions, which control the substrate patterns or stiffness, thus mimic the *in vivo* situations. The surface modifications that use poly-L-lysine, poly-D-lysine, laminin, polyethylene glycol, and albumin have been widely used to control cell adhesion or growth (Wheeler and Brewer 2010). Additionally, the cell ratio also plays a crucial role in modeling diseases in a microfluidic device. For instance, in the microfluidic platform, we can generate both normal and abnormal status by controlling the ratio of co-cultured neurons and glia (Nam, Brewer et al. 2007). This has proved an essential technique to give diverse disease models for the research of degenerative disease and drug discovery.

In human brain tissue, the key factors of the microenvironment, which contain the fluid flow, extracellular matrix, and essential growth factors, determine the property of *in vivo* structure together with brain cells (Figure 1.22 a). In the 3D organogenesis of the human brain *in vitro*, the human brain organoids are usually formed from the hPSCs via a process in which the embryoid bodies (EBs) are formed (Figure 1.22 b). In a specific microfluidic chip, an individual culture channel is screened off by the surrounding micropillar and the EBs are embedded in Matrigel and cultured inside (Figure 1.22 c and d). The organoids formation within 33 days, and all the timeline and representative images are showed in Figure 1.22 e and f.

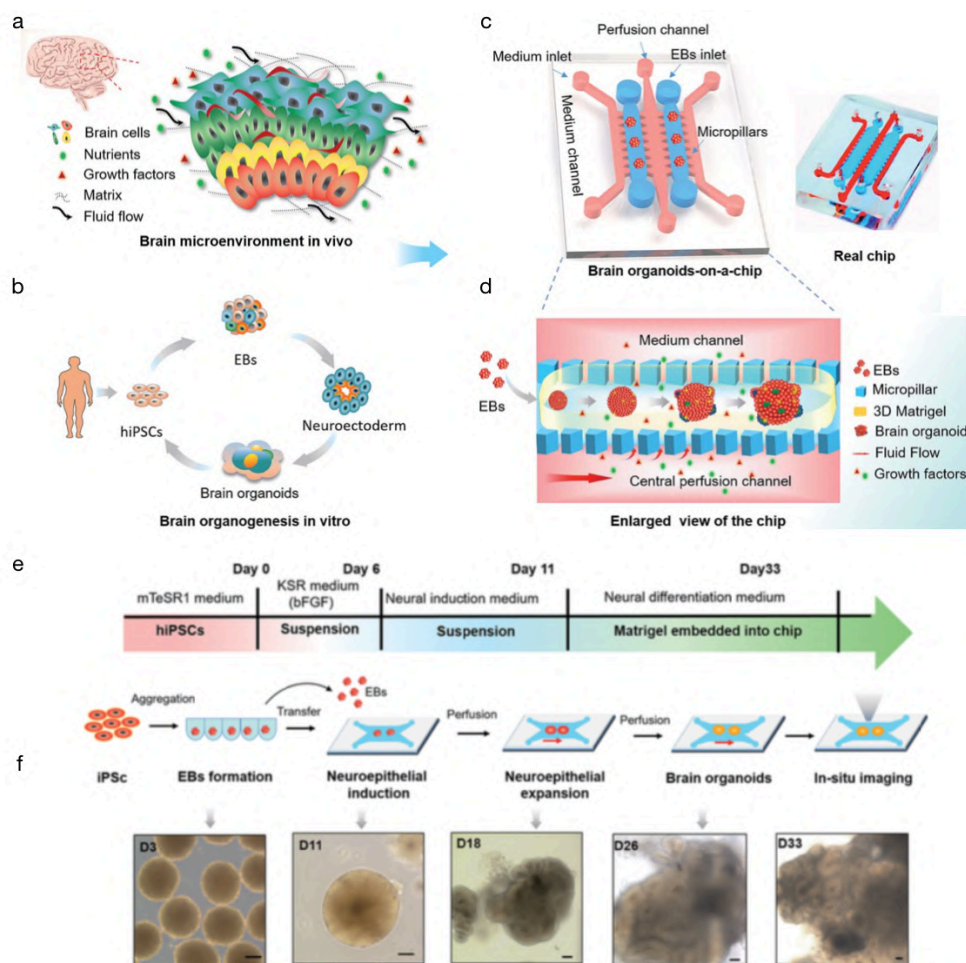


Figure 1.22: Formation of brain organoids on microfluidic platform. a) Microenvironment of brain tissue *in vivo*. b) Development process of organoids *in vitro*. c) Configuration of the microfluidic

device. d) Enlarged view of brain organoids generation on the chip. e) Timeline of organoids formation. f) Representative images of cell aggregate in different culture steps.

CHAPTER 2

MOTIVATION AND AIM

During gastrulation, the cells in the embryo are allocated into Endoderm, Mesoderm, and Ectoderm layers in an ordered spatiotemporal organization. It makes excellent sense to investigate the *in vitro* cell differentiation with the source of human pluripotent stem cells (hPSCs) to mimic the *in vivo* human cell-fate-decision. As reported in the recent year, the use of micropatterns has shown that self-organization of human embryonic stem cells (hESCs) can be influenced by both geometric and chemical cues and generate several ring-like cell populations of different cell-fates, similar to those observed at gastrulation (Warmflash, Sorre et al. 2014). These self-organizing patterns emerge as a consequence of the interaction between receptor localization and the production of the BMP-inhibitor NOGGIN. This system represents an *in vitro* model ideally suited to reveal the complex interaction between signaling (Chhabra., Liu. et al. 2018, Martyn, Kanno et al. 2018, Britton, Heemskerk et al. 2019, Manfrin, Tabata et al. 2019, Martyn, Brivanlou et al. 2019), fate (Knight, Lundin et al. 2018, Morgani, Metzger et al. 2018), and shape(Xue, Sun et al. 2018), as well as explore symmetric-breaking events (Manfrin, Tabata et al. 2019) and the self-organization properties (Warmflash, Sorre et al. 2014, Martyn, Kanno et al. 2018) of pluripotent stem cells. Considering the complexity of human embryogenesis, this model lack several morphological features of human early post-implantation structure like amnion and amniotic cavity. According to the requirement of the *in vitro* model, different 3D structures undergo spontaneous symmetric-breaking (Simunovic, Metzger et al. 2018) and self-organization (Harrison, Sozen et al. 2017) have been reported, the more complex developing in vitro model is attracting more and more attention. For example, the amniotic cavity can be formed by the addition of 3D ECM (extracellular matrix). Assemble extra-embryonic and embryonic stem cells in culture can be used to generate embryo-like structure (Harrison, Sozen et al. 2017). However,

in contrast to micropattern technology, the formation of these embryo-like structures or embryoids is currently less efficient and robust.

The first aim listed in this project is to develop and establish a robust 2D micropattern technology with the topologically controlled substrate. The micropatterned hPSCs are sufficient to differentiate into gastruloid, primitive streak (Martyn, Kanno et al. 2018), and neural rosette (Knight, Sha et al. 2015, Knight, Lundin et al. 2018, Xue, Sun et al. 2018). In the dual-Smad neural induction model, the destabilization of TGF- β and NANOG-mediated pluripotency network together with the promote neuralization of primitive ectoderm through BMP inhibitor induce the generation of CNS population at a high cell density while PNS population at a low density. Thus, we plan to investigate if we can establish a neurulation model with the specific cell population generated from primitive ectoderm, such as CNS, PNS, and neuroectoderm. This will give a promising model that can be used to study the process of neural plate folding.

After the establishment of the micropatterned neural induction model to generate different cell populations, those represent neural plate (CNS), neural plate border (PNS), and neuroectoderm (neuroepithelia, NE). We now have a great chance to expand future differentiation into co-culture layered patterns, which can be used to investigate the self-organization ability of the post-seeded germ layer (meso-endoderm) and how the pre-seeded/formed neuroectoderm lineages will affect the post-seeded germ layer. In this part, we set out two specific aims: 1) Establish a hESCs-GFP cell line to distinguish the co-cultured germ layers; 2) Develop the meso-endoderm population induction protocol, and characterize the specific markers for both mesoderm and endoderm.

CHAPTER 3

METHODS AND MATERIALS

3.1 METHODS

3.1.1 H9 human embryonic stem cells (H9 hESCs) culture

3.1.1.1 Medium preparation

StemMACS™ iPS-Brew XF (Miltenyi Biotech) medium was used to support feeder-free maintenance of H9 hESCs. Before StemMACS iPS-Brew XF can be used in cell culture, the two kit components need to be mixed according to the following protocol to obtain the complete medium.

1. Thaw StemMACS iPS-Brew XF, 50× Supplement at 2–8 °C prior to use.
2. To obtain the complete medium add 10 mL StemMACS iPS- Brew XF, 50× Supplement to 500 mL StemMACS iPS-Brew XF, Basal Medium. Mix well. The media is ready-to-use now. Use the complete medium within 2 weeks when stored at 2–8 °C.
3. For longer storage, prepare 50 mL aliquots and store at –20 °C for up to 2 months. Thaw aliquots of complete medium overnight at 2–8 °C. Once thawed, keep aliquots at 2–8 °C and use within 2 weeks.

3.1.1.2 Cell thawing

1. Warm the culture medium in a water bath to 37 °C.
2. Quickly transfer cryovials from liquid nitrogen to 37 °C water bath and leave until thawed. Swirl the vial to promote thawing.
3. Wipe the cryovials thoroughly with 70 % ethanol.
4. Slowly transfer the cell suspension from the cryovials to a 15 mL conical tube containing 5 mL warm medium.

5. Centrifuge cell suspension at 1,100 RPM for 5 minutes.
6. Remove most of the supernatant.
7. Gently resuspend cell pellet into small clusters (pipette not more than 3 times) in fresh medium supplemented with 10 μ M ROCK inhibitor (Miltenyi Biotech) and place in a 6-well tissue culture petri dish. Keep the cells in a 37 °C, 5 % CO² incubator for 24 hours with ROCK inhibitor, then withdraw ROCK inhibitor from the next day and change the medium every day.

3.1.1.3 Passaging

1. Coat 6-well plates with 0.5 % Matrigel (Corning) and incubate at room temperature for at least 2 hours. The coated plates can be used immediately after incubation or stored at 2–8 °C less than 1 month. Pre-warm the stored one at 37 °C for 15 minutes before using
2. Aspirate the cell culture supernatant.
3. Wash the cell layer 2 times with DPBS (GIBCO), 2 mL each wash.
4. Add 1 mL EDTA (GIBCO), gently rock the plate to distribute the solution evenly. Incubate at room temperature for 5 minutes.
5. Remove the suspension gently, not suck out cell clusters.
6. Add 1 mL of the culture medium and detach all the cells from the substrate. Collect in a 15 mL conical tube.
7. Wash the petri dish with 2 mL DPBS (GIBCO) for 2 times, collect the DPBS (GIBCO) in the same tube.
8. Centrifuge cell suspension at 1,100 RPM for 5 minutes.
9. Remove most of the supernatant.
10. Gently resuspend cell pellet into small clusters (pipette not more than 3 times) in

fresh medium and place in a 6-well tissue culture petri dish. Keep the cells in a 37 °C, 5 % CO₂ incubator.

11. After 48 hours, change the medium every day.

3.1.1.4 Single-cell splitting

1. Coat 6-well plates with 0.5 % Matrigel (Corning) and incubate at room temperature for at least 2 hours. The coated plates can be used immediately after incubation or stored at 2–8 °C less than 1 month. Pre-warm the stored one at 37 °C for 15 minutes before using
2. Aspirate cell medium, wash each well with 3 mL of DPBS (GIBCO).
3. Add 0.7 mL of 0.05% TrypLE™ Select (1X) per well. Gently rock the plate to ensure even distribution of the enzyme solution.
4. Incubate for 5 minutes at 37 °C.
5. Stop enzymatic reaction by adding 2 mL of Soybean Trypsin Inhibitor (0.5 mg/mL) per well.
6. Using a 5 mL serological pipette, dissociate to a single-cell suspension by carefully pipetting up and down.
7. Determine the cell number.
8. Depending on the cell line, seed 70,000–150,000 cells per well (7000–16,000 cells/cm²). Transfer the desired cell number into a 15 mL conical tube.
9. Centrifuge for 5 minutes at 1,100 RPM.
10. Aspirate supernatant.
11. Resuspend the cell pellet in culture medium supplemented with a small molecule ROCK inhibitor. Use 2 mL medium per well.
12. After 48 hours, replace media with fresh culture medium without ROCK inhibitor

and continue with daily media changes.

3.1.1.5 Cryopreservation

1. Ensure that the freezing jar is at room temperature and filled with isopropanol.
2. Prepare the freezing medium by adding DMSO (Sigma) to the culture medium to a final concentration of 10 % (v/v).
3. Label 2 mL cryogenic vials with name, date, passage number, and cell type.
4. Collect the cell clusters via normal cell passage.
5. Centrifuge at 1,100 for 5 minutes.
6. Remove the suspension and resuspend the pellet gently, pipette not more than 3 times.
7. Suspend cells in freezing medium.
8. Transfer the cells into pre-labeled cryovials.
9. Transfer cryovials into the freezing jar.
10. Leave the freezing jar at -80 °C overnight to allow a slow and reproducible decrease in temperature.
11. Transfer cryovials into liquid nitrogen for long term storage.

3.1.2 Lentiviral production and stable cell line generation

3.1.2.1 Lentivirus infection

Day 0: Keep the H9 hESCs in culture and when the cells are confluent, seed 0.5×10^6 cells as single-cell with culture medium (10 μ M ROCK inhibitor, Miltenyi Biotech) in one 6-well plate.

Day 1: prepare to work in virus infection room.

- a. Put on shoe covers, gloves and wear special protective suits before enter then

virus infection room.

- b. Wear another pair of gloves after enter the virus room.
- c. Prepare a 50 mL conical tube and add 5 mL bleach inside.
- d. Move the seeded cells in the incubator in the virus infection room.
- e. Lentivirus Puro-GFP (pLenti PGK GFP Puro, w509-5) was kept in -80 °C fridge, and each aliquot is 5 µL. Move the cells out of the incubator, switch the pipette to 10 µL and pipette 5 µL lentivirus Puro-GFP into cell culture medium. All tips and virus tube should be disposed into a conical tube containing bleach. Do not mix the virus many times and the virus as soon after thawing, plate virus on ice if the experiment lasts long.
- f. After the infection, clean the biological hood with bleach and water, then 70 % ethanol. Trash all reagents and outer gloves into a biological trash can, and the shoe covers trashed into a normal trash can inside the virus infection room. The inner gloves should be trashed outside the virus infection room.

Day 2: Check the cells and change the medium. If cells are cultured in StemMACS iPS-Brew, the medium change is not necessary.

Day 3: Remove the culture medium (dispose in a conical tube containing bleach) and replace with new medium supplemented with Puromycin (1.25 µg/mL, the stock is 10 mg/mL, stored at -20 °C, ThermoFisher Scientific).

Day 4: Replace with new medium supplemented with 1.25 µg/mL Puromycin. Medium removed and tips used to be trashed in a conical tube containing bleach.

Day 5: Replace with new medium supplemented with 1.25 µg/mL Puromycin. Medium removed and tips used to be trashed in a conical tube containing bleach.

Day 6: Replace with new medium supplemented with 1.25 µg/mL Puromycin. Medium removed and tips used to be trashed in a conical tube containing bleach. From

now on, cells can be moved out the virus infection room, check the GFP condition.

Day 7: Cells will most likely need to be split.

3.1.2.2 Single-cell picking and expansion

After virus infection, we can generate over 95 % GFP-positive cells in the established cell line. But after few passages, the number of GFP-positive cells is decreasing because of the expansion of GFP-negative clusters. To get a pure GFP cell line, we have three ways to solve the problem:

- 1) Cell sorting before every experiment.
- 2) Detach negative colony before passaging.
- 3) Single-cell picking and establish new cell line.

Cell sorting introduces contamination easily. Cell detachment result the loss of cell source and bring cell damage. Thus, here, we use single-cell picking and expansion to establish the GFP-positive hESCs cell line. The detailed procedure is:

1. Keep the lentivirus infected GFP-positive cells in culture in a normal 6-well plate.
Few of the cells lost the GFP signal.
2. Coat a 10 cm tissue culture petri dish with 0.5 % Matrigel (Corning), and seed 20,000 cells from step 1 as single-cell in the petri dish. The proper seeding density ensures the formation of the single-cell-derived colony.
3. Keep the medium the first 2 days, and then start to do medium change every day till the present of individual colonies.
4. When the colonies grow big enough and express homogeneous and pure GFP signal, pick the colony under the microscopy by using 100 μ L or 200 μ L tips. The selected colonies are seeded into Matrigel (Corning) coated 96-well plate.

5. Check the GFP condition every day, trash those with heterogeneous GFP signal.
6. Cell expansion and cryopreservation.

3.1.3 Micropatterned surface preparation

3.1.3.1 Glass slide functionalization

1. Treat the glass coverslips with plasma cleaner machine for 3 minutes (3×10^{-1} mbar) to oxidize the surface.
2. Prepare solution A: Add 10 μ L of 3-(trimethoxysilyl) propyl methacrylate (Fluka) into 950 μ L ethanol, then add 50 μ L acetic acid. Treat coverslip surface with 3-4 drops of solution A. After 3 minutes of incubation at room temperature, wash with ethanol for 3 times and then let it dry naturally.
3. Prepare photo-patterning solution, solution B: 8 % (w/v) acrylamide in 50mM HEPES. All solution should be stored in 4 °C, the stock of acrylamide (Sigma) is 40 % (w/v)
4. Prepare solution C: 20 mg/100 μ L IRGACURE2959 (Ciba) in methanol, then dilute 100 μ L solution C in 900 μ L solution B. Switch the light of chemical hood off.
5. Degas the mixed solution for 15 minutes, protect from light.
6. Plate square glass coverslips and drop 10 μ L mixed solution on top, cover the liquid drop with dried 12mm glass coverslips.
7. Switch on the UV lamp 5 minutes before using, expose the glass coverslips to UV with the interposition of photo-mask. The irradiation time is 40 seconds, the distance between glass coverslip and UV source is 5.5 cm.
8. Remove the square glass coverslip and wash the functionalized surface with deionized water for 2 times.

3.1.3.2 Sterilization and coating

1. Immerse the functionalized glass coverslips in 70 % ethanol, then move them into 24-well plate with the functionalized surface up and exposed to UV light under the biological hood for 20 minutes.
2. Keep the plate always under the biological hood after sterilization.
3. Rehydrate the glass coverslips with sterile water (milli-Q water) and then let them dry.
4. Coat the sterilized glass coverslips with 0.5 mL 50 µg/mL poly-L-lysine (Sigma, in milli-Q water) for each well, incubate at room temperature for 2 hours.
5. Wash 3 times with milli-Q water as gradient wash, add 1 mL and then move 1 mL. Wash 2 times with milli-Q water as complete wash, add 1 mL and then move all. Store them at 4 °C.
6. Cool DPBS at 4 °C.
7. Dilute Matrigel (Corning, the stock is 50 %) to 1 % in DMEM/F12 (Gibco) medium and introduce 0.5 mL into each well, keep Matrigel (Corning) always cold to avoid gelification. Introduce 0.5 mL Matrigel (Corning) into each well (24-well plate) and coat the plate overnight at 4 °C.
8. Wash 5 times with milli-Q water as gradient wash, add 1 mL and then move 1mL. Do not let the plate dry during Matrigel (Corning) coating, and leave the last wash solution inside. The coated glass coverslips can be stored at 4°C within 1-2 weeks. Keep the plate always on the ice during this two steps coating to avoid gelification.

3.1.4 Mouse embryonic fibroblast conditioned medium (MEF-CM) preparation

a. MEF culture

1. Prepare the MEF culture medium as: DMEM high glucose (GIBCO) 44.5 mL, FBS-Fetal Bovine Serum (GIBCO), 5 mL (10 %), β -Mercaptoethanol (GIBCO), 50 μ L (1:1000), NEAA 500 μ L (1:100). Filter the medium with 0.22 μ m filter (Millipore).
2. Coat the T175 flask with 12 mL 0.1 % Gelatin (0.1 g/100 mL in milli-Q water) for at least 1 hour at room temperature.

b. MEF inactivation

1. Prepare the inactivation medium as: MEF culture medium supplemented with Mitomycin (Sigma, 1:100)
2. The MEF are cultured in the culture medium, incubate cells with 5 mL Trypsin at 37 °C for 2 minutes. Split cells into single cells and then cryopreserve in vials as 1×10^6 cells each vial.

c. HUESM medium

Prepare the HUESM medium as: 38 mL of DMEM high glucose (GIBCO) with 10 mL of knockout serum replacement (GIBCO), 0.5 mL of GlutaMAX (GIBCO), 0.5 mL of NEAA (GIBCO), 0.1 mL of β -mercaptoethanol (GIBCO), and 1 ml of B27-Supplement (50 \times), minus vitamin A (GIBCO). 0.5 mL of Sodium pyruvate (Sigma). Then filter with 0.22 μ m filter (Millipore), and store it for up to 4 weeks at 4 °C.

d. MEF-CM medium

1. Coat the 10 cm² petri dish with 5 mL Gelatin (0.1 g/100 mL in milli-Q water) for at least 1 hour at room temperature.
2. Thaw 1 vial of MEF (1×10^6 cells) in the MEF culture medium and seed as 0.7×10^6 cells/dish and incubate at 37 °C overnight.

3. The next day, remove the medium and replace it with 10 mL HUESM medium, incubate overnight to condition the medium.
4. Harvest the medium every 24 hours for 10 days.
5. Collect all medium in the same flask and then filter with μm filter (Millipore), freeze the aliquots at $-80\text{ }^{\circ}\text{C}$ and store them for up to 6 months. When they are ready to use, add fresh bFGF at a concentration of 20 ng/ml.

3.1.5 Micropatterned cell culture

All experiments were performed with H9 hESCs cell line. For routine culture maintenance, H9 hESCs were cultured in StemMACSTM iPS-Brew XF (Miltenyi Biotech) pluripotent stem cell medium and passaged 1:5 to 1:10 every 3-5 days in clusters. The culture plate was coated with 0.5 % Matrigel (Corning) and incubated at room temperature for at least 2 hours. Coated plates were stored at $4\text{ }^{\circ}\text{C}$ and pre-warmed at $37\text{ }^{\circ}\text{C}$ for at least 15 minutes before used.

3.1.5.1 Micropatterned neural induction

Cells already suspended as single-cell in growth medium supplemented with $10\text{ }\mu\text{M}$ Rock-inhibitor Y27632 (Miltenyi Biotech) were seeded onto the glass coverslips (plated in 24-well petri dish) immediately after the removal of DPBS. Introduce 0.5×10^6 cells in 0.5 ml growth medium) to each well. After 3 hours, the medium was replaced with new growth medium without Rock-inhibitor Y27632 (Miltenyi Biotech), two times of pre-warmed DPBS ($37\text{ }^{\circ}\text{C}$) wash procedure was necessary to remove cells outside micropatterns. 3 hours later, neural induction was initiated by replacing the medium to neural induction medium contains sufficient small molecular inhibitors. The method showed in this part is a general neural induction method. When applied

MEF-CM differentiation medium in micropatterned neural induction, H9 hESCs cultured in growth medium was passaged in clusters with half StemMACS™ iPS-Brew XF (Miltenyi Biotech) medium and half MEF-CM medium, the next day after cell passage, medium was replaced to MEF-CM medium supplemented with 20 ng/ml bFGF and then changed medium every day till 60-80% confluent before cell seeding onto micropatterns. Cells were seeded as single-cell in the same cell density in MEF-CM (20 ng/ml bFGF) supplemented with 10μM Rock-inhibitor Y27632. Rock-inhibitor Y27632 was removed as described in the general method. For neural induction, MEF-CM medium supplemented with the same combination of small molecular inhibitors (without bFGF) was changed every day for at least five days.

3.1.5.2 Standard and micropatterned meso-endoderm induction

Meso-endoderm induction medium comprised RPMI 1640 (GIBCO), 2% B27-ins (GIBCO) and 1× MEM NEAA (GIBCO), once initiate meso-endoderm induction, the basal medium was supplemented with 100ng/ml Activin A (R&D), 10ng/ml BMP4 (R&D), 20ng/ml bFGF (PeproTech) and 3μM CHIR99021 (Miltenyi Biotech).

Meso-endoderm differentiation was induced in 6-well petri dish. H9 hESCs were seeded (1:5 passage) onto 2.5 % matrigel coated plate as clusters. Cells reached 30-50 % confluency the next day, and then the meso-endoderm induction was initiated by replacing medium to induction medium. 24 hours later, cells were differentiated to meso-endoderm cell fate. One day more culture time will lead the cells differentiated to more endoderm cell fate.

For the micropatterned meso-endoderm induction, H9 hESCs are cultured in 6-well

plate petri dish as in the standard induction protocol. Collect cells after one day of the induction, then seed cells as single-cell onto the functionalized and coated micropatterns. Replace the medium to MEF-CM without supplements and change the medium every day for 3 days.

3.1.5.3 Micropatterned neuroectoderm co-cultured with meso-endoderm

Micropatterned neuroectoderm cell fates were induced as described above after 5 days of cell differentiation. Meso-endoderm cell induction was initiated at day3 of neuroectoderm differentiation to keep in step. Meso-endoderm cells were cultured in 6-well petri dish with RPMI (GIBCO) medium, through a single cell splitting, 0.25×10^6 cells (in 0.5 mL MEF-CM medium) were seeded on top of micropatterned neuroectoderm cells. The medium was changed every day for 3 days.

3.1.6 Micropatterns inside of microfluidic chips

Chip production:

a. Note:

1. Use gloves and never touch PDMS, glass slides, and wafer mold directly with your hands.
2. Clean the bench before starting.
3. PDMS surface must be absolutely flat for adhesion.
4. Free of dust and PDMS debris on PDMS.

b. Cleaning of glass slides:

1. Wash both sides of the glass slides with distilled water.
2. Clean carefully both sides of the glass slides with the cleaning solution (2% Micro90 from Sigma in distilled water)

3. Rinse both sides of the glass slides with distilled water.
4. Dry the slides with compressed air and then keep them in a clean box.
- c. Preparation of PDMS:
 1. Blow a polystyrene glass with compressed air to remove dust.
 2. Cover the glass with a piece of clean aluminum foil to keep the glass clean.
 3. Cover the bench with paper.
 4. Define the total quantity of PDMS you need to prepare (Named A)
 5. Weight on the scale $1/11$ of A (in mass) of curing agent of the “Dow Corning Sylgard 184-Silicone Elastomer” kit.
 6. Weight on the scale $10/11$ of A (in mass) of base of the “Dow Corning Sylgard 184-Silicone Elastomer” kit.
 7. Under the chemical hood, stir for at least 2 minutes with a clean wooden stick until the mixture is full of bubbles.
 8. Leave the wooden stick inside and cover the mixture with aluminum foil.
 9. Put the covered cup into the desiccator for PDMS.
 10. Connect the vacuum tube to the inlet of the desiccator.
 11. Switch on the vacuum pump and pay attention to the PDMS increase of volume in the cup.
 12. Switch off the pump when the PDMS fills completely the cup.
 13. Remove the vacuum tube from the desiccator.
 14. Leave the mixture inside the desiccator under vacuum for 20-30 minutes, until PDMS is completely transparent.
 15. Blow the wafer mold as well as petri dish with compressed air to remove small debris.
 16. Open the valve of the desiccator slowly until it reaches atmospheric pressure.

17. Pour the desired mass of PDMS in the wafer mold.
18. Cover the model with the cover of the petri dish.
19. Put the petri dish containing the mold into the desiccator.
20. Degas again as steps 10-14.

d. Baking:

1. Put the petri dish containing the mold on the hot plate.
2. Switch on and set one of the baking protocol:
 - i) 1h at 80 °C.
 - ii) 1h 30min at 75 °C.
 - iii) 2h at 70 °C.
 - iv) ON at 40 °C.
3. Set the “AUTO OFF” option on the hot plate.

e. Cut and punch of PDMS:

1. When the mold is at room temperature, remove it from the hot plate.
2. Cut the borders of the chip with a sharp scalpel.
3. Remove the PDMS from the mold.
4. Punch the chip with the desired size of punch, from the pattern side.

f. Plasma bonding:

1. Before starting, turn the compressed air regulator to 0.5 bar.
2. Clean PDMS pieces and glass slides carefully with tape.
3. Check that the 3-way valve is closed.
4. Put the cleaned samples inside the plasma chamber.
5. Close the front door.
6. Turn on the plasma main power.
7. Turn on the pump main power.

8. Wait until $P=9.6 \times 10^{-1}$ mbar.
 9. Turn the 3-way valve to the metering valve position.
 10. Turn RF power level switch to HI position.
 11. Look through the plasma chamber to check the plasma is activated.
 12. Treat samples for 30s.
 13. Turn RF power level switch to OFF position.
 14. Close the 3-way valve.
 15. Turn off the vacuum pump.
 16. Turn the 3-way valve to vent position.
 17. Turn off the plasma main power.
 18. Once the atmospheric pressure is reached, close the 3-way valve.
 19. Open the front door and attach the PDMS onto glass by pressing slightly.
 20. Put the attached samples immediately onto the hot plate, incubate at 100 °C for 15 minutes.
 21. At the end of the work, close the compressed air regulator.
- g. Functionalization of the microfluidic channels:
1. Prepare the reagents used for the glass functionalization, see chapter 3.1.3, preparation of the functionalized surface.
 2. Treat 2-3 chips at one time.
 3. Fill the channels with solution C.
 4. Switch on the UV lamp 5 minutes before using, expose the glass coverslips to UV with the interposition of photo-mask. The irradiation time is 40 seconds, the distance between the glass and UV source is 5.5 cm.
 5. Wash the channels with deionized water for 2 times immediately after the UV activation.

3.1.7 Immunofluorescence

1. After cell culture or differentiation, fix cells with 4 % PFA (Sigma) for 10 minutes at room temperature. For the fixation of micropatterned neural induction, the samples are easy to detach when using PFA directly. Thus, keep 0.5 mL of the culture medium and add 0.5 mL of 4 % PFA, incubate for 10 minutes. Then do the 4 % PFA fixation again.
2. Wash the samples gently 3 times with DPBS, 5 minutes for each wash.
3. Treat cells with Triton ×-100 (Sigma) for 10 minutes to increase the permeabilization of cells. The Triton ×-100 stock is 100 %, dilute it in DPBS with the working concentration of 0.5 %.
4. Prepare the blocking solution: 0.1 % Triton ×-100 plus 5 % heat-inactivated HS (house serum). Treat cells with blocking solution for 45-60 minutes at room temperature.
5. Dilute the primary antibody in the antibody solution (Ab solution, blocking solution: 0.1 % PBST = 1:3) and incubate overnight at 4 °C. In this step, put wet paper (DPBS) in the plate to keep the sample wet.
6. After the overnight incubation, wash the samples gently with 0.1 % PBST for 3 times, each wash incubates for 5 minutes.
7. Dilute the secondary antibody in Ab solution and incubate for 30 minutes at 37 °C or 1-2 hours at room temperature. The Hoechst (Polysciences) can be diluted as 1:1000 together with the secondary antibody.
8. Wash 3 times with DPBS, each wash for 5 minutes.
9. Wash the glass slides with milli-Q water and mount the glass slide by using the mounting medium (Sigma).

3.2 MATERIALS

3.2.1 Media and supplements

StemMACS™ iPS-Brew XF, human (Miltenyi Biotech, cat.no. 130-104-368)

DMEM/F12, HEPES (GIBCO, cat.no. 31330-038)

KnockOut Serum Replacement (GIBCO, cat.no. 10828028)

GlutaMAX™ (GIBCO cat.no. 35050-061)

RPMI 1640 (GIBCO, cat.no. 22400089)

DMEM high glucose (GIBCO, cat.no. 41965-039)

MEM NEAA (GIBCO, cat.no. 11140-50)

β-Mercaptoethanol (GIBCO, cat.no. 31350-010)

B27-Supplement (50x), minus vitamin A (GIBCO, cat.no. 12587-010)

Sodium pyruvate (Sigma, cat.no. 11360070)

Corning Matrigel Matrix - Growth Factor Reduced (Corning, cat.no. L003975)

TrypLE™ Select (1×) (GIBCO, cat.no. 12563-011)

3.2.2 Reagents

3-(trimethoxysilyl) propyl methacrylate (Fluka, cat.no. 64210)

IRGACURE 2959 (Ciba, cat.no. 0298913AB)

acrylamide (Sigma, cat.no. A4058)

Poly-L-lysine (Sigma, cat.no. P8920)

EDTA (GIBCO)

DPBS (GIBCO)

DMSO (Sigma)

pLenti PGK GFP Puro (Addgene, cat.no. w509-5)

Puromycin (ThermoFisher Scientific, cat.no. A11138-03)
poly-L-lysine (Sigma, cat.no. P8920)
FBS-Fetal Bovine Serum (GIBCO, cat.no. 1020-106)
0.22 μ m filter (Millipore, cat.no. MPPG002A1)
Mitomycin C from Streptomyces (Sigma, cat.no. M0503-2MG)
PFA, Paraformaldehyde (Sigma, cat.no. P6148)
Triton \times -100 (Sigma, cat.no. 93426)
Horse serum for cell-HS (GIBCO, cat.no. 16050-122)
Hoechst (Polysciences, cat.no. 09460-100)
Fluoroshield with DAPI-histology mounting medium (Sigma, cat.no. F6057)
Silicone Elastomer Curing Agent (Sigma, cat.no. 184)

3.2.3 Antibodies

AP-2 α (3B5) (Santa Cruz Biotechnology, cat.no. sc-12726)
Sox2 (EMD Millipore, cat.no. AB5603)
Anti-p75 pAb (Promega, cat.no. G323A)
Human Nestin (R&D, cat.no. MAB1259)
Pax6 (Biolegend, cat.no. 901301/PRB-278P)
Phalloidin647 (Invitrogen, cat.no. A22287)
Tuj (Biolegend, cat.no. 801202/MMS-435P)
Sox17 (R&D, cat.no. AF1924)
Brachyury (R&D, cat.no. AF2085)
Sox1 (R&D, cat.no. AF3369)
OCT4 (Santa Cruz Biotechnology, cat.no. sc-5279)
Nanog (Reprocell, cat.no. RACB004P-F)

3.2.4 Small molecules

Rock-inhibitor Y27632 (Miltenyi Biotech, cat.no. 130-103-922)

A83-01 (Tocris, cat.no. 2939)

PNU-74654 (Tocris, cat.no. 3534)

Dorsomorphin (Sigma, cat.no. P5499)

Activin A (R&D, cat.no. 338-AC)

BMP4 (R&D, cat.no. 314-BP-010)

bFGF (PeproTech, cat.no. 100-18B)

CHIR99021 (Miltenyi Biotech, cat.no. 130-103-926)

SB431542 (Stemgent, cat.no. 04-0010-10)

LDN193189 (Sigma, cat.no. SML0559)

CHAPTER 4

RESULTS

4.1 ESTABLISHMENT OF THE MICROPATTERN TECHNOLOGY

During the past decades, micropattern technology has developed a lot, and many techniques are available for modeling the microenvironment at different scales and complexities. As reported, all micropattern techniques involve three basic steps: 1) Generation of a pattern of controlled surface adhesiveness, 2) Cell seeding onto the adhesion surface, and 3) Washing to remove cells outside adherent surface/on top of cell repellent surface. If a multiphase tissue containing multiple cell types is needed for co-culture, three additional steps are required: 1) Treatment to render cell repellent substrate regions adhesive, 2) Seeding of a second cell population targeted to adhere to vacant regions of the substrate that do not contain the previous cell type, and 3) Wash again to remove excess cells, thus generate the pattern used for co-culture.

We have already established a new micropatterned method used for hPSCs cell culture and differentiation, and all the method includes the three main steps, as explained above (Figure 4.1 a). We can generate a micropatterned surface on the glass substrate, and both the size and shape of the cell adherent region are controllable by using different photomasks (Figure 4.1 b). Different from the so-called “microcontact” printing and “polyacrylamide patterning”, our micropattern technique takes advantage of surface silanization by using photopatterning technology (Figure 4.1 d). The photo-initiated surface functionalization procedure is showed in Figure 4.1 c. The photo-preserved area corresponds to the cell adhesion island.

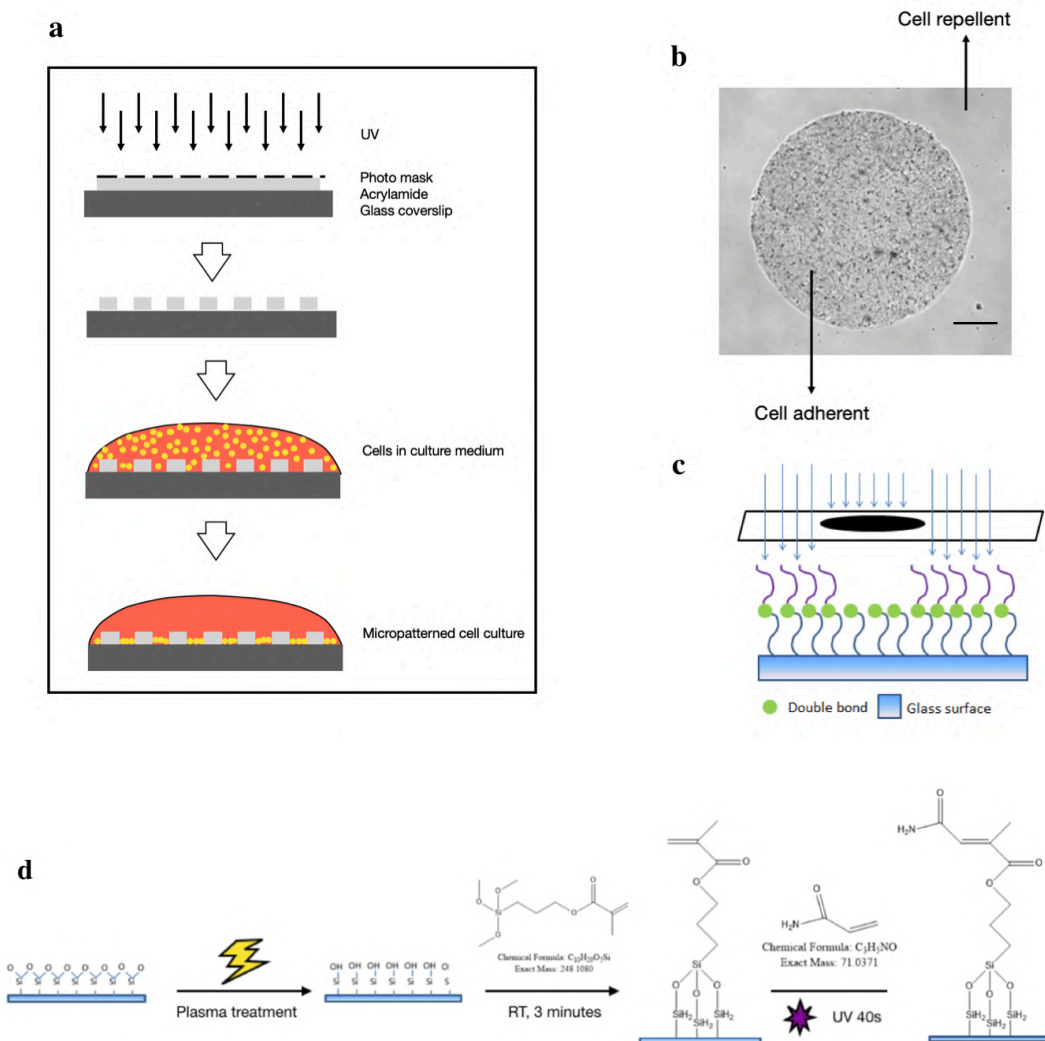


Figure 4.1: Micropattern technology. (a) Detailed strategies include surface functionalization, surface coating, and micropatterned cell culture. (b) Well-formed cell colony. Scare bar = 200 μm . (c) Enlarged surface structures of cell repellent and adherent areas. (d) Surface functionalization. Step1: Plasma treatment to oxidized the surface. Step2: Reaction between 3-(trimethoxysilyl) propyl methacrylate and the activated surface. Step3: Photo-initiator mediated reaction between acrylamide and 3-(trimethoxysilyl) propyl methacrylate.

In micropatterned cell maintenance or differentiation, the two evaluation indexes are the quality and stability of the micropatterns. Quality means if the cell colonies are well-formed with apparent border to the cell repellent surface correlate with the

photomask. Stability means if the colonies will detach from the substrate or lost the desired shapes. In our early research, it is hard to always harvest homogeneous micropatterns on the 12mm-diameter glass coverslips substrate (Figure 4.2 a), and even most of the well-formed colonies detached within 3 days of cell differentiation (Figure 4.2 c). To solve this problem, we modified our micropatterned culture protocol by testing different influence factors, such as Poly-L-lysine and Matrigel coating time, coating temperature, seeding density, ROCK inhibitor incubation time, and culture medium used. At the same time, we also modified the way we performed the experiment, such as cell seeding and washing operations to avoid both batch-to-batch unrepeatability and physical damage.

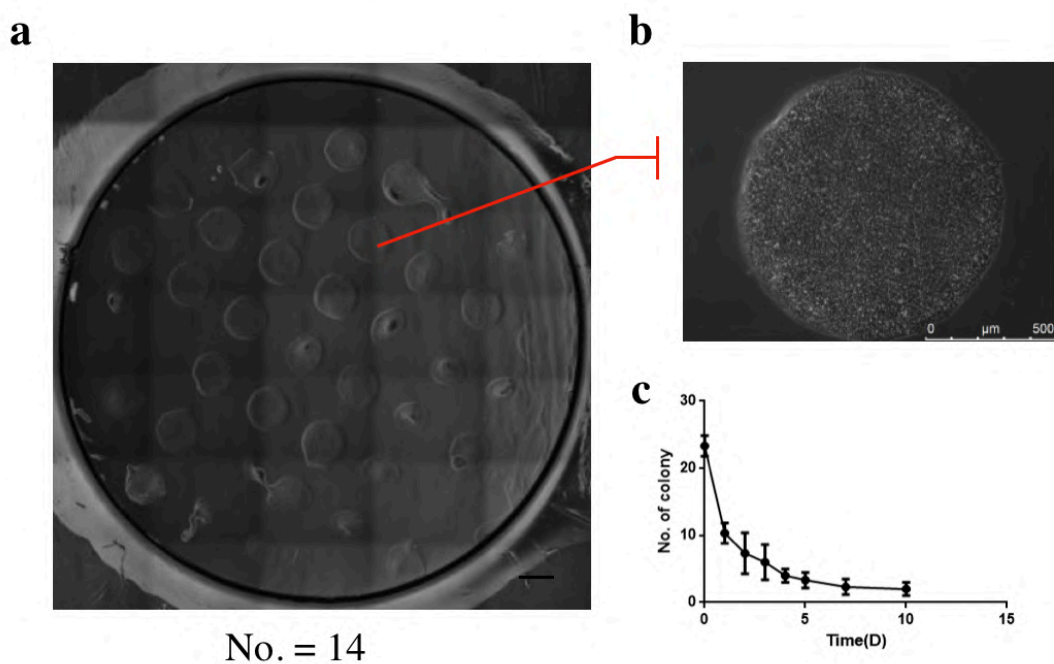


Figure 4.2: Heterogeneous micropatterns on 12mm-diameter glass coverslips. (a) One day after seeding without ROCK inhibitor. The total number of well-formed colony is around 14. Scare bar = 1mm. (b) The well-formed micropattern with compact cell morphology. Scare bar = 500 μ m. (c) The number of the well-formed colonies decreased over time. After 10 days of culture, nearly all cell colonies detached. Data is from three individual experiments. Shown are the mean \pm SD.

Similar to the troubleshooting table reported by Warmflash based on the CYTOO™ Chip - micropattern technology, here, we conclude our troubleshooting table from diverse influence factors (Table 4.1).

Problem	Possible reason	Solution
Cell attach outside of the micropatterned colonies	Concentration of Matrigel is too high	Find the working dilution of Matrigel for each batch; test in the range of 0.5 %-1.0 %
	Substrate dried up during coating or washing steps	Ensure that the chips are kept immersed in liquid
	Substrate was not washed properly	Properly wash the substrate according to the protocol Use precooled DPBS and always keep the glass coverslips cold
	Cells were left in Rock inhibitor too long	Ensure that the cells are exposed to Y-27632 for the appropriate time
Uneven seeding	Too many cells were seeded	Adjust the number of cells used
	Washing procedure	Wash for more times
	Poor mixing	Gently mix the cells when seeding the chip, taking care not to swirl, as this will concentrate cells in the center of the dish
Holes form in colonies upon removal of ROCK inhibitor	Cells were not reduced to a single-cell suspension	Single cells are critical for accurate counting and seeding; if colonies are difficult to break up into single colonies, incubate them longer with TypLE™ select
	Too many or too few cells were seeded	Adjust the number of cells used
	Poor seeding	Adjust the number of cells used
Cells or colonies detach from the chip	Plate is moved within 15 minutes after seeding	Keep plate in incubate without any movement for at least 15 minutes
	Washing procedure	Wash gently and not pipette the cell colonies
	Problems with coating	Try a higher concentration or a longer coating time
Cells or colonies detach from the chip	Cell density is too high	Try lowering the cell concentration
	Medium used result a cell colony shrink after removal of ROCK inhibitor	Use MEF-CM instead to avoid cell detachment
	Washing procedure and the time to wash	Long incubation with ROCK inhibitor leads cell attach) patterns while short incubation leads cell detachment, test

and find the balance and choose proper wash time

Table 4.1: Troubleshooting table.

After a series of modification, the micropatterned hESCs culture are fixed. We use MEF-CM as the growth and basal differentiation medium. Cells cultured with conditioned medium showed a flatter morphology and did not get retraction after the media change. This also can be solved by initiating cell differentiation immediately after the removal of the ROCK inhibitor. The protocol is concluded in chapter 3.

We next test the reproducibility of the established method. For every glass coverslips, the number of cell adherents island is randomly between 40-44. In three independent replicates, we demonstrated that our micropatterns are stable and around 94% (we assume that the full number of micropatterns on each glass coverslips) of the patterns are well organized during 5 days of differentiation (Figure 4.3).

3 individual replicates in MEF-CM culture condition

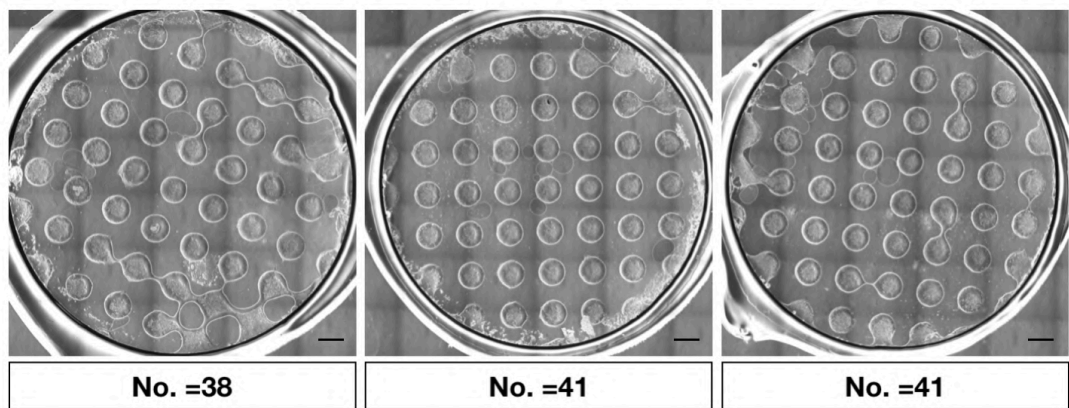


Figure 4.3: Micropatterning conditions on 3 individual glass coverslips. Scare bar = 1mm.

4.2 MICROPATTERNED NEURAL INDUCTION

4.2.1 Standard neural induction protocol with dual-Smad inhibition

We sought to develop an *in vitro* model to investigate the micropatterned neural induction under geometric confinement. In contrast with the published work, the micropatterned hPSCs can be differentiated into gastrulation-stage patterns: the three germ layers located regionally along the axis, we hypothesis that the micropatterned hPSCs which in response to specific stimulation can self-organize into different cell fates within the ectoderm cell populations. To investigate the micropatterned neural patterning, a well-defined neural induction protocol is necessary. As reported, concomitant inhibition of the BMP and TGF- β 1 branches of TGF- β signaling pathways by the endogenous antagonists will induce efficient neuralization, and this method is known as dual-Smad inhibition. We used SB431542 and LDN193189 as the small molecule combination to induce standard neural induction within 10 days of cell differentiation. The timeline and strategy showed in Figure 4.4.

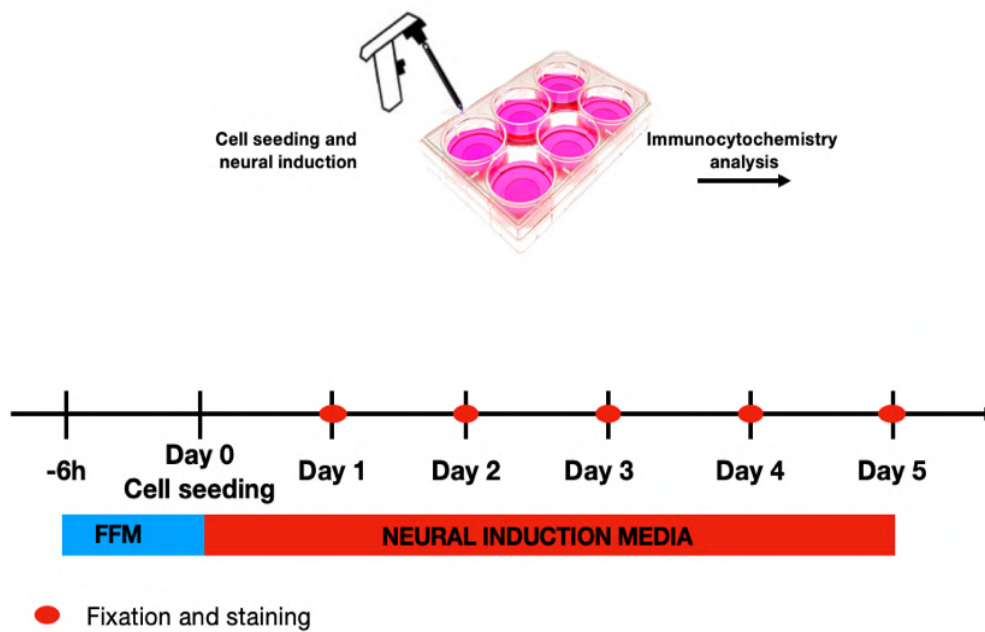
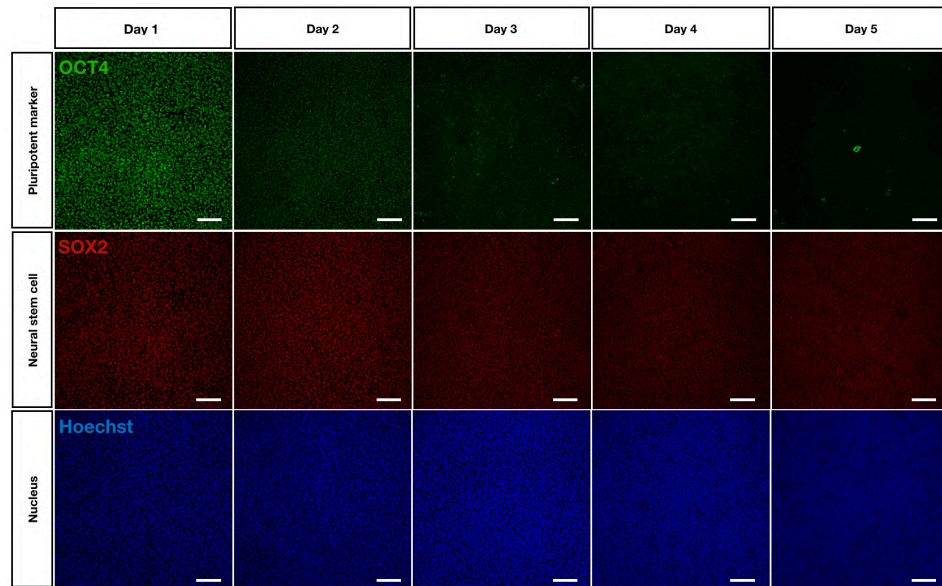


Figure 4.4: Characterization of dual-Smad inhibitor neural induction protocol. Timeline and protocol used. Cell fixation at day5 after initiation of differentiation. All the experiment was performed in standard cell culture.

We found that the central nervous system (CNS) markers PAX6 and SOX1 expressed significantly from day3 and reached the peak at day5, neural stem cell marker SOX2 expressed nearly 100 % all the time while pluripotent marker OCT4 expressed highly at day1 and kept decreasing till day3. We can conclude that day3 is the time when the neural induction starts, and we harvested neural progenitors efficiently after 5 days of dual-Smad inhibition protocol (Figure 4.5).

a



b

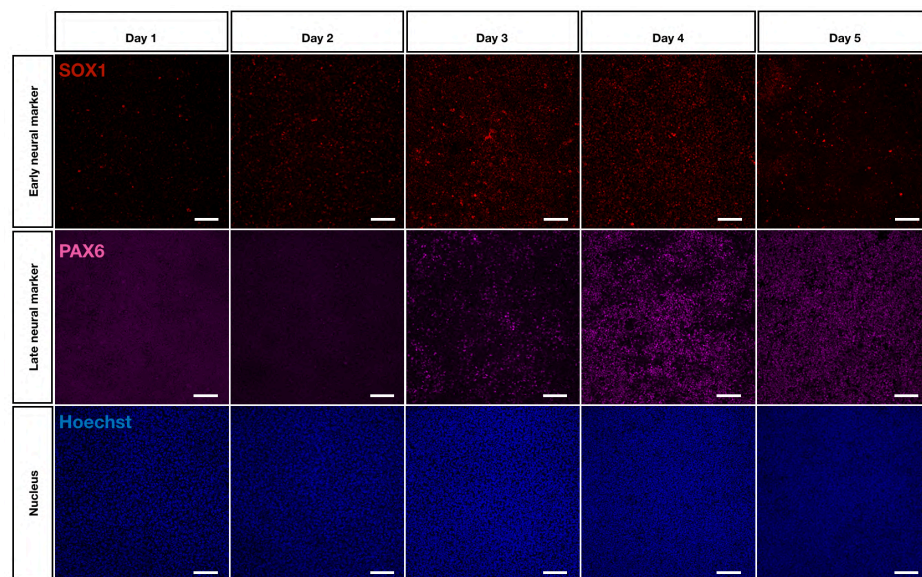


Figure 4.5: Characterization of dual-Smad inhibitor neural induction protocol. (a) Pluripotent markers expression condition within 5 days of neural induction. (b) Neural markers expression condition within 5 days of neural induction. Data is from three individual experiments. Scale bar = 100 μm .

Within 5 days of neural induction, we determined a specific time point to harvest cell population that present the process of neurulation. Specific marker expression condition showed in Figure 4.6.

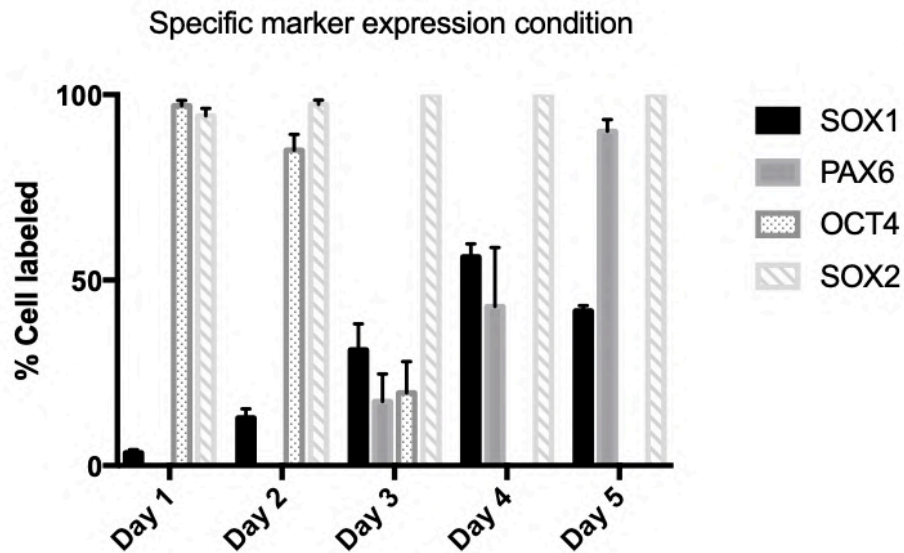


Figure 4.6: Characterization of dual-Smad inhibitor neural induction protocol. Specific marker expression condition within 5 days. Markers selected: SOX1, PAX6, OCT4, and SOX2. Shown are the means \pm SD, n=3 images. We got similar marker expression results from 3 independent experiments.

The same experiment, we keep the differentiation for 5 days more (till day 10) to check how the cell morphology changed during neural induction. We found a huge change of phalloidin expression while SOX2 expression is relatively stable. This may reflect cell migration and the appearance of cell polarity during neurulation (Figure 4.7). Later we tested another neural induction differentiation medium, which contains A83-01 (TGF- β inhibitor), PNU-74654 (WNT inhibitor) and Dorsomorphin (BMP4 inhibitor). Within 5 days of neural induction, we got similar differentiation results.

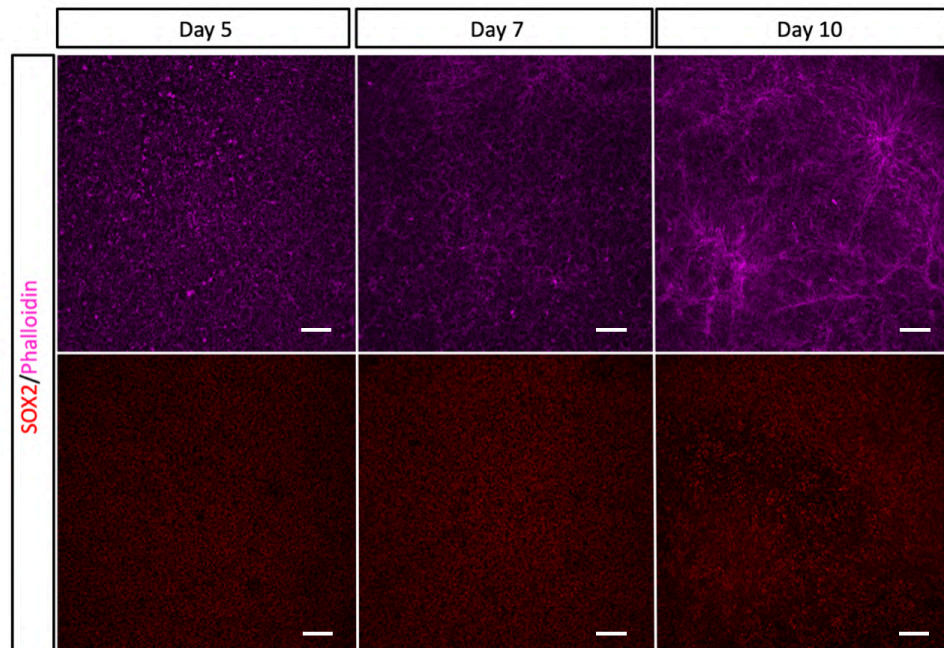


Figure 4.7: Characterization of dual-Smad inhibitor neural induction protocol. Phalloidin and SOX2 expression condition at day5, 7, and 10. Data is from three individual experiments. Scare bar = 100 μm .

4.2.2 Micropatterned neural induction

We have already developed and established robust micropattern technology and succeeded in forming cell colonies with diverse sizes and shapes. In the meantime, the neural induction protocols were also available. We next started to apply our neural protocol to the micropatterned hPSCs to investigate how the neural induction will be influenced under geometric confinement. The H9 ESCs are maintained in StemMACSTM iPS-Brew XF medium, change the medium to MEF-CM (bFGF) one day before the micropatterned cell seeding to avoid significant apoptosis. Then, initiate neural induction by switching to the differentiation medium (Figure 4.8).

Micropatterned neural induction

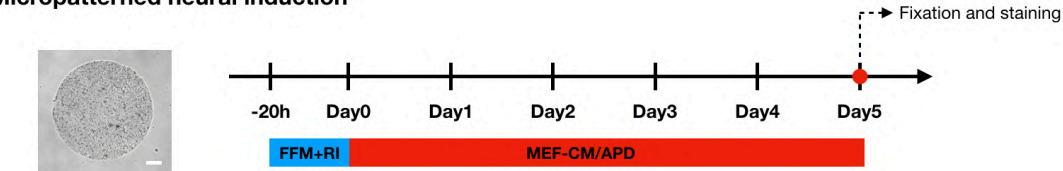


Figure 4.8: Characterization of micropatterned neural induction. Timeline and protocol used. Here we use MEF-CM plus APD as the differentiation medium. Cell fixation at day5 after initiation of differentiation.

In response to the stimulation of dual-Smad inhibitors, we can generate neuroectoderm (Marked by PAX6+ / SOX1+ / NESTIN+ / OCT4-, Figure 4.9) within 5 days of differentiation. As we know, WNT signaling pathway is a crucial parameter for the patterning of ectoderm. It also plays an essential role in neural plate border (NPB) specification. Thus, we used a combination of differentiation factors, including PNU (β -Catenin, inhibits Wnt signals) to check if we can generate the NPB population. Up to now, this micropatterned neural induction method has been demonstrated efficient under different differentiation protocols include: 1) KnockOut DMEM basal medium 2) MEF-Conditioned medium supplemented with LSB (LDN193189 and SB431542) or APD (A83-01, PNU and Dorsomorphin).

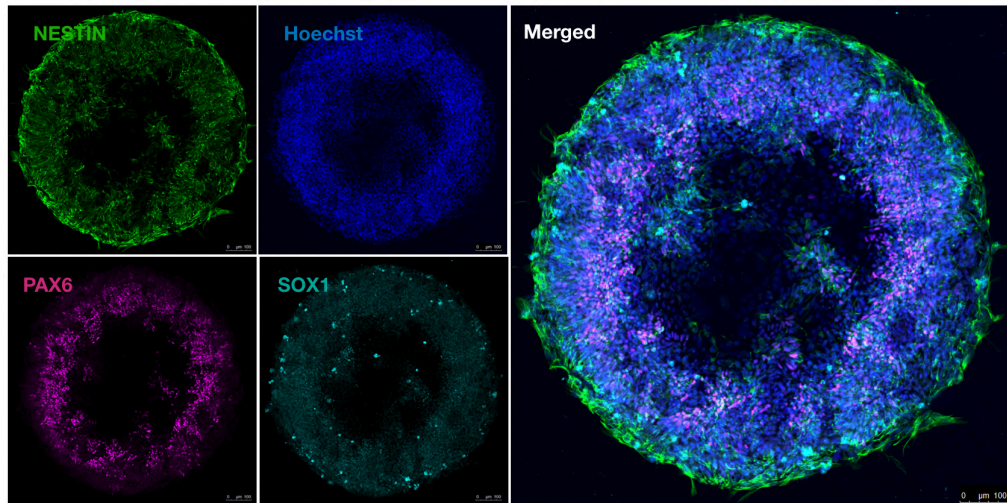


Figure 4.9: Characterization of micropatterned neural induction. Neural markers expression at day 5 of micropatterned neural induction. Neural markers located at the colony boundary. Scare bar = 100 μm . Data is from three individual experiments. Replicates on each sample is more than 30.

As expected, we can generate the new cell fate, neural crest (Marked by AP-2 α + / P75+/PAX6-/SOX1-/NESTIN-, Figure 4.10) population, at day 5 of cell differentiation with MEF-CM supplemented with APD.

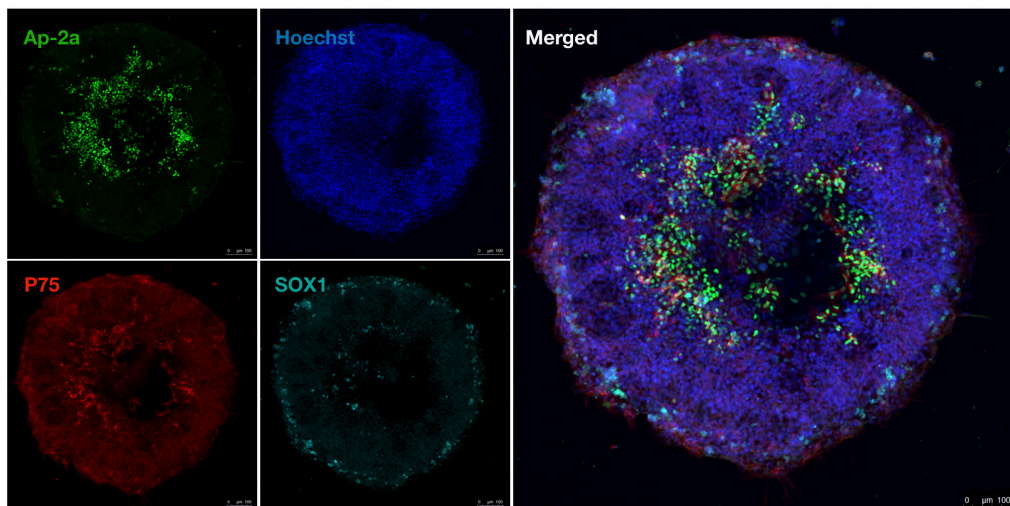


Figure 4.10: Characterization of micropatterned neural induction. Neural crest marker expression condition. Scare bar = 100 μm . Data is from three individual experiments. Replicates on each sample is more than 30.

Generally speaking, these protocols we established are reproducible for neural induction and useful to investigate the deep mechanism of ectoderm patterning which happened during gastrulation. When we analyze the distribution of these main markers from the center, we can find one notable peak of PAX6 ranged at 300-400 μm , and another notable but a little lower at 200 μm (Figure 4.11).

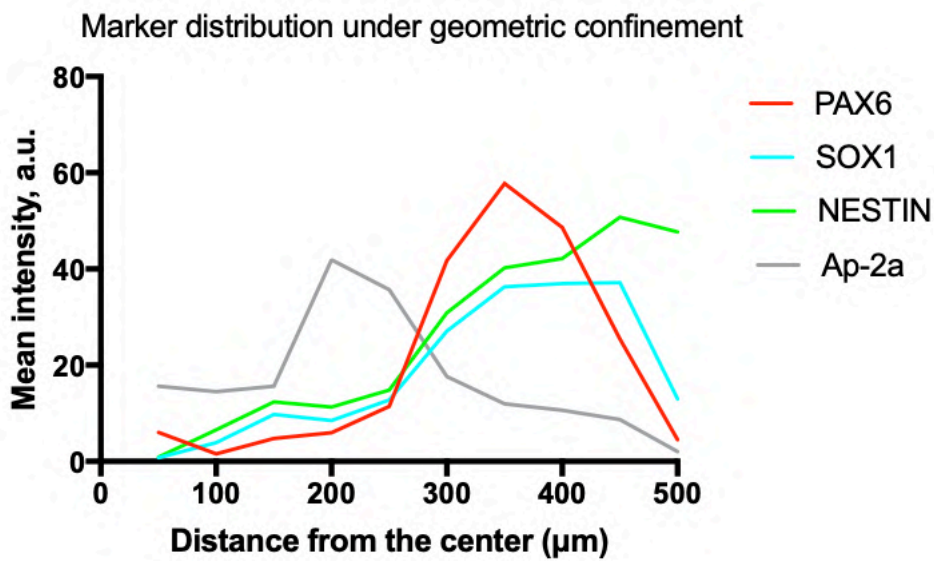


Figure 4.11: Characterization of micropatterned neural induction. Specific marker distribution in 1000 μm -diameter micropatterns. Each marker was quantified in three independent experiments. a.u., arbitrary units. The intensity of the indicated markers was normalized to the Hoechst intensity. We got similar marker expression results from 3 independent experiments.

According to the cell fates distribution, we have at least three cell populations along the axis: 1) Neural stem cells at the very border. 2) Neuroectoderm between the border and center. 3) Neural crest in the center, and the approximate size/location of each pattern is showed in Figure 4.12. we found that the size variation after 5 days of differentiation is ubiquitous, all the micropatterns showed an appropriate 50 μm shrink

(data not showed). Here, we still use 1000 μm as the size in the schematic diagrams.

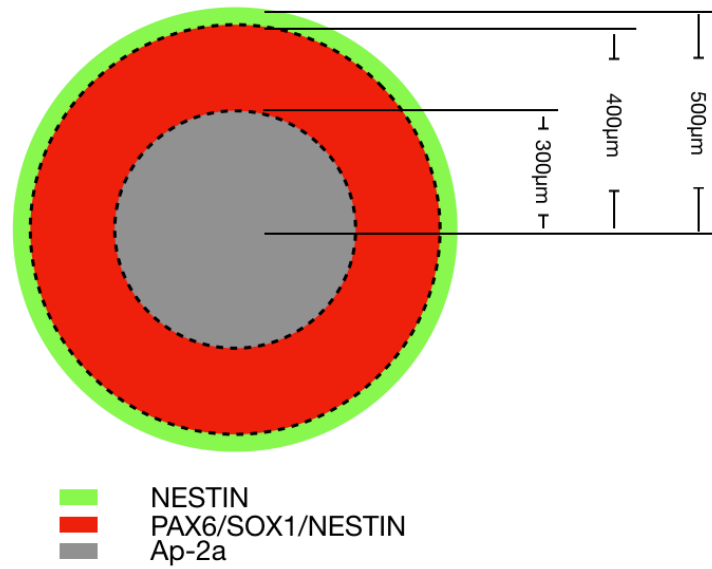


Figure 4.12: Cell fate allocations inside the micropattern. Center: Neural crest/Non-neural ectoderm (AP-2a+/PAX6-). Ring between: CNS/neural progenitors (PAX6+/SOX1+/NESTIN+). Border: NSC (NESTIN+/PAX6-/SOX1-).

4.3 MICROPATTERNED CO-CULTURE SYSTEM

4.3.1 H9 hESCs-GFP cell line

To develop the co-culture system, the hESCs cell line with GFP labeling is needed. We used the commercial pLenti PGK GFP Puro (Addgene) and performed the lentiviral production as introduced in the last chapter, and finally established the hESCs GFP cell line. However, the established GFP⁺ cell line did not express a homogeneous GFP signal, and some of them even lost the signal (Figure 4.13). This loss was caused by the multiple cell passage of GFP-negative aggregates.

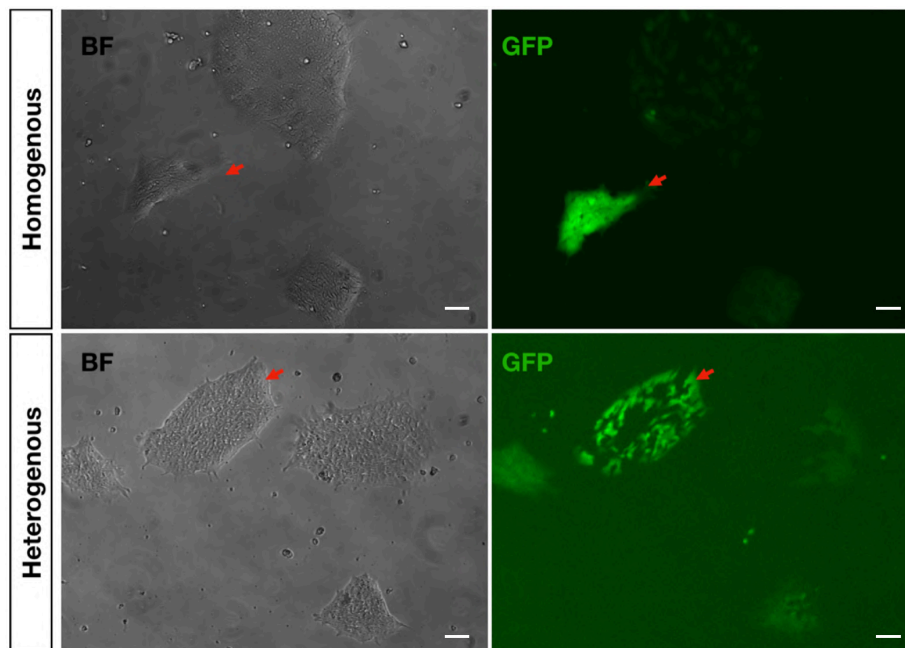


Figure 4.13: Establishment of H9 hESCs GFP cell line. Up, homogeneous GFP signal one passage after lentivirus infection. Down, heterogeneous GFP signal after three passages. Red arrow showed the GFP signal. Scale bar = 100 μ m. n = 3 images.

To solve this problem and establish a pure GFP-positive H9 human ES cell line, we performed a single-cell-picking purification operation (Figure 4.14): 1) The lentivirus

infected GFP cells are cultured in the growth medium in a 10 cm petri dish. 2) Split cells into single-cell and seed 20,000 cells into another 10 cm petri dish. Cells are maintained in culture medium supplemented with ROCK inhibitor. 3) Keep ROCK inhibitor at least for 3 days and withdraw it only when the cells grow to small colonies. 4) Before cell picking, we should check if the colony is big enough (it will offer a better chance of cell survival with more cell seeding). Moreover, the colony we picked must be an individual cell colony and has enough space between the surrounding colonies to ensure the accuracy of cell picking. The picked aggregates are cultured individually in a 96-well plate. 4) Expand the picked cells and analyze the purity via Fluorescence Activated Cell Sorting (FACS).

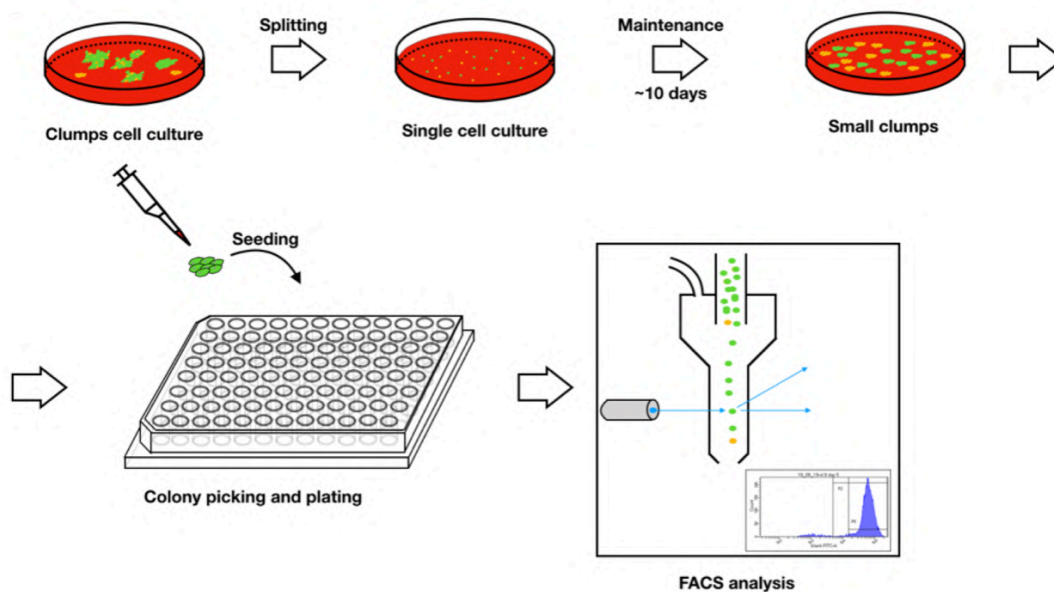
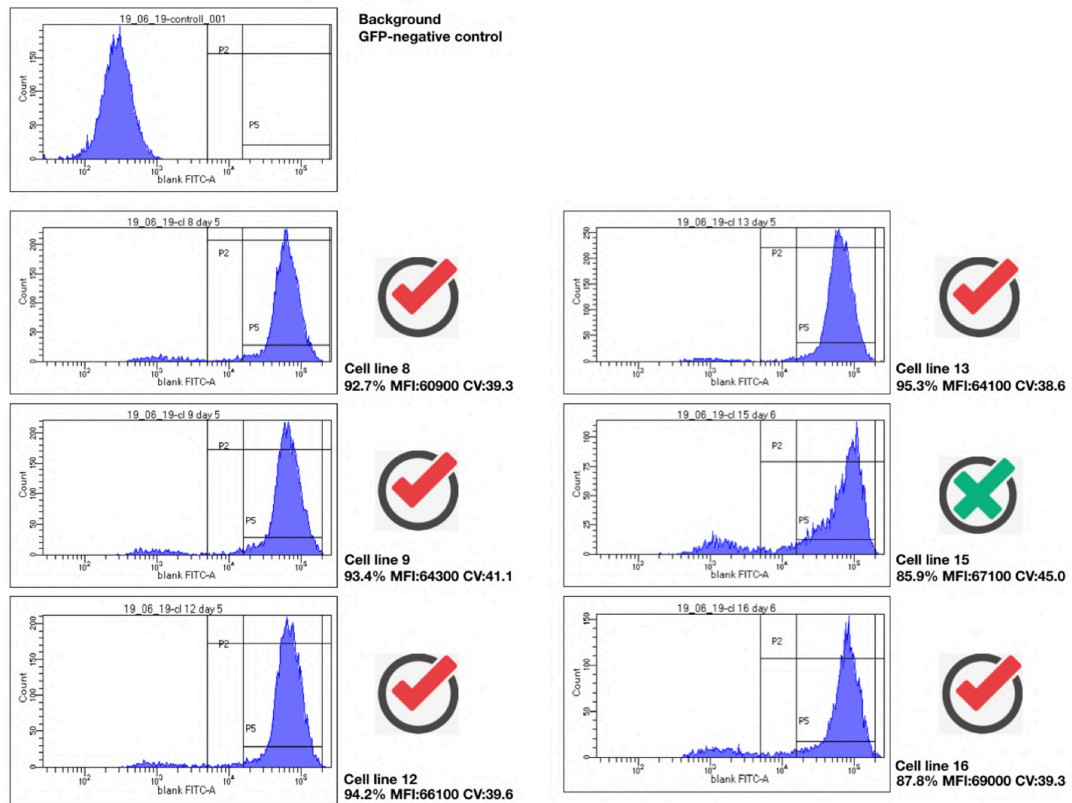


Figure 4.14: Establishment of H9 hESCs GFP cell line. Details of single cell picking operation.

As a result, we established 5 H9 hESCs cell lines (Figure 4.15a), and one of them showed homogeneous and pure GFP signal (Figure 4.15b).

a



b

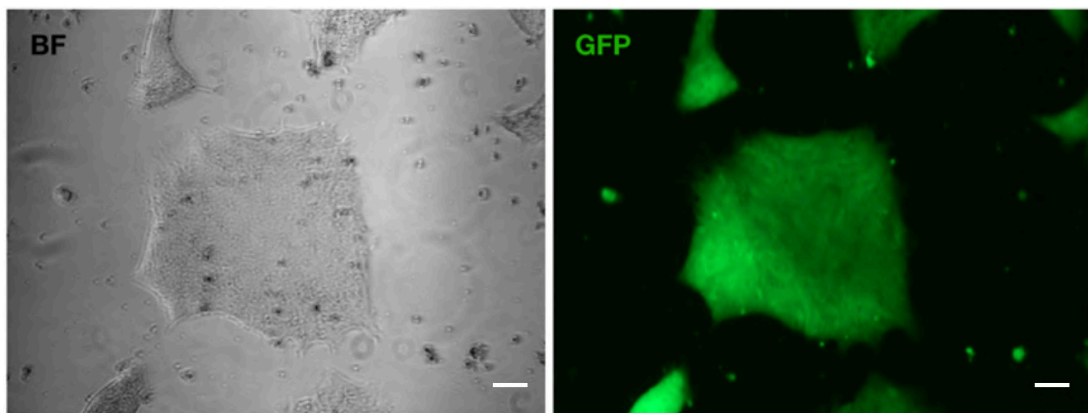


Figure 4.15: Establishment of H9 hESCs GFP cell line. (a) Fluorescence Activated Cell Sorting (FACS) results. Line 8,9,12, and 13 showed over 90% GFP positive. (b) GFP signal of cell line 13.

Scale bar = 100 μ m. n = 3 images.

4.3.2 Characterization of meso-endoderm cell fates

Before the micropatterned co-culture trial, we need to establish a meso-endoderm differentiation, which can induce the differentiation of these two cell populations. We

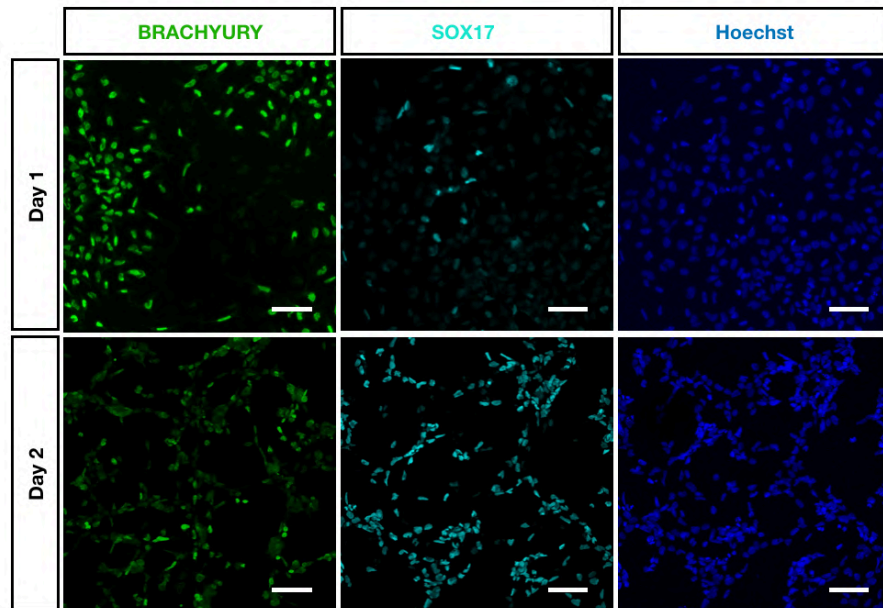
can use more defined cell fate, but this may result in adding the complexity of co-culture cell seeding. Thus, we decide to use the mixture of both endoderm and mesoderm, which is also called meso-endoderm. Firstly, we tested the marker expression condition within 48 hours of meso-endoderm induction in standard petri-dish cell culture (Figure 4.7 a).



Figure 4.16: Characterization of meso-endoderm cell fates. Strategies of meso-endoderm induction protocol.

BRACHYURY presents early mesoderm fate. Within 24 hours of induction, we can harvest more mesoderm cell population, and even the SOX17 started to express. SOX17 presents early endoderm cell fate. In the first 24 hours, SOX17 express not that much, but it was significantly upregulated in the next 24 hours (Figure 4.17 a and b).

a



b

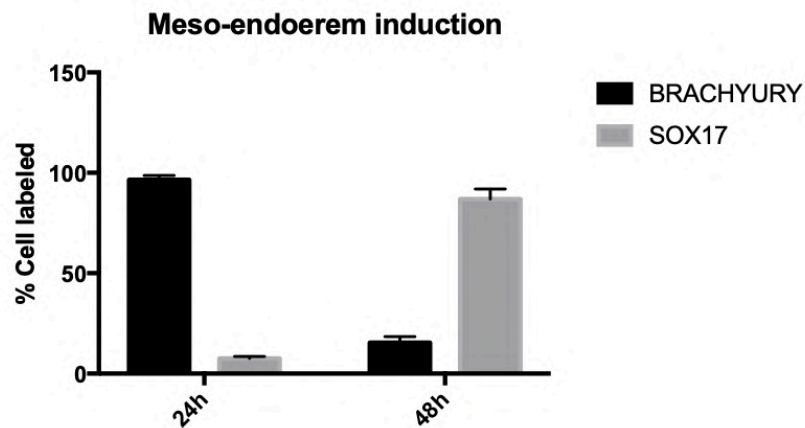


Figure 4.17: Characterization of meso-endoderm cell fates. (a) BRACHYURY and SOX17 expression conditions after 24 hours and 48 hours of differentiation. Scale bar = 100 μ m. (b) The percentage of BRACHYURY+ and SOX17+ cells at each time point. Shown are the means \pm SD, n=3 images. We got similar marker expression results from 3 independent experiments.

4.3.3 Micropatterned neuroectoderm co-culture with meso-endoderm

Based on the cell fates outcome under the geometric confinement, we took advantage

of this micropatterning platform to expand monolayer stem cell differentiation into co-culture differentiation, which can be used to investigate the self-organization ability of different germ layers, and their interactions between each other. In particular, we have evaluated the influence of the meso-endoderm layer co-cultured on top of the patterns of the neuroectoderm (Figure 4.18).

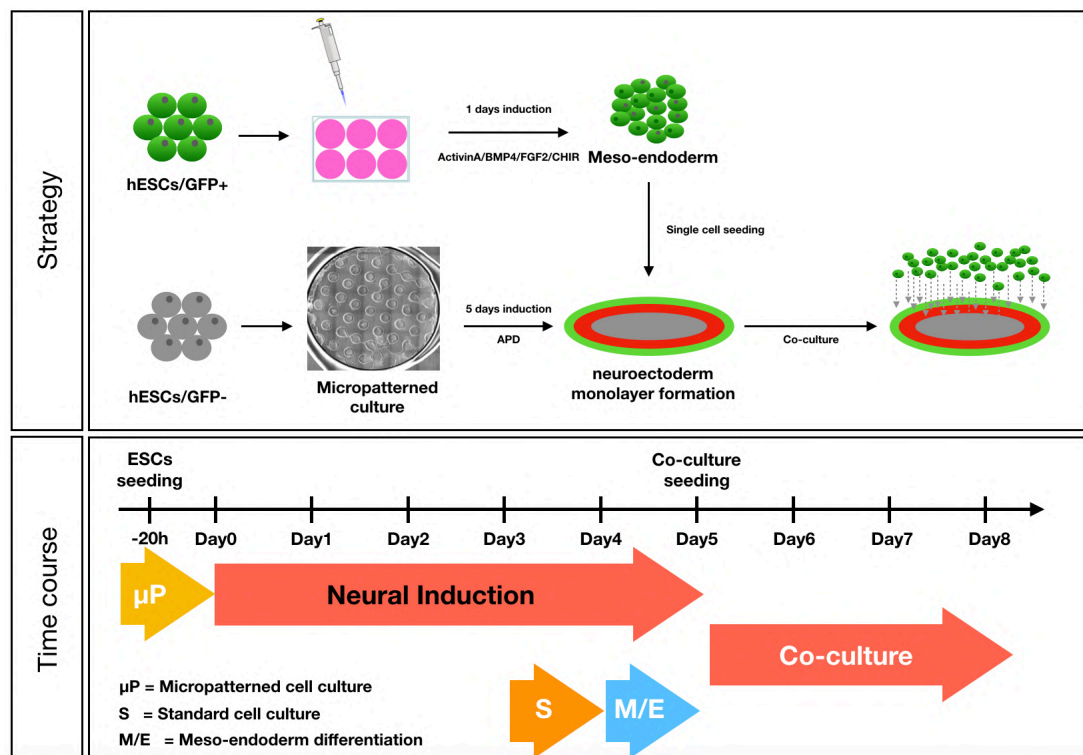
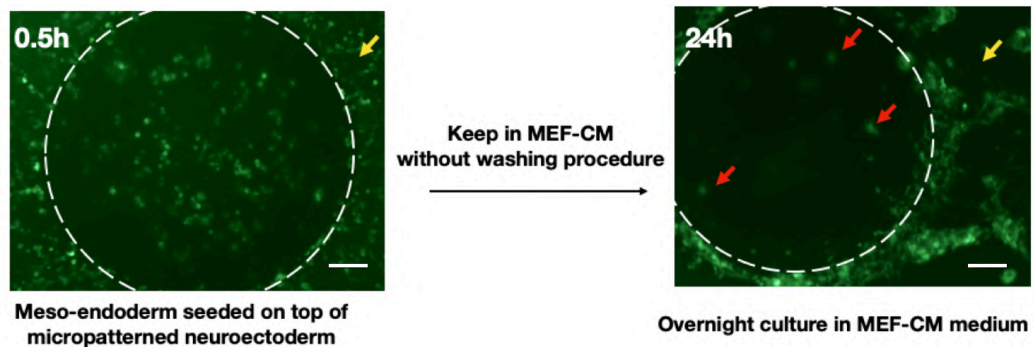


Figure 4.18 Micropatterned neuroectoderm co-culture with meso-endoderm. Strategies and time course of the micropatterned co-culture system.

We used GFP signal as the label to show how the subsequently seeded meso-endoderm cells interact with micropatterned neuroectoderm. 0.5 hour after seeding, the meso-endoderm cells are almost homogeneous and cover all the surface, including the cell patterns and also the cell repellent surface. However, the next day, after 24 hours of cell maintenance in MEF-CM, the GFP+ meso-endoderm cells tend to “move” out of

the micropatterns, but dramatically adhere and accumulate as a ring structure to the border. Interestingly, the GFP+ meso-endoderm cells seem to be “friendly” to only a specific cell population and locate only at the edge of the neuroectoderm region (Figure 4.19 a and b).

a



b

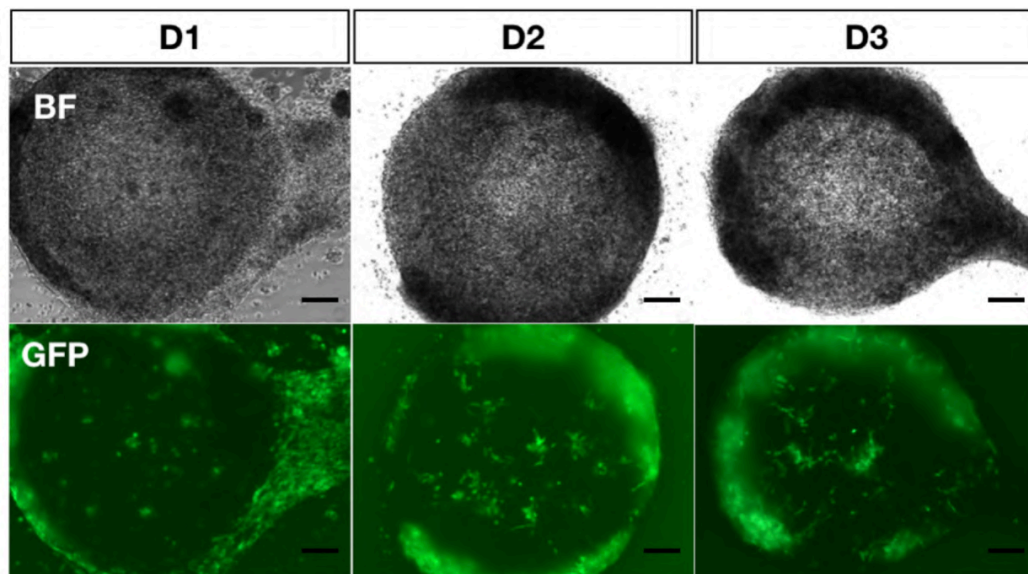


Figure 4.19 Micropatterned neuroectoderm co-culture with meso-endoderm. (a) Distribution of GFP+ cells at first 24 hours after seeding. The white dash line indicates the range of neuroectoderm micropattern. The yellow arrow indicates the meso-endoderm cells on the cell repellent area. Red arrow indicates the meso-endoderm cells on top of the neuroectoderm. Scare bar = 100 μ m. (b) Distribution of GFP+ cells in the next 3 days. Scare bar = 100 μ m. We got similar marker expression results from 3 independent experiments.

Immunostaining results show that the expression condition of BRACHYURY and SOX17 were identical with those under normal cell culture (data not showed). Nevertheless, we found that there occurs a new cell fate in this co-culture system which marked by Pax6 with GFP label (Figure 4.20).

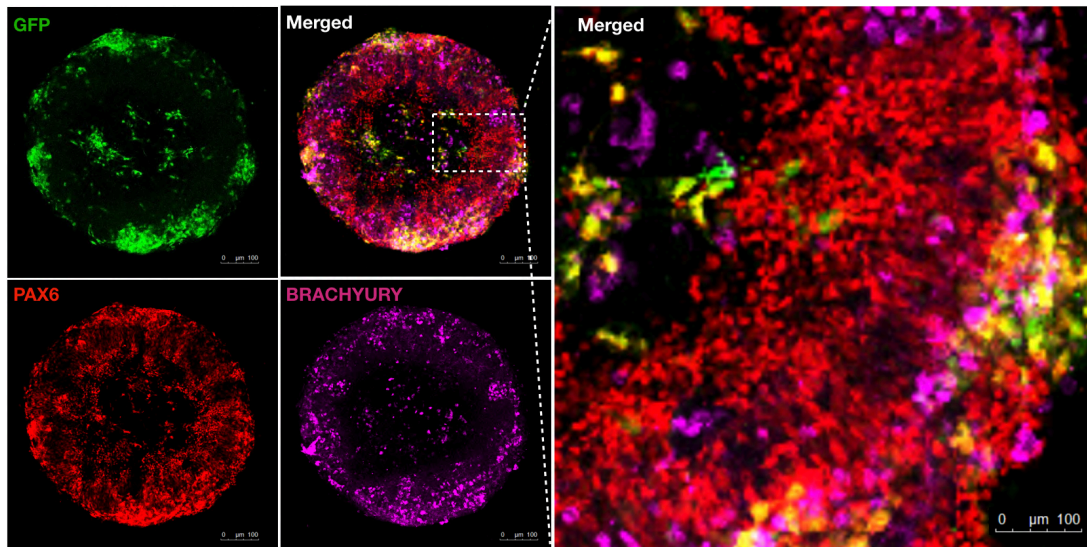


Figure 4.20 Micropatterned neuroectoderm co-culture with meso-endoderm. GFP, PAX6, and BRACHYURY expression conditions. Scale bar = 100 μm . We got similar marker expression results from 3 independent experiments.

From micropatterned meso-endoderm differentiation results (data not showed), we can demonstrate that these PAX6⁺ cells are generated from subsequent meso-endoderm cells within 3 days of co-culture, but more markers are still needed to characterize the cell fate. In the meantime, the connecting linear cell aggregates, which connect the inner and outer GFP⁺ cell populations over PAX6⁺ region, aroused our interest (Figure 4.21).

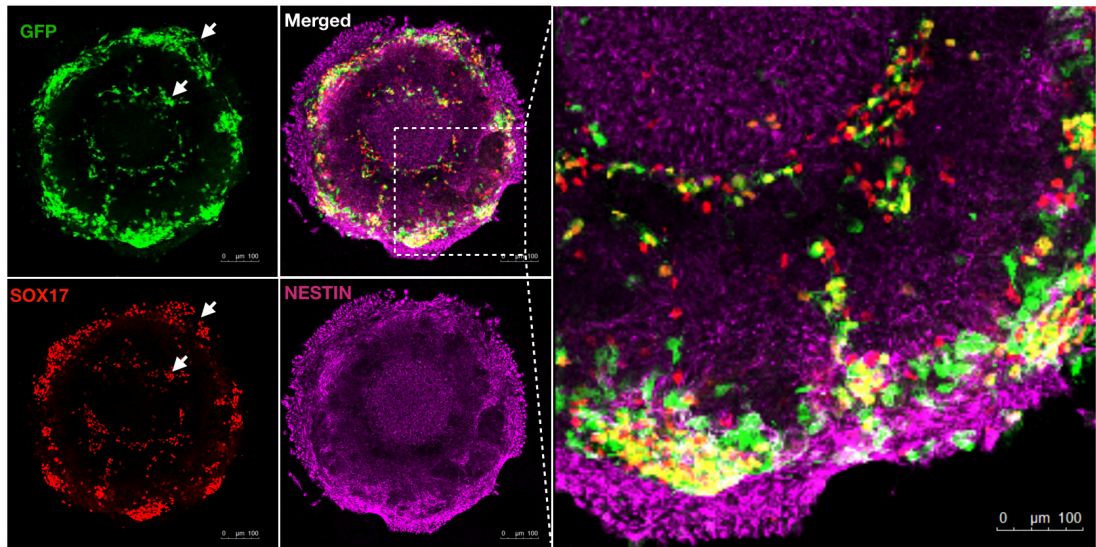


Figure 4.21 Micropatterned neuroectoderm co-culture with meso-endoderm. GFP, SOX17, and Nestin expression conditions. Scare bar = 100 μm . We got similar marker expression results from 3 independent experiments.

4.3.4 Micropatterned meso-endoderm culture

To investigate how the subsequently seeded meso-endoderm self-organize themselves during the 3 days of co-culture, we performed a micropatterned meso-endoderm cell culture by using the same medium (Figure 4.22).

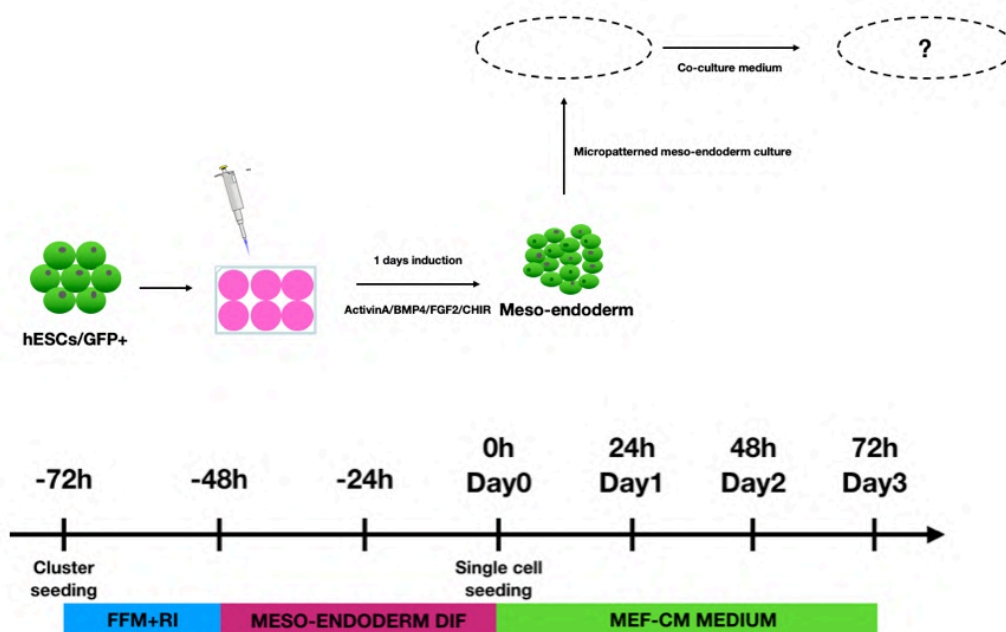
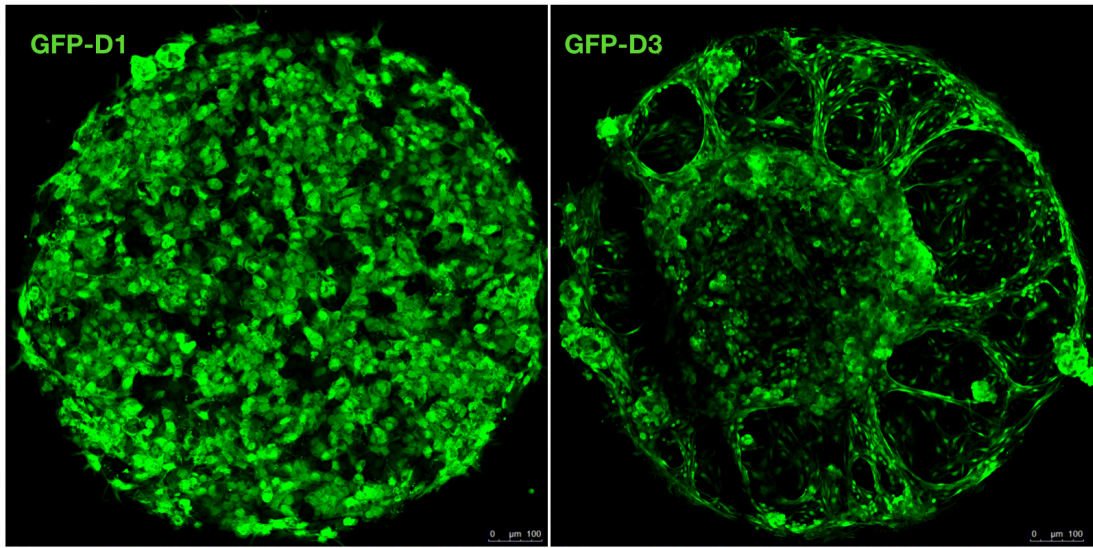


Figure 4.22: Micropatterned meso-endoderm (Up) Strategy of cell culture and differentiation. (Down)

Timeline.

Surprisingly, we found that the cells under geometric confinement showed amazing migration property and they can self-organized into a multiple layer structure: The cells in the colony center proliferated a lot and showed a very thick morphology while the cells around tended to organize into a linear structure, and the cells obtain an elongated cell morphology (Figure 4.23 a and b). We found that these cells showed elongated morphology then others and all express SOX17. As reported, SOX17 is known as a regulator of endodermal and hematopoietic differentiation, but it also plays an indispensable role in the acquisition and maintenance of arterial identity. Further characterization is needed to identify cell fates.

a



b

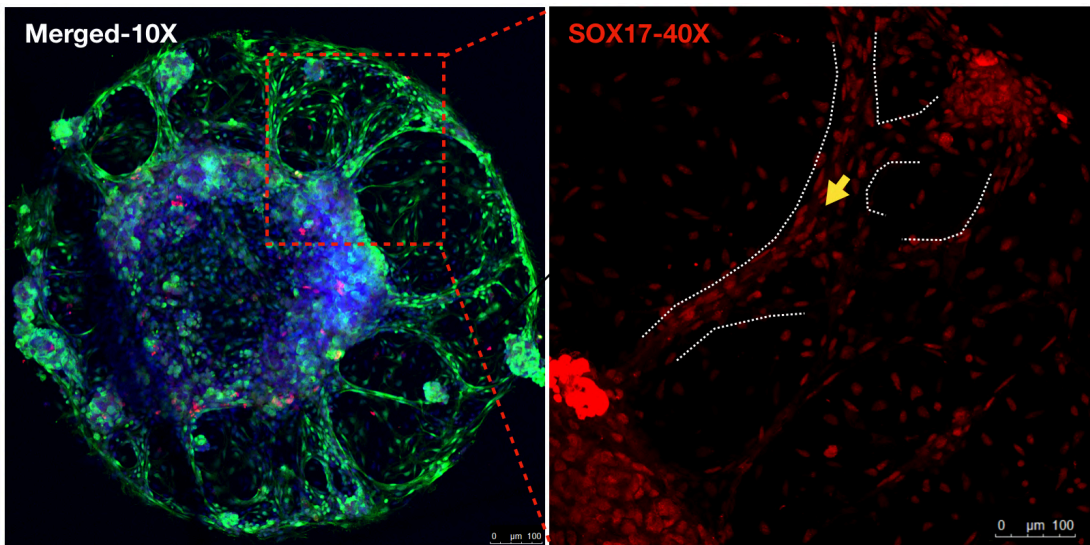


Figure 4.23: Micropatterned meso-endoderm. (a) Cell morphology maintained in MEF-CM at day1 and day3 after seeding. Scale bar = 100 μm. (b) Local details of SOX17+ cell population. Scale bar = 100 μm. Yellow arrow showed the linear structure of SOX17+ population between the center and boundary.

4.3.5 Micropatterns inside of microfluidic chips

To expand the application of our micropattern technology, we took advantage of glass surface functionalization to make micropatterns inside of microfluidic chips. First of all, we modified the protocol to do the functionalization inside the microfluidic channels. Later we detached the PDMS layer from the glass and fabricated together with a PDMS “wall” to test the quality of micropatterns (Figure 4.24). 24 hours after cell seeding, we can form cell patterns with the desired size and shape. We also found that the medium and seeding density are critical factors that affect the outcome of cell morphology. More importantly, when the culture volume was decreased to microliter, cell behavior and morphology were different from the micropatterned culture in a normal multi-well plate.

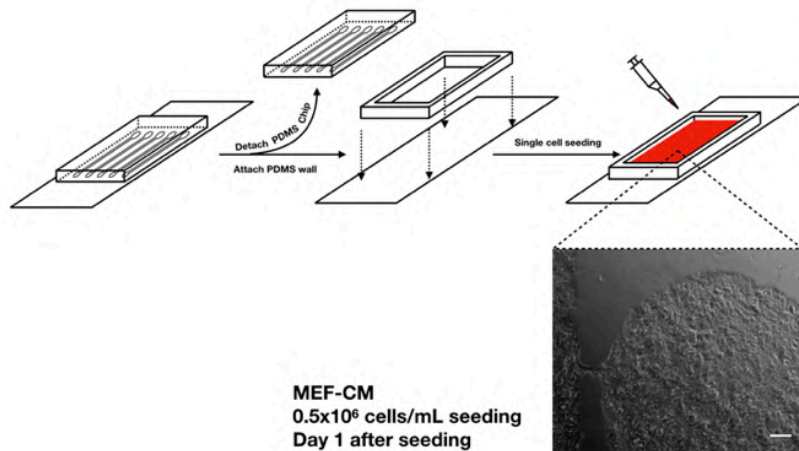


Figure 4.24: Glass functionalization inside microfluidic chip. Step 1, Glass functionalization. 2, PDMS detachment. 3, Cell seeding and micropatterns formation. Scare bar = 100 μm . We got similar results from 3 independent experiments.

We later modified the microfluidic channel functionalization protocol. For the seeding density, we tested both 125,000 cells/cm² and 250,000 cells/cm² when MEF-CM was applied in this protocol. In the low-density group, cells did not cover all of one micropattern and kept growing during 5 days of cell differentiation. Because of this, cells inside of the colony formed some compact cell populations. This heterogeneous property can lead to a disorder of cell fates allocation. In the high-density group, the micropattern was not well-formed within the first 20 hours, and cells proliferated and migrated a lot to the cell repellent surface during the time. Considering the culture system and medium volume between microfluidic and normal multi-well culture, we still have to fix the protocol in specific culture condition.

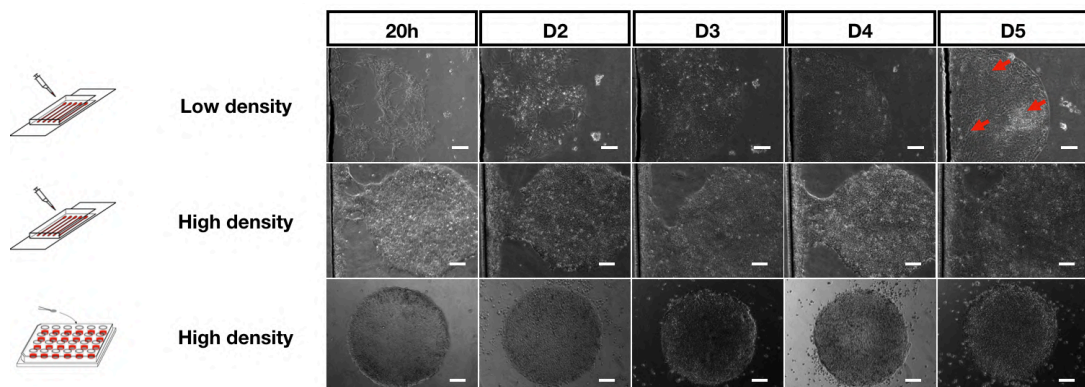


Figure 4.25: Comparison between microfluidic and multi-well plate culture. (Up) Low seeding density in MEF-CM, in microfluidic chips. (Mid) High seeding density MEF-CM, in microfluidic chips. (Down) High seeding density MEF-CM, in 24-well plate. Low density = 125,000 cells/cm². High density = 250,000 cells/cm². Scare bar = 100 μ m. We got similar results from 3 independent experiments.

We tested the marker expression condition after 5 days of neural induction when applied the protocol by using MEF-CM supplemented with APD cocktail (Introduced above). Surprisingly, the neural marker, both early expressed NESTIN and later expressed PAX6 did not show the geometric confinements of cell fates. This may be caused by the flat cell morphology in microfluidic chips (Figure 4.26). We assume that the MEF-CM promoted the stability of the cell colony and also the secreted matrix can improve the adhesion property of the microfluidic channel even on the repellent surface.

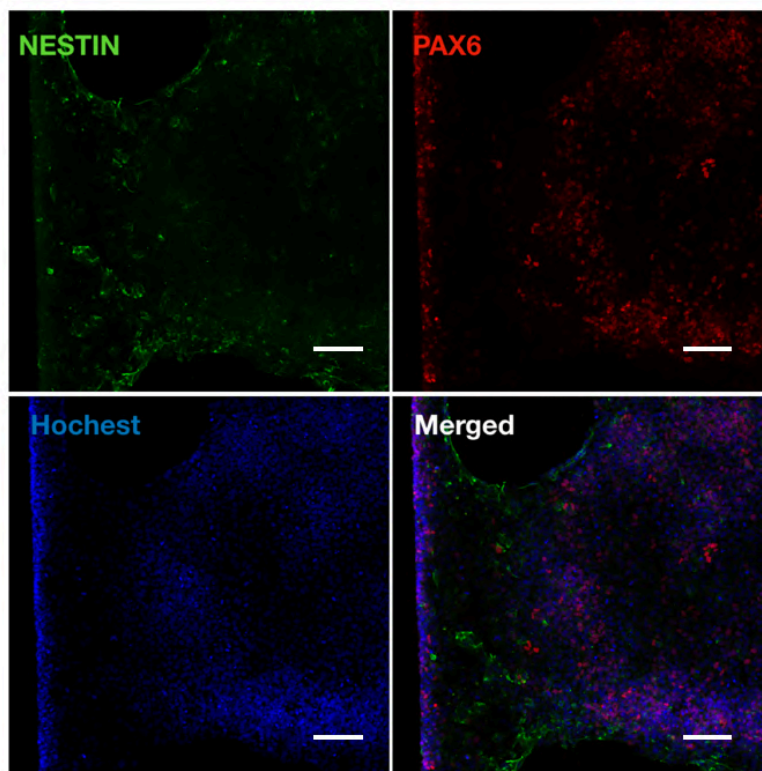
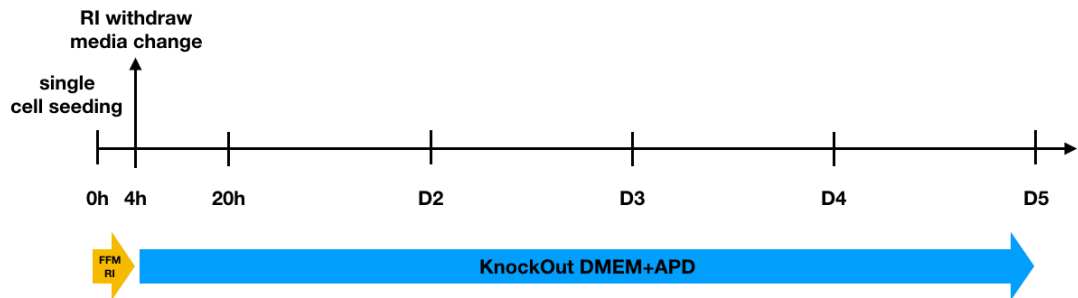


Figure 4.26: Immunostaining of micropattern inside of the microfluidic chip. Scare bar = 100 μ m. We got similar results from 3 independent experiments.

Considering the small culture volume and extremely good adhesion property in microfluidic channels, we decided to fix the protocol by using: 1) KnockOut DMEM as basal medium instead of conditional medium to avoid cell adhesion on the

repellent surface; 2) 800 μm (diameter) circular micropatterns instead of 1000 μm (diameter) ones to make more space between the edge of the channel. The method and cell patterning formation results showed in Figure 4.27a & b.

a



b

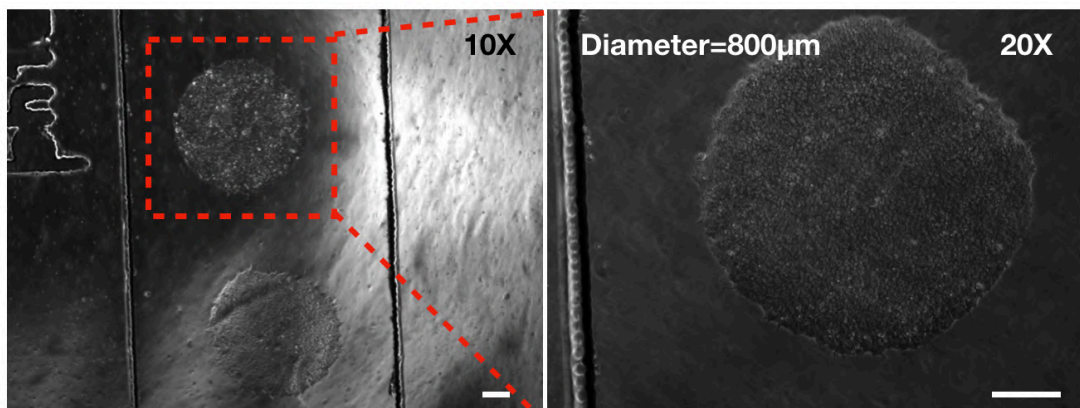


Figure 4.27: Micropatterns inside of microfluidic chips. (a) Strategy and timeline of the applied protocol. (b) Left, 10x, 2 well-formed colonies inside of the microfluidic channel. Scare bar = 200 μm Right, 20x. Scare bar = 200 μm . Diameter of each colony is 800 μm . We got similar results from 3 independent experiments.

CHAPTER 5

DISSCUSSION

In this study, we developed an *in vitro* model in which hESCs differentiate into self-organized patterns of human neural, neural crest, and neural stem cells on the micropatterned surface. It has been demonstrated a robust *in vitro* model to mimic the *in vivo* processes of neurulation, which later form the dorsal-ventral axis patterning. Recent work reported that three phases of neural induction protocol could induce similar neural progenitors, including the human neural, neural crest, placode, and epidermal progenitors (Britton, Heemskerk et al. 2019). In this method, the initial phase starts with the inhibition of TGF- β signal pathway. Then, the patterning factor BMP4 is introduced in this system. As the last phase, the WNT inhibitor is combined with BMP4 to prevent the activation of the Wnt signal pathway, and also promote the generation of neural crest population.

In our preliminary experiment, we used the combination of LDN193189 and SB431542, known as the dual-Smad inhibitor, to induce the micropatterned neural induction. The results showed an extensive promotion of neural plate or CNS cell fates with no possibility to generate the neural crest population. Considering the crucial role of WNT signaling pathway in the neurulation and neural tube formation, we modified our protocol to another combination, which uses three small molecules as the cocktail, to enrich the cell fates outcome. A83-01, PNU74654, and Dorsomorphin, the cocktail we used to inhibit TGF- β , WNT- β catenin, and BMP signal pathways, respectively. As a result, we showed the possibility to mimic neural fate specification during neurulation. We can generate a neural crest cell population in the center together with a CNS cell population as a ring outside. On the contrary, in the published work of 3 phases induction, the CNS occurs in the center while neural crest fate occurs outside. This reverse of cell fates location may be caused by the culture system, especially the

medium applied, but the intrinsic reason is not clear. We also observed a higher cell density close to the border and extremely low density in the center. Thus, another explanation could be that there are different cell communications under different cell density. This result correlates with the work published in 2009, in which they demonstrated that high cell density promotes CNS and low cell density promotes PNS with dual-Smad inhibitor differentiation protocol (by using Noggin and SB431542). The data showed here explained the phenomenon we found and laid the foundation of the co-culture system, and there is a lot of extend work to do in the next stage.

To develop the germ layer co-culture system, we used the established protocol to generate a meso-endoderm cell population. Considering the complexity of the system, we used the mesoderm and endoderm mixture as the second layer instead of two individual layers. After 24 hours of co-culture seeding, the homogeneous meso-endoderm cells were arranged only to the border of the colony. This cell migration or cell accumulation pointed out the existence of germ layer communication in our co-culture system. Based on the data processed, we found a new cell population generated from the co-culture system. Some cells from the subsequently seeded meso-endoderm cells (with GFP labeling) start to express PAX6, which is not observed in the control of micropatterned meso-endoderm maintenance. This discovery is another evidence that can demonstrate the intrinsic “guidance” between different germ layers.

Another impressive result is the phenotype change of meso-endoderm after three days of cell maintenance in MEF-CM without any supplements. From the co-culture staining result, the linear cellular structure over the patterns which connected the border and center caught our attention. We hypothesis that these SOX17+ cells are

induced from the co-culture system and represent the appearance of early vascular fate. To explore this, we applied the same induction protocol to the micropatterned meso-endoderm induction and observed one attractive self-organization property even without co-culture. The radial and linear connecting branches occur even more apparent. Additionally, in contrast with the two days of meso-endoderm induction plus 3 days of maintenance in MEF-CM under standard cell culture, the micropatterned one showed a signal wave transmit from border to center or center to border.

We also got the preliminary data about how to form micropatterns inside of microfluidic chips. Compare with the normal micropattern technology, which we used to generate cell colony from the multi-well culture system, microfluidic culture system may lead to surprising induction results because of its intrinsic differences both in media change and culture volume. More work needs to be done after the establishment of the protocol.

CHAPTER 6
CONCLUSIONS AND FUTURE
PERSPECTIVES

We have developed and established a new micropattern technology that is useful in stem cell research. Also, this method is flexible to be applied to other micro-engineering techniques. As a general conclusion, we can generate the micropatterned neural induction within 5 days of cell differentiation. When we use the small molecule cocktail APD (A83-01, PNU74654, and Dorsomorphin) with MEF-CM as the induction medium, the cells inside the micropattern showed a specific cell-fates-allocation: Neural stem cell population locates at the border, central nervous system population locates as a ring-structure between, while neural crest cell population presents only in the center. In contrast, the MEF-CM with dual-Smad inhibition (LDN193189 and SB431542) cannot induce AP-2 α in the center. This evidence indicates the crucial role of WNT signal pathway in the neural crest fate specification.

We next sought to develop a co-culture system that can be used to investigate the interaction between different germ-layers. In this part, we used MEF-CM supplemented with an APD cocktail as the differentiation medium. Then another meso-endoderm differentiation protocol was defined and applied to induce a subsequently seeded meso-endoderm population. We succeeded in making a complex in vitro model, which can be treated as a multiple germ layer organoids. Based on the staining results, we found that the subsequent meso-endoderm cells adhered mainly to the border of the PAX6⁺ cell population. This cell location indicates that different cell fates of neuroectoderm have diverse adherent properties. In the meantime, we found two new cell fates from our system after 3 days of co-culture. The cells with GFP label co-expressed PAX6 are generated from meso-endoderm cells, and this probably could be direct evidence of the interaction between germ layers. When we looked into the SOX17 expression condition, we found the subsequently seeded meso-endoderm cell

showed an elongated cell morphology, and they acted as a “bridge” over PAX6+ population region. From the micropatterned meso-endoderm differentiation experiment, we can confirm that the micropatterned meso-endoderm cells can self-organize into some linear structure between the micropattern center and border, and these SOX17+ cells are quite possibly early vascular cells. So, we hypothesis that these linear cells are the early vascular cells generated from our co-culture system. Additional, the self-organization property we observed in the micropatterned meso-endoderm induction and maintenance opens up a new horizon for us to investigate the signal wave inside micropatterns.

This study has developed a novel system in which human embryonic stem cells can be used to generate the patterns during neurulation. This system can be used to gain a new understanding of human embryonic development and to develop new differentiation protocols. Future studies can take advantage of this system together with live-cell reporters of signaling and fate to understand in detail how the patterning happens when under geometric confinement. Similar approaches are now available to generate patterning based on mesoderm, endoderm, or even particular organs.

CHAPTER 7

REFERENCES

Andersson, A. S., K. Glasmästar, D. Sutherland, U. Lidberg and B. Kasemo (2003). "Cell adhesion on supported lipid bilayers." Journal of Biomedical Materials Research Part A: An Official Journal of The Society for Biomaterials, The Japanese Society for Biomaterials, and The Australian Society for Biomaterials and the Korean Society for Biomaterials **64**(4): 622-629.

Aragona, M., T. Panciera, A. Manfrin, S. Giullitti, F. Michielin, N. Elvassore, S. Dupont and S. Piccolo (2013). "A mechanical checkpoint controls multicellular growth through YAP/TAZ regulation by actin-processing factors." Cell **154**(5): 1047-1059.

Arias, A. M. and A. Stewart (2002). Molecular principles of animal development, Oxford University Press.

Artavanis-Tsakonas, S., M. D. Rand and R. J. Lake (1999). "Notch signaling: cell fate control and signal integration in development." Science **284**(5415): 770-776.

Asch, R., C. Simerly, T. Ord, V. Ord and G. Schatten (1995). "The stages at which human fertilization arrests: microtubule and chromosome configurations in inseminated oocytes which failed to complete fertilization and development in humans." MHR: Basic science of reproductive medicine **1**(5): 239-248.

Azioune, A., M. Storch, M. Bornens, M. Théry and M. Piel (2009). "Simple and rapid process for single cell micro-patterning." Lab on a chip **9**(11): 1640-1642.

Barbaric, I. and N. J. Harrison (2012). "Rediscovering pluripotency: from teratocarcinomas to embryonic stem cells." International Journal of Developmental Biology **56**(4): 197-206.

Barber, T. A., S. L. Golledge, D. G. Castner and K. E. Healy (2003). "Peptide-modified p (AAm-co-EG/AAc) IPNs grafted to bulk titanium modulate osteoblast behavior in vitro." Journal of Biomedical Materials Research Part A: An Official Journal of The Society for Biomaterials, The Japanese Society for Biomaterials, and The Australian

Society for Biomaterials and the Korean Society for Biomaterials **64**(1): 38-47.

Bauwens, C. L., R. Peerani, S. Niebruegge, K. A. Woodhouse, E. Kumacheva, M. Husain and P. W. Zandstra (2008). "Control of human embryonic stem cell colony and aggregate size heterogeneity influences differentiation trajectories." Stem cells **26**(9): 2300-2310.

Bearinger, J., D. Castner and K. Healy (1998). "Biomolecular modification of p(AAm-co-EG/AA) IPNs supports osteoblast adhesion and phenotypic expression." Journal of Biomaterials Science, Polymer Edition **9**(7): 629-652.

Bédier, A., C. Vieu, F. Arnauduc, J.-C. Sol, I. Loubinoux and L. Vaysse (2012). "Engineering of adult human neural stem cells differentiation through surface micropatterning." Biomaterials **33**(2): 504-514.

Bhatia, S. N. and D. E. Ingber (2014). "Microfluidic organs-on-chips." Nature biotechnology **32**(8): 760.

Bietsch, A. and B. Michel (2000). "Conformal contact and pattern stability of stamps used for soft lithography." Journal of Applied Physics **88**(7): 4310-4318.

Britton, G., I. Heemskerk, R. Hodge, A. A. Qutub and A. Warmflash (2019). "A novel self-organizing embryonic stem cell system reveals signaling logic underlying the patterning of human ectoderm." bioRxiv: 518803.

Chhabra., S., L. Liu., R. Goh. and A. Warmflash. (2018). "The timing of signaling events in the BMP, WNT, and Nodal cascade determines self-organized fate patterning in human gastruloids." bioRxiv.

D'Arcangelo, E. and A. P. McGuigan (2015). "Micropatterning strategies to engineer controlled cell and tissue architecture in vitro." Biotechniques **58**(1): 13-23.

Deglincerti, A., F. Etoc, M. C. Guerra, I. Martyn, J. Metzger, A. Ruzo, M. Simunovic, A. Yoney, A. H. Brivanlou, E. Siggia and A. Warmflash (2016). "Self-organization of

human embryonic stem cells on micropatterns." Nat Protoc **11**(11): 2223-2232.

di Magliano, M. P. and M. Hebrok (2003). "Hedgehog signalling in cancer formation and maintenance." Nature reviews cancer **3**(12): 903.

Dorsky, R. I., R. T. Moon and D. W. Raible (1998). "Control of neural crest cell fate by the Wnt signalling pathway." Nature **396**(6709): 370.

Engler, A. J., M. A. Griffin, S. Sen, C. G. Bönnemann, H. L. Sweeney and D. E. Discher (2004). "Myotubes differentiate optimally on substrates with tissue-like stiffness: pathological implications for soft or stiff microenvironments." J Cell Biol **166**(6): 877-887.

Falconnet, D., G. Csucs, H. M. Grandin and M. Textor (2006). "Surface engineering approaches to micropattern surfaces for cell-based assays." Biomaterials **27**(16): 3044-3063.

Fleming, A., R. J. Keynes and D. Tannahill (2001). "The role of the notochord in vertebral column formation." The Journal of Anatomy **199**(1-2): 177-180.

Folch, A., B. H. Jo, O. Hurtado, D. J. Beebe and M. Toner (2000). "Microfabricated elastomeric stencils for micropatterning cell cultures." Journal of Biomedical Materials Research: An Official Journal of The Society for Biomaterials, The Japanese Society for Biomaterials, and The Australian Society for Biomaterials and the Korean Society for Biomaterials **52**(2): 346-353.

Fujimura, N. (2016). "WNT/ β -catenin signaling in vertebrate eye development." Frontiers in cell and developmental biology **4**: 138.

Goubko, C. A. and X. Cao (2009). "Patterning multiple cell types in co-cultures: A review." Materials Science and Engineering: C **29**(6): 1855-1868.

Hall, B. K. (2000). "The neural crest as a fourth germ layer and vertebrates as quadroblastic not triploblastic." Evolution & development **2**(1): 3-5.

Harrison, R. G., M. Greenman, F. P. Mall and C. Jackson (1907). "Observations of the living developing nerve fiber." The Anatomical Record **1**(5): 116-128.

Harrison, S. E., B. Sozen, N. Christodoulou, C. Kyprianou and M. Zernicka-Goetz (2017). "Assembly of embryonic and extraembryonic stem cells to mimic embryogenesis in vitro." Science **356**(6334).

Hogberg, H. T., J. Bressler, K. M. Christian, G. Harris, G. Makri, C. O'Driscoll, D. Pamies, L. Smirnova, Z. Wen and T. Hartung (2013). "Toward a 3D model of human brain development for studying gene/environment interactions." Stem cell research & therapy **4**(1): S4.

Hopkins, A. M., E. DeSimone, K. Chwalek and D. L. Kaplan (2015). "3D in vitro modeling of the central nervous system." Progress in neurobiology **125**: 1-25.

Hurtado, L., C. Caballero, M. P. Gavilan, J. Cardenas, M. Bornens and R. M. Rios (2011). "Disconnecting the Golgi ribbon from the centrosome prevents directional cell migration and ciliogenesis." The Journal of cell biology **193**(5): 917-933.

Hynes, R. O. (2002). "Integrins: bidirectional, allosteric signaling machines." cell **110**(6): 673-687.

Ingber, D. E. (2003). "Tensegrity II. How structural networks influence cellular information processing networks." J Cell Sci **116**(Pt 8): 1397-1408.

James, J., E. D. Goluch, H. Hu, C. Liu and M. Mrksich (2008). "Subcellular curvature at the perimeter of micropatterned cells influences lamellipodial distribution and cell polarity." Cell motility and the cytoskeleton **65**(11): 841-852.

Jiang, X., D. A. Bruzewicz, A. P. Wong, M. Piel and G. M. Whitesides (2005). "Directing cell migration with asymmetric micropatterns." Proceedings of the National Academy of Sciences **102**(4): 975-978.

John, P. M. S., L. Kam, S. W. Turner, H. G. Craighead, M. Issacson, J. N. Turner and

W. Shain (1997). "Preferential glial cell attachment to microcontact printed surfaces." Journal of neuroscience methods **75**(2): 171-177.

Kam, L., W. Shain, J. N. Turner and R. Bizios (1999). "Correlation of astroglial cell function on micro-patterned surfaces with specific geometric parameters." Biomaterials **20**(23-24): 2343-2350.

Kanning, K. C., A. Kaplan and C. E. Henderson (2010). "Motor neuron diversity in development and disease." Annual review of neuroscience **33**: 409-440.

Kato-Negishi, M., Y. Morimoto, H. Onoe and S. Takeuchi (2013). "Millimeter-Sized Neural Building Blocks for 3D Heterogeneous Neural Network Assembly." Advanced healthcare materials **2**(12): 1564-1570.

Kaufman, D. S., E. T. Hanson, R. L. Lewis, R. Auerbach and J. A. Thomson (2001). "Hematopoietic colony-forming cells derived from human embryonic stem cells." Proceedings of the National Academy of Sciences **98**(19): 10716-10721.

Kaufmann, T. and B. J. Ravoo (2010). "Stamps, inks and substrates: polymers in microcontact printing." Polymer Chemistry **1**(4): 371-387.

Kenausis, G. L., J. Vörös, D. L. Elbert, N. Huang, R. Hofer, L. Ruiz-Taylor, M. Textor, J. A. Hubbell and N. D. Spencer (2000). "Poly (L-lysine)-g-poly (ethylene glycol) layers on metal oxide surfaces: attachment mechanism and effects of polymer architecture on resistance to protein adsorption." The Journal of Physical Chemistry B **104**(14): 3298-3309.

Keselowsky, B. G., D. M. Collard and A. J. García (2003). "Surface chemistry modulates fibronectin conformation and directs integrin binding and specificity to control cell adhesion." Journal of Biomedical Materials Research Part A: An Official Journal of The Society for Biomaterials, The Japanese Society for Biomaterials, and The Australian Society for Biomaterials and the Korean Society for Biomaterials **66**(2):

247-259.

Khademhosseini, A., L. Ferreira, J. Blumling III, J. Yeh, J. M. Karp, J. Fukuda and R. Langer (2006). "Co-culture of human embryonic stem cells with murine embryonic fibroblasts on microwell-patterned substrates." Biomaterials **27**(36): 5968-5977.

Knight, G., J. Sha and R. Ashton (2015). "Micropatterned, clickable culture substrates enable in situ spatiotemporal control of human PSC-derived neural tissue morphology." Chemical Communications **51**(25): 5238-5241.

Knight, G. T., B. F. Lundin, N. Iyer, L. M. Ashton, W. A. Sethares, R. M. Willett and R. S. Ashton (2018). "Engineering induction of singular neural rosette emergence within hPSC-derived tissues." Elife **7**.

Komiya, Y. and R. Habas (2008). "Wnt signal transduction pathways." Organogenesis **4**(2): 68-75.

Lake, B. B., R. Ai, G. E. Kaeser, N. S. Salathia, Y. C. Yung, R. Liu, A. Wildberg, D. Gao, H.-L. Fung and S. Chen (2016). "Neuronal subtypes and diversity revealed by single-nucleus RNA sequencing of the human brain." Science **352**(6293): 1586-1590.

Lancaster, M. A., M. Renner, C.-A. Martin, D. Wenzel, L. S. Bicknell, M. E. Hurles, T. Homfray, J. M. Penninger, A. P. Jackson and J. A. Knoblich (2013). "Cerebral organoids model human brain development and microcephaly." Nature **501**(7467): 373.

Langer, R. and D. A. Tirrell (2004). "Designing materials for biology and medicine." Nature **428**(6982): 487.

Lauer, L., C. Klein and A. Offenhäusser (2001). "Spot compliant neuronal networks by structure optimized micro-contact printing." Biomaterials **22**(13): 1925-1932.

Lee, L. H., R. Peerani, M. Ungrin, C. Joshi, E. Kumacheva and P. Zandstra (2009). "Micropatterning of human embryonic stem cells dissects the mesoderm and endoderm lineages." Stem cell research **2**(2): 155-162.

Liu, C., G. Peng and N. Jing (2017). "TGF- β signaling pathway in early mouse development and embryonic stem cells." Acta biochimica et biophysica Sinica **50**(1): 68-73.

Londono, C., M. J. Loureiro, B. Slater, P. B. Lückner, J. Soleas, S. Sathanathan, J. S. Aitchison, A. J. Kabla and A. P. McGuigan (2014). "Nonautonomous contact guidance signaling during collective cell migration." Proceedings of the National Academy of Sciences **111**(5): 1807-1812.

Luk, Y.-Y., M. Kato and M. Mrksich (2000). "Self-assembled monolayers of alkanethiolates presenting mannitol groups are inert to protein adsorption and cell attachment." Langmuir **16**(24): 9604-9608.

Ma, Z., J. Wang, P. Loskill, N. Huebsch, S. Koo, F. L. Svedlund, N. C. Marks, E. W. Hua, C. P. Grigoropoulos and B. R. Conklin (2015). "Self-organizing human cardiac microchambers mediated by geometric confinement." Nature communications **6**: 7413.

Manfrin, A., Y. Tabata, E. R. Paquet, A. R. Vuaridel, F. R. Rivest, F. Naef and M. P. Lutolf (2019). "Engineered signaling centers for the spatially controlled patterning of human pluripotent stem cells." Nature Methods **16**(7): 640.

Martyn, I., A. H. Brivanlou and E. D. Siggia (2019). "A wave of WNT signalling balanced by secreted inhibitors controls primitive streak formation in micropattern colonies of human embryonic stem cells." Development.

Martyn, I., T. Y. Kanno, A. Ruzo, E. D. Siggia and A. H. Brivanlou (2018). "Self-organization of a human organizer by combined Wnt and Nodal signalling." Nature **558**(7708): 132-135.

McNulty, J. D., T. Klann, J. Sha, M. Salick, G. T. Knight, L.-S. Turng and R. S. Ashton (2014). "High-precision robotic microcontact printing (R- μ CP) utilizing a vision guided selectively compliant articulated robotic arm." Lab on a Chip **14**(11): 1923-

1930.

Metzger, J. J., M. Simunovic and A. H. Brivanlou (2018). "Synthetic embryology: controlling geometry to model early mammalian development." Current opinion in genetics & development **52**: 86-91.

Mohr, J. C., J. J. de Pablo and S. P. Palecek (2006). "3-D microwell culture of human embryonic stem cells." Biomaterials **27**(36): 6032-6042.

Montero, J.-A. and C.-P. Heisenberg (2004). "Gastrulation dynamics: cells move into focus." Trends in cell biology **14**(11): 620-627.

Morgani, S. M., J. J. Metzger, J. Nichols, E. D. Siggia and A. K. Hadjantonakis (2018). "Micropattern differentiation of mouse pluripotent stem cells recapitulates embryo regionalized cell fate patterning." Elife **7**.

Nam, Y., G. J. Brewer and B. C. Wheeler (2007). "Development of astroglial cells in patterned neuronal cultures." Journal of Biomaterials Science, Polymer Edition **18**(8): 1091-1100.

Nelson, C. M., S. Raghavan, J. L. Tan and C. S. Chen (2003). "Degradation of micropatterned surfaces by cell-dependent and-independent processes." Langmuir **19**(5): 1493-1499.

Nuzzo, R. G. and D. L. Allara (1983). "Adsorption of bifunctional organic disulfides on gold surfaces." Journal of the American Chemical Society **105**(13): 4481-4483.

Ostuni, E., R. Kane, C. S. Chen, D. E. Ingber and G. M. Whitesides (2000). "Patterning mammalian cells using elastomeric membranes." Langmuir **16**(20): 7811-7819.

Pasche, S., S. M. De Paul, J. Vörös, N. D. Spencer and M. Textor (2003). "Poly (l-lysine)-g raft-poly (ethylene glycol) Assembled Monolayers on Niobium Oxide Surfaces: A Quantitative Study of the Influence of Polymer Interfacial Architecture on Resistance to Protein Adsorption by ToF-SIMS and in Situ OWLS." Langmuir **19**(22):

9216-9225.

Pasche, S., J. Vörös, H. J. Griesser, N. D. Spencer and M. Textor (2005). "Effects of ionic strength and surface charge on protein adsorption at PEGylated surfaces." The Journal of Physical Chemistry B **109**(37): 17545-17552.

Peerani, R., B. M. Rao, C. Bauwens, T. Yin, G. A. Wood, A. Nagy, E. Kumacheva and P. W. Zandstra (2007). "Niche-mediated control of human embryonic stem cell self-renewal and differentiation." The EMBO journal **26**(22): 4744-4755.

Rajagopalan, P., W. A. Marganski, X. Q. Brown and J. Y. Wong (2004). "Direct comparison of the spread area, contractility, and migration of balb/c 3T3 fibroblasts adhered to fibronectin-and RGD-modified substrata." Biophysical journal **87**(4): 2818-2827.

Rathjen, J. (2014). "The states of pluripotency: pluripotent lineage development in the embryo and in the dish." ISRN Stem Cells **2014**.

Ratner, B. D. and S. J. Bryant (2004). "Biomaterials: where we have been and where we are going." Annu Rev Biomed Eng **6**: 41-75.

Reubinoff, B. E., P. Itsykson, T. Turetsky, M. F. Pera, E. Reinhartz, A. Itzik and T. Ben-Hur (2001). "Neural progenitors from human embryonic stem cells." Nature biotechnology **19**(12): 1134.

Revzin, A., R. G. Tompkins and M. Toner (2003). "Surface engineering with poly(ethylene glycol) photolithography to create high-density cell arrays on glass." Langmuir **19**(23): 9855-9862.

Rowe, R. G. and G. Q. Daley (2019). "Induced pluripotent stem cells in disease modelling and drug discovery." Nature Reviews Genetics: 1.

Sahni, G., J. Yuan and Y. C. Toh (2016). "Stencil Micropatterning of Human Pluripotent Stem Cells for Probing Spatial Organization of Differentiation Fates." J

Vis Exp(112).

Sanz-Ezquerro, J. J., A. E. Münsterberg and S. Stricker (2017). "Signaling pathways in embryonic development." Frontiers in cell and developmental biology **5**: 76.

Sasai, Y. (2013). "Next-generation regenerative medicine: organogenesis from stem cells in 3D culture." Cell stem cell **12**(5): 520-530.

Shen, K., S. Luk, D. F. Hicks, J. S. Elman, S. Bohr, Y. Iwamoto, R. Murray, K. Pena, F. Wang and E. Seker (2014). "Resolving cancer–stroma interfacial signalling and interventions with micropatterned tumour–stromal assays." Nature communications **5**: 5662.

Simunovic, M., J. J. Metzger, F. Etoc, A. Yoney, A. Ruzo, I. Martyn, G. Croft, A. H. Brivanlou and E. D. Siggia (2018). "Molecular mechanism of symmetry breaking in a 3D model of a human epiblast." BioRxiv: 330704.

Singh, V. K., M. Kalsan, N. Kumar, A. Saini and R. Chandra (2015). "Induced pluripotent stem cells: applications in regenerative medicine, disease modeling, and drug discovery." Frontiers in cell and developmental biology **3**: 2.

Stemple, D. L. (2005). "Structure and function of the notochord: an essential organ for chordate development." Development **132**(11): 2503-2512.

Takahashi, K., K. Tanabe, M. Ohnuki, M. Narita, T. Ichisaka, K. Tomoda and S. Yamanaka (2007). "Induction of pluripotent stem cells from adult human fibroblasts by defined factors." cell **131**(5): 861-872.

Takahashi, K. and S. Yamanaka (2016). "A decade of transcription factor-mediated reprogramming to pluripotency." Nature reviews Molecular cell biology **17**(3): 183.

Tao, Y. and S. C. Zhang (2016). "Neural Subtype Specification from Human Pluripotent Stem Cells." Cell Stem Cell **19**(5): 573-586.

They, M. (2010). "Micropatterning as a tool to decipher cell morphogenesis and

functions." J Cell Sci **123**(Pt 24): 4201-4213.

Thomson, J. A., J. Itskovitz-Eldor, S. S. Shapiro, M. A. Waknitz, J. J. Swiergiel, V. S. Marshall and J. M. Jones (1998). "Embryonic stem cell lines derived from human blastocysts." science **282**(5391): 1145-1147.

Tseng, Q., E. Duchemin-Pelletier, A. Deshieri, M. Balland, H. Guillou, O. Filhol and M. Théry (2012). "Spatial organization of the extracellular matrix regulates cell–cell junction positioning." Proceedings of the National Academy of Sciences **109**(5): 1506-1511.

Urich, E., C. Patsch, S. Aigner, M. Graf, R. Iacone and P.-O. Freskgård (2013). "Multicellular self-assembled spheroidal model of the blood brain barrier." Scientific reports **3**: 1500.

Vaez Ghaemi, R., I. L. Co, M. C. McFee and V. G. Yadav (2019). "Brain Organoids: A New, Transformative Investigational Tool for Neuroscience Research." Advanced Biosystems **3**(1): 1800174.

Vaillancourt, C. and J. Lafond (2009). Human embryogenesis: overview. Human Embryogenesis, Springer: 3-7.

van der Meer, A. D. and A. van den Berg (2012). "Organs-on-chips: breaking the in vitro impasse." Integrative Biology **4**(5): 461-470.

Wagner, M., S. Pasche, D. G. Castner and M. Textor (2004). "Characterization of poly (L-lysine)-graft-poly (ethylene glycol) assembled monolayers on niobium pentoxide substrates using time-of-flight secondary ion mass spectrometry and multivariate analysis." Analytical chemistry **76**(5): 1483-1492.

Wang, N., E. Ostuni, G. M. Whitesides and D. E. Ingber (2002). "Micropatterning tractional forces in living cells." Cell motility and the cytoskeleton **52**(2): 97-106.

Warmflash, A., B. Sorre, F. Etoc, E. D. Siggia and A. H. Brivanlou (2014). "A method

to recapitulate early embryonic spatial patterning in human embryonic stem cells." Nature methods **11**(8): 847.

Weibel, D. B., W. R. Diluzio and G. M. Whitesides (2007). "Microfabrication meets microbiology." Nat Rev Microbiol **5**(3): 209-218.

Wen-Wen, L., C. Zhen-Ling and X.-Y. JIANG (2009). "Methods for cell micropatterning on two-dimensional surfaces and their applications in biology." Chinese Journal of Analytical Chemistry **37**(7): 943-949.

Wheeler, B. C. and G. J. Brewer (2010). "Designing neural networks in culture." Proceedings of the IEEE **98**(3): 398-406.

Whitesides, G. M., E. Ostuni, S. Takayama, X. Jiang and D. E. Ingber (2001). "Soft lithography in biology and biochemistry." Annual review of biomedical engineering **3**(1): 335-373.

Wong, J. Y., J. B. Leach and X. Q. Brown (2004). "Balance of chemistry, topography, and mechanics at the cell–biomaterial interface: Issues and challenges for assessing the role of substrate mechanics on cell response." Surface Science **570**(1-2): 119-133.

Xia, Y. and G. M. Whitesides (1998). "Soft lithography." Annual review of materials science **28**(1): 153-184.

Xue, X., Y. Sun, A. M. Resto-Irizarry, Y. Yuan, K. M. A. Yong, Y. Zheng, S. Weng, Y. Shao, Y. Chai and L. Studer (2018). "Mechanics-guided embryonic patterning of neuroectoderm tissue from human pluripotent stem cells." Nature materials: 1.

Yao, R., J. Wang, X. Li, D. Jung Jung, H. Qi, K. K. Kee and Y. Du (2014). "Hepatic differentiation of human embryonic stem cells as microscaled multilayered colonies leading to enhanced homogeneity and maturation." Small **10**(21): 4311-4323.

Yu, J., M. A. Vodyanik, K. Smuga-Otto, J. Antosiewicz-Bourget, J. L. Frane, S. Tian, J. Nie, G. A. Jonsdottir, V. Ruotti and R. Stewart (2007). "Induced pluripotent stem

cell lines derived from human somatic cells." science **318**(5858): 1917-1920.

Zhang, S.-C., M. Wernig, I. D. Duncan, O. Brüstle and J. A. Thomson (2001). "In vitro differentiation of transplantable neural precursors from human embryonic stem cells." Nature biotechnology **19**(12): 1129.

Zhu, Z. and D. Huangfu (2013). "Human pluripotent stem cells: an emerging model in developmental biology." Development **140**(4): 705-717.

ACKNOWLEDGEMENT

First of all, I would like to thank both the University of Padova (UNIPD) and China Scholarship Council (CSC) for giving me this opportunity to study in Italy, meeting so many helpful people, and enriching my academic experiences. I want to take this opportunity to express my sincere gratitude to my supervisor, professor Nicola Elvassore. he has offered me constructive guidance for the planning of the project thesis and invaluable advice and encouragement for its completion and improvement.

Besides, I wish to extend my sincere gratitude to all the teachers in the school of chemical and environmental engineering. They have taught me and given me generous support during my three years of Ph.D. It is my great honor to have known all those respectable teachers. Also, many thanks to my colleagues and friends, Anna Urciuolo, Cecilia Laterza, Onelia Gagliano, Hannah Stuart, Anna Maria Tolomeo, Luca Brandolino, Valentina Scattolini, Paolo Raffa, Elisa Cesare, Silvia Angiolillo, Davide Scantamburlo, etc., I cannot succeed without the help the form them.

At last, my thanks would go to my beloved family for their thoughtful considerations and great confidence through these years. It is their support that confirmed my determination to finish my research during the time of great hardships. Thank myself, always enjoy the life in science, and never give up at any time.

致谢

在过去的三年多时间里，我数次构思着这一份写在最后的致谢。幻想着一部分，渴望着一部分，也慢慢地遗忘了一部分。

曾经幻想着在最后写一份最滑稽的致谢，把所有的喜怒哀乐都裹藏在其中，然后三五十年之后的某一天，偶然打开，让如今这份年轻的冲动再给苍老的心一点慰藉。

曾经也有很多渴望，渴望着用几百页的文字总结一下博士的工作，厚厚一沓，以后拿给师弟师妹，或许也能凹一个成功大师兄的人设出来。

曾经也想说，有些人有些事，都是我成长道路上不可遗忘的部分，但如今细细去想，那些人那些事，却都变成了哪些人哪些事。

...

我难以分清现在是否拥有，却真真切切体会到了过程的真实，在博士期间，我遇到了太多，懂得了太多，也在这最后，拥抱了太多。那些甜蜜抑或是苦涩的经历，此时看来，也正是它们，成就了如今的我。

首先，我想感谢我的祖国，感谢国家留学基金委，感谢母校中国科学技术大学，给了我这个机会，资助我完成博士学业！

其次，感谢 PADOVA 大学，感谢我的导师 Nicola Elvassore 教授，为我提供了完善的博士教育，并帮助我完成博士课题！

同时我还要感谢我的同事，同学，以及跟我一起奋斗在实验室的工作人员们，感谢你们对我无私的帮助！

最后，我想感谢我的家人们。感谢我的姐姐，在我海外求学期间，担负起照顾整个家庭的重担。是你的无私，给予了我继续探求科学真理的机会！感谢我的父母，无论何时都为我着想，爱护并鼓励我，支持我在自己的道路上愈发向前！

也要感谢我自己，满怀希望，顽强而乐观！

2019/12/01 帕多瓦大学